SANDIA REPORT

SAND94—2693
Unlimited Release
Printed December 1994

Comparison of Stress-Measuring Techniques at the DNA-UTP Site, Rodgers Hollow, Kentucky

R. E. Finley

Prepared by
Sandia National Laboratories
Albuquerque, New Mexico 87185 and Livermore, California 94550
for the United States Department of Energy
under Contract DE-AC04-94AL85000

Approved for public release; distribution is unlimited.

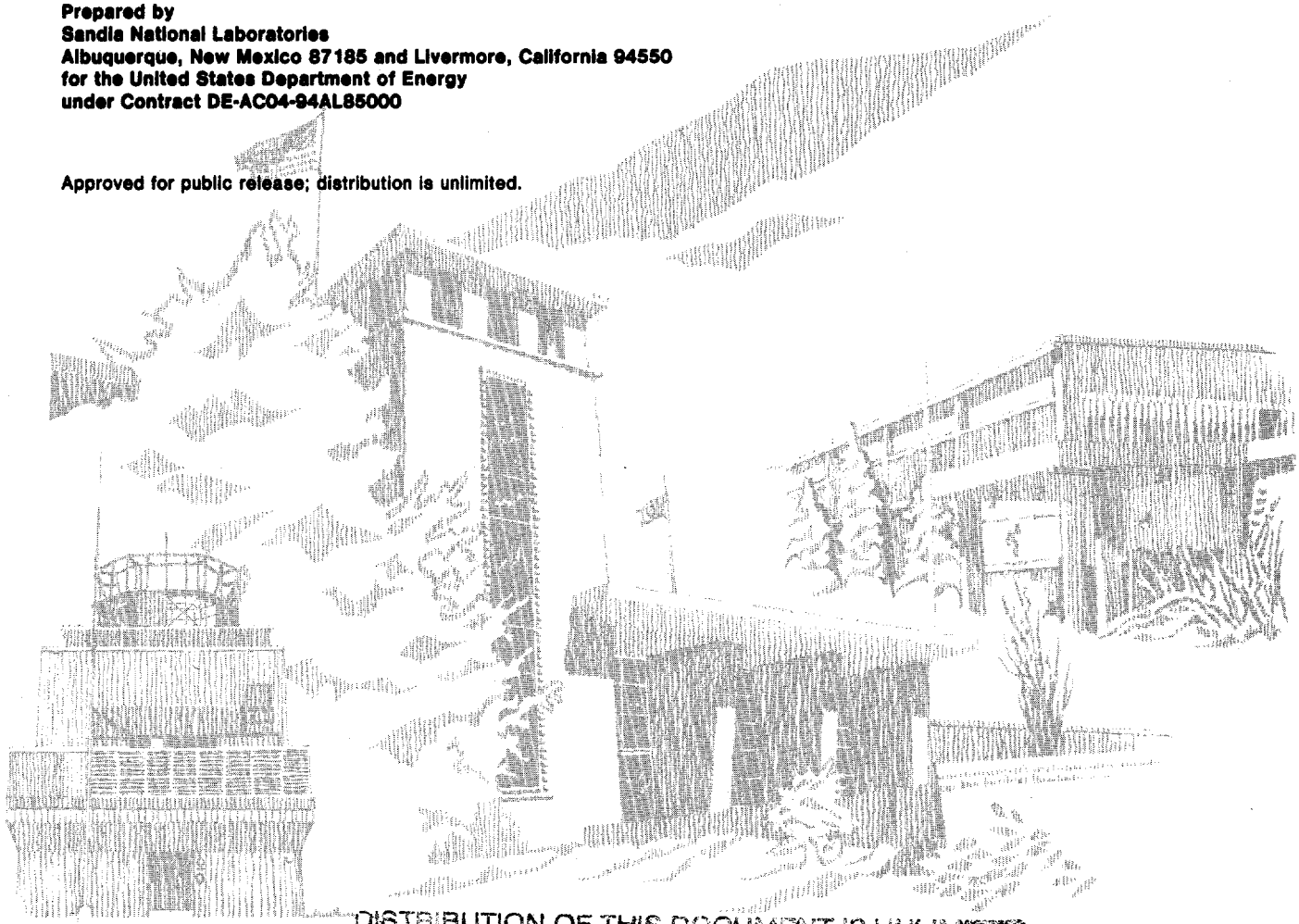

Issued by Sandia National Laboratories, operated for the United States Department of Energy by Sandia Corporation.

Available to DOE and DOE contractors from
Office of Scientific and Technical Information
PO Box 62
Oak Ridge, TN 37831

Prices available from (615) 576-8401, FTS 626-8401

Available to the public from
National Technical Information Service
US Department of Commerce
5285 Port Royal RD
Springfield, VA 22161

NTIS price codes
Printed copy: A07
Microfiche copy: A01

DISCLAIMER

DISCLAIMER

Portions of this document may be illegible in electronic image products. Images are produced from the best available original document.

SAND94-2693
Unlimited Release
Printed December 1994

Comparison of Stress-Measuring Techniques at the DNA-UTP Site, Rodgers Hollow, Kentucky

Sandia National Laboratories
Performance Assessment Applications Department 6313
Geomechanics Department 6117
and
J.F.T. Agapito and Associates

Abstract

Three different stress-measuring techniques were used to measure the in situ stress and near-field stress at the Defense Nuclear Agency-Underground Technology Program (DNA-UTP) test facility at Rodgers Hollow, near Fort Knox, Kentucky. US Bureau of Mines (USBM) Overcoring, Anelastic Strain Recovery (ASR), and flatjack techniques were used to measure far- and near-field stresses in the New Providence Shale Member at a depth of about 350 ft (107 m) below the surface. In addition, the flatjack technique was used to estimate the deformation modulus of the shale member parallel and perpendicular to bedding. In general, the test techniques met with limited success, due largely to the material behavior of the stratigraphic horizon tested. The New Providence Shale Member exhibited strongly anisotropic time-dependent behavior both in laboratory tests and in situ. The USBM overcoring technique produced the most repeatable, realistic in situ stress values of: σ_1 = 373 psi (2.57 MPa) at 34°N 63°E, σ_2 = 281 psi (1.94 MPa) at 122°N 40°E, and σ_3 = 176 psi (1.21 MPa) at 101°N 137°E. Simple calculation of the in situ stress from the overburden support the overcoring results. The flatjack in situ stress testing resulted in extremely complex rock response suggesting that the flatjack results be treated with care when drawing conclusions. Unfortunately, the ASR testing did not produce results useable for in situ stress determinations. The modulus of deformation determinations using the flatjack technique suggest a value of between 435,000 and 1,450,000 psi (3 and 10 GPa) for the rock mass. These values are consistent with the results from the laboratory testing and the USBM overcoring.

CONTENTS

Figures

Tables

1.0 Introduction

The Defense Nuclear Agency (DNA) is developing explosives technology through its Underground Technology Program (UTP). Sandia National Laboratories (SNL) has supported the DNA by conducting research to characterize the in situ stress and rock mass deformability at one of the UTP underground sites at Rodgers Hollow, near Louisville, Kentucky on the Fort Knox Military Reservation (see Figure 1-1).

1.1 Purpose/Objectives of the Test

The purpose of SNL's testing was to determine the in situ stress using three different measurement techniques and, if possible, to estimate the rock mass modulus near the underground opening. The three stress-measuring techniques are 1) borehole deformation measurements using overcoring, 2) Anelastic Strain Recovery (ASR) complemented by laboratory ultrasonic and mechanical properties testing, and 3) the in situ flatjack technique using cancellation pressure. Rock mass modulus around the underground opening was estimated using the load deformation history of the flatjack and surrounding rock.

Borehole deformation measurements using the overcoring technique probably represent the most reliable method for in situ stress determination in boreholes up to 50 ft (15 m) deep in competent rock around an isolated excavation. The technique is used extensively by the tunneling and mining industries. The ASR technique is also a core-based technique and is used in the petroleum and natural gas industries for characterization of in situ stress from deep boreholes. The flatjack technique has also been used in the tunneling and mining industries, and until recently has been limited to measurement of the stress immediately around the excavation. Results from the flatjack technique must be further analyzed to calculate the in situ stress in the far field.

1.2 Geology of the Site

The geology of the site consists of a layered stratigraphic sequence of sedimentary rocks as shown in Figure 1-2. The local topography (see Figure 1-3) is hilly with a total relief of about 280 ft (85 m) from valley to hilltop. The tunnel portal is located in a hard silty calcareous shale and is driven downward at a 10% slope to a total depth of approximately 260 ft (79 m) from which point the test drift was driven horizontally an additional 1,000 ft (305 m) (see Figure 1-3). The horizontal drift is located in the New Providence Shale Member of the Borden Formation, which consists of an approximately 100-ft (30.5-m)-thick sequence of dark gray, moderately hard shale. This shale is horizontally bedded and feels "greasy" when wet. The water table in the vicinity of the in situ tests is about 155 ft (47 m) above the base of the New Providence Shale Member (UTP, 1991).

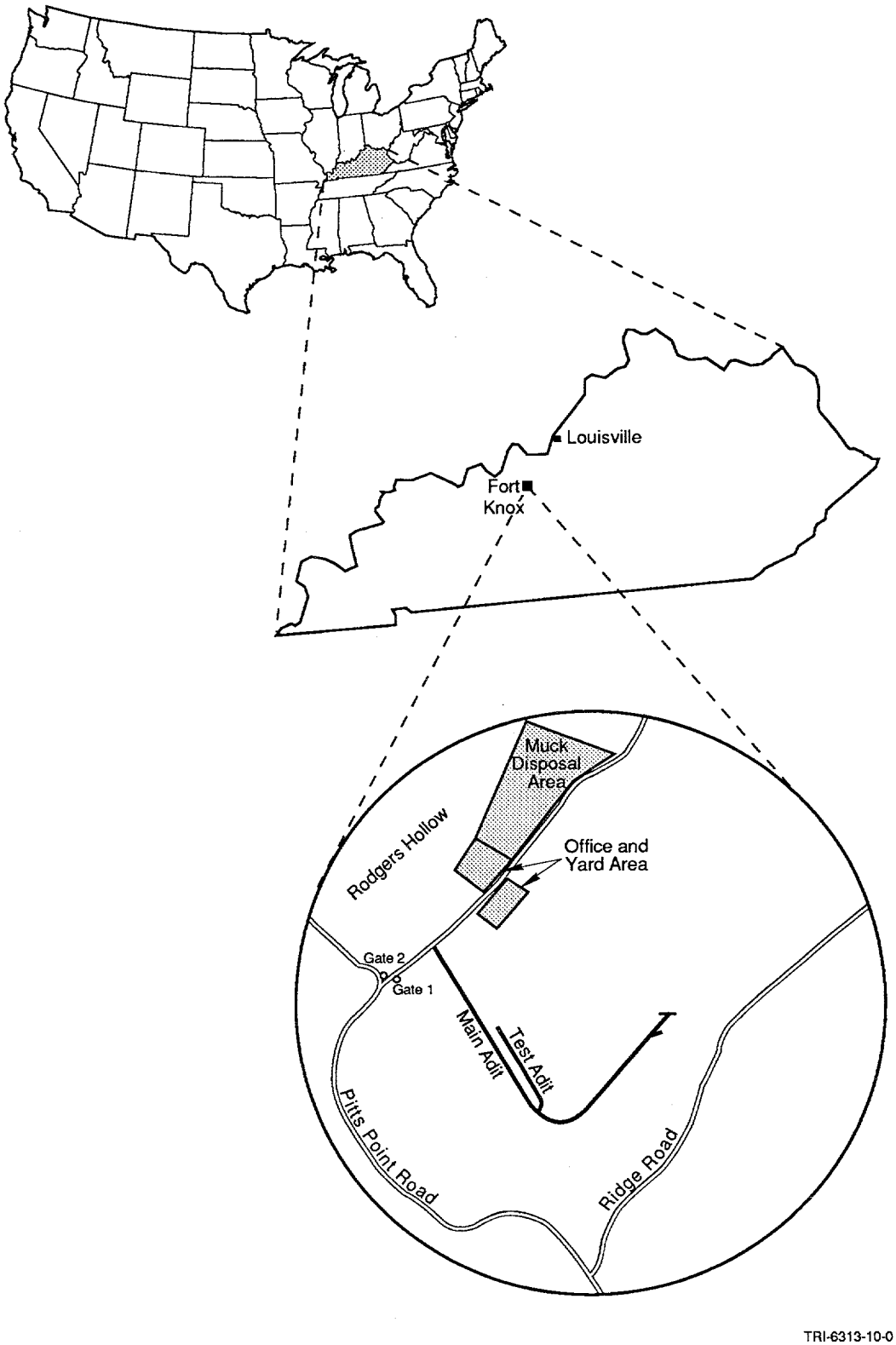

Figure 1-1. Maps showing the location of the DNA-UTP test facilities.

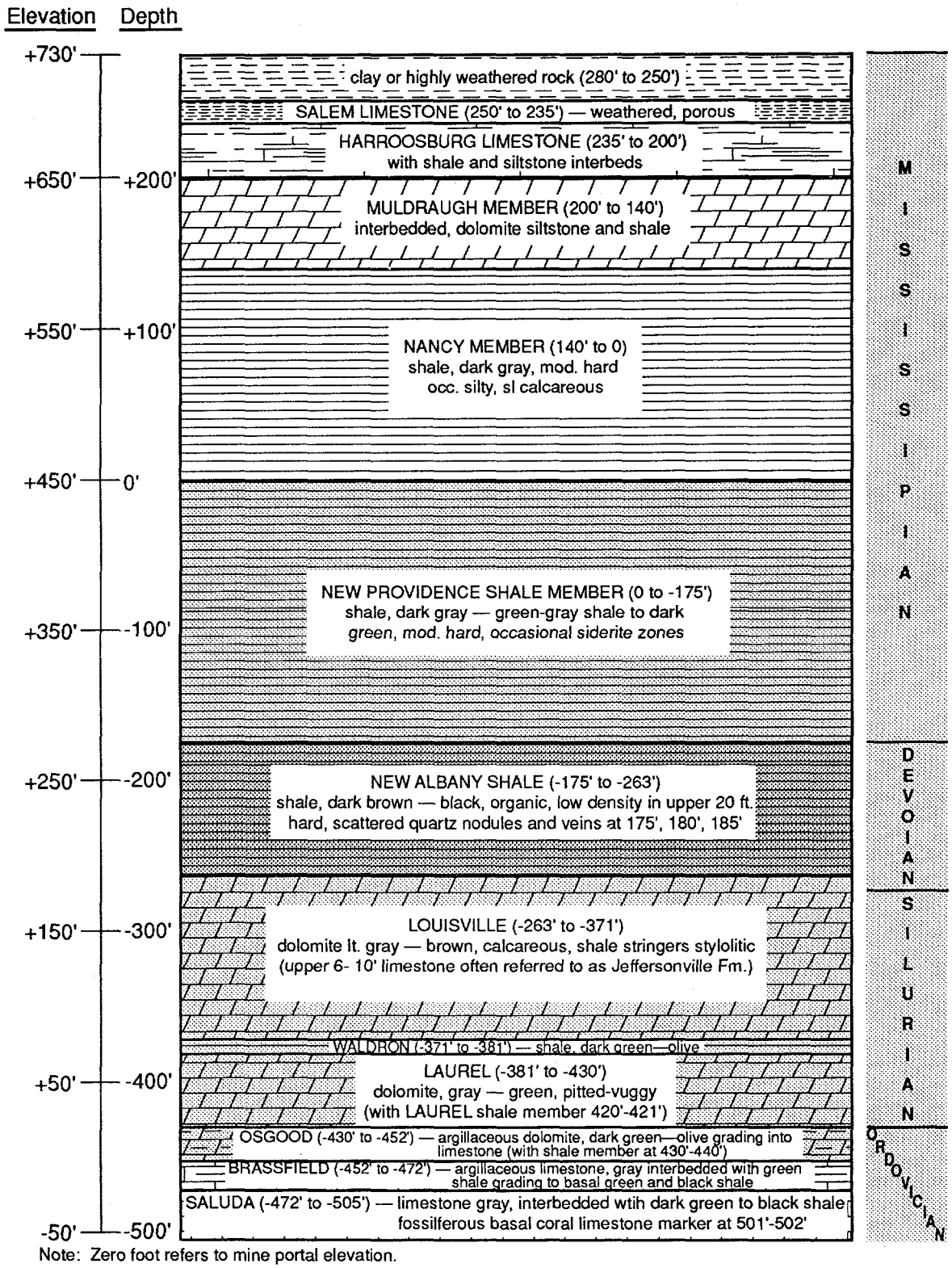

Note: Zero foot refers to mine portal elevation.

TRI-6313-12-0

Figure 1-2. Stratigraphy of the test area showing formation, elevation, and depth above and below the Tunnel Portal.

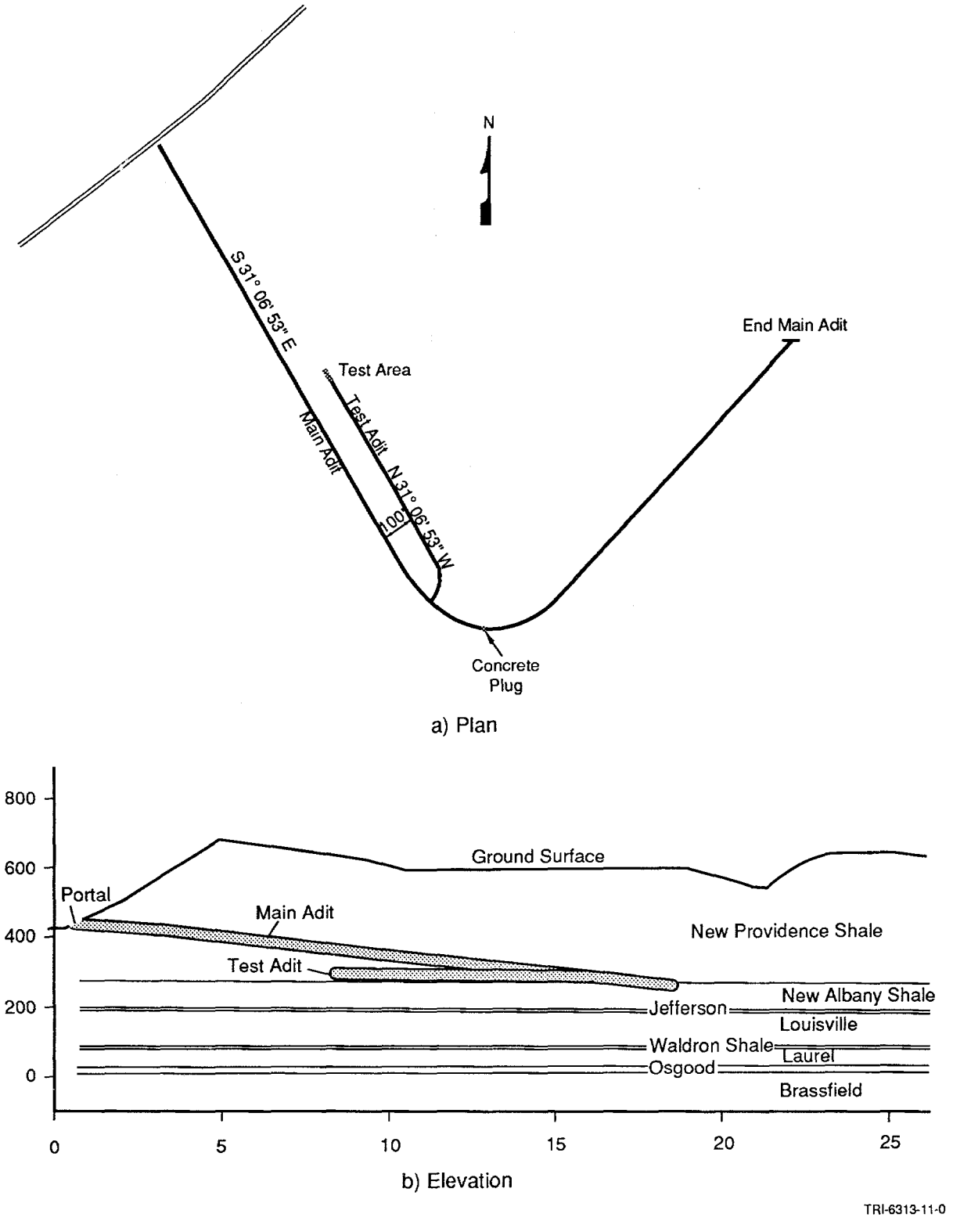

Figure 1-3. Elevation and plan views in the vicinity of the DNA-UTP site.

1.3 Test Configuration (general)

The underground facility consists of an access ramp and a horizontal test drift as shown in Figure 1-3. The drifts were excavated using a mechanical excavator and were covered with a 2-in (5.1-cm) layer of shotcrete immediately after excavation. The in situ stress and rock mass modulus testing was conducted near the end of the test drift. Figure 1-4 shows the general layout and locations of the in situ experiments. The overcoring was performed at about 35 ft (10.7 m) depth from three non-parallel holes, two at right angles, and the third angled upward at about 45°. The ASR tests were conducted on core from a borehole approximately 2 ft (0.6 m) above one of the overcoring boreholes. The flatjack tests were conducted in a vertical and a horizontal slot cut into the rib of the drift about 30 ft (9.1 m) from the drift end.

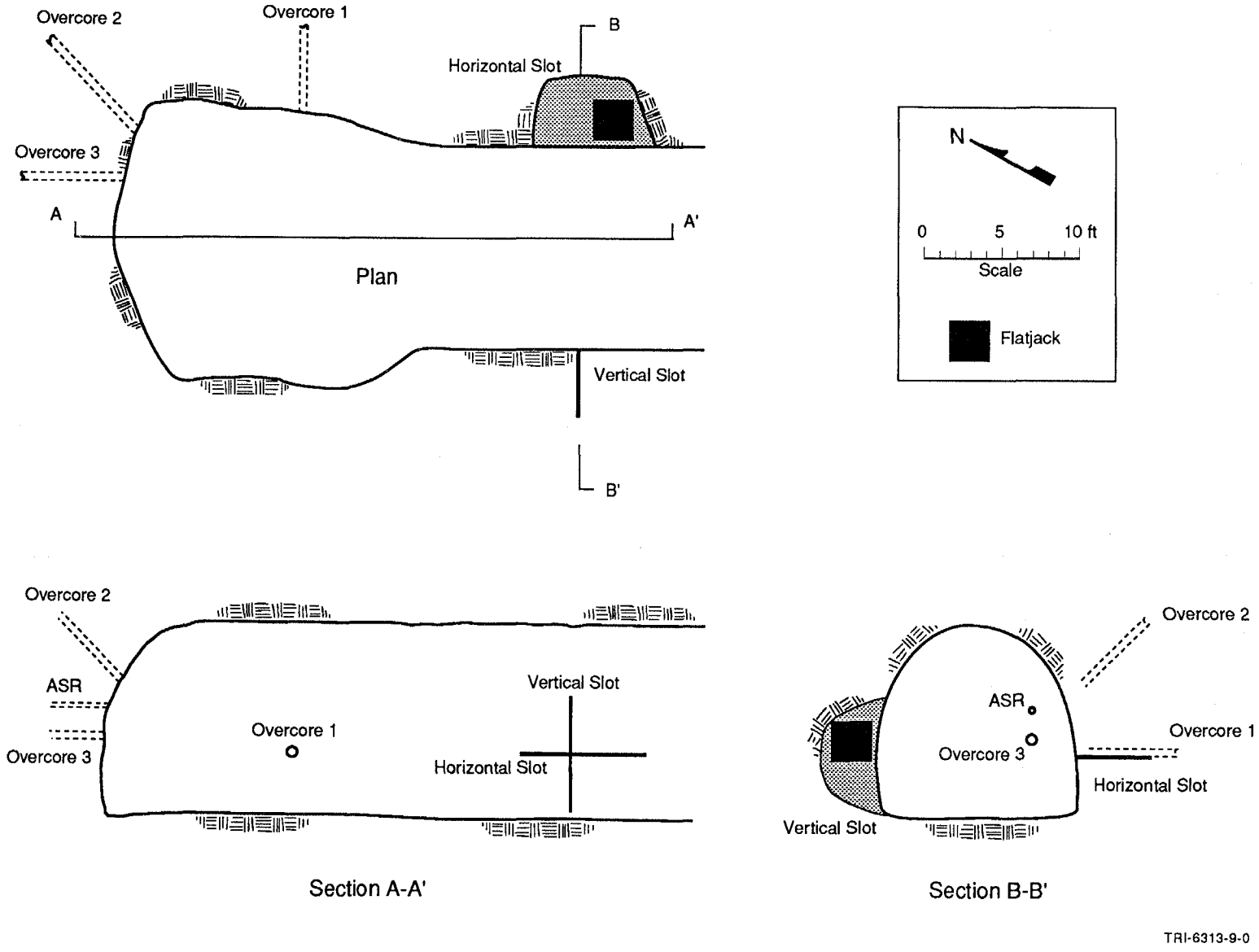

Figure 1-4. Close-up of test adit showing locations of overcore and ASR boreholes and flatjack tests.

2.0 Overcore Stress Tests

2.1 Method of Overcoring Stress Measurement

Overcoring stress measurement techniques using the USBM borehole deformation gage (BDG) were used to determine the in situ stress state. In this technique, the deformations of 1.5-in (3.8-cm) diameter boreholes were measured as stresses were relieved by drilling a larger-diameter 6-in (15.2-cm) coaxial borehole. The deformations were then related to the in situ stresses using the elastic solution for a circular hole in an isotropic material. The overcoring technique typically uses two to three nonparallel boreholes in which multiple measurements are made. Three nonparallel boreholes allow a complete and redundant determination of the three-dimensional stress field from the borehole measurements. In addition, the depth at which the measurements are made must be as removed from the underground openings as possible to minimize stress concentration effects due to proximity to the excavation. For the DNA-UTP testing, three non-parallel boreholes, as shown in Figure 1-4, were used. In each borehole, multiple measurements were made at depths ranging from 30 to 35 ft (9.1 to 10.7 m) from the excavation. In situ stresses determined using the overcoring technique are presented as compression-positive.

The USBM-type borehole deformation gage measures deformation of the hole on three diameters, U1, U2, and U3, located 60° apart as shown in Figure 2-1. Initial readings of the hole diameter are made prior to overcoring when the gage is initially inserted into the hole. A 6-in (15.2-cm) diameter hole is then drilled concentrically over the BDG using a thin-walled coring bit, thereby relieving the in situ stresses on the resulting cylinder of rock (shown in Figure 2-2).

Deformations are continuously measured as the overcore is advanced past the gage. Figure 2-3 presents a typical record of the depth of drilling versus bore deformation. The record shows minor compression of the hole as the overcore bit approaches the gage, then expansion of the hole as the bit passes the gage and relieves the in situ stress. The expansion of the hole gradually reduces and ceases altogether after the bit is several centimeters beyond the gage.

After the run is completed, the overcored cylinder of rock is removed from the hole and tested in a biaxial pressure chamber. Uniform pressure increments are applied to the overcore to determine the elastic modulus. The elastic deformation of the borehole and the elastic modulus from the biaxial tests allow calculation of the biaxial stress relieved by the overcoring.

The overcoring technique employed in these measurements uses only deformations measured normal to the axis of the drill hole. Consequently, analysis of the results yields the secondary principal stresses and their directions in the plane normal to the hole axis. To determine the complete in situ state of stress, borehole deformation measurements are required in the three noncoplanar holes. Data reduction techniques assumed linear elastic isotropic rock.

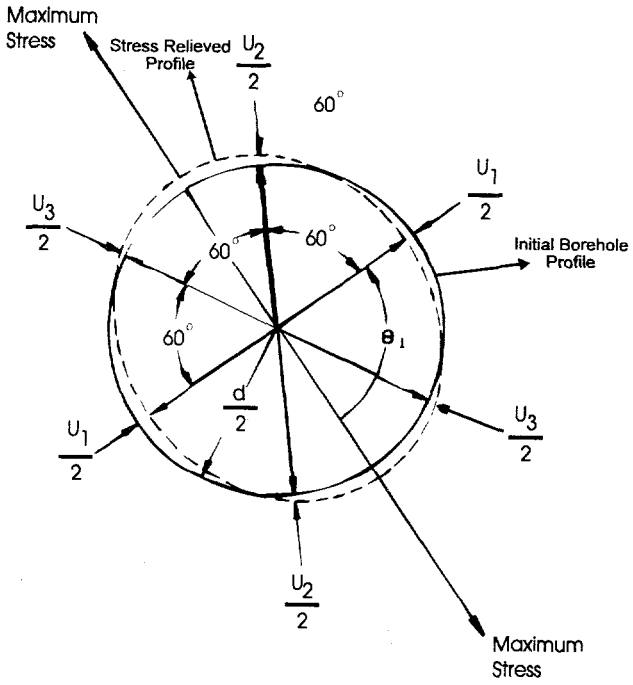

Figure 2-1. Cross section of pilot borehole illustrating the 60° deformation rosette with USBM BDG (Merrill and Peterson, 1961).

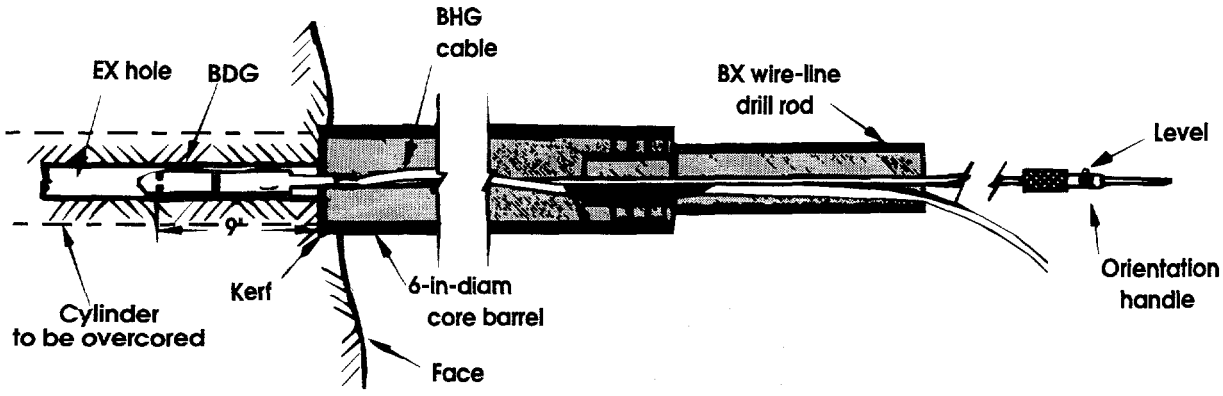

Figure 2-2. Schematic cross section illustrating borehole overcoring equipment (Bickel, 1985).

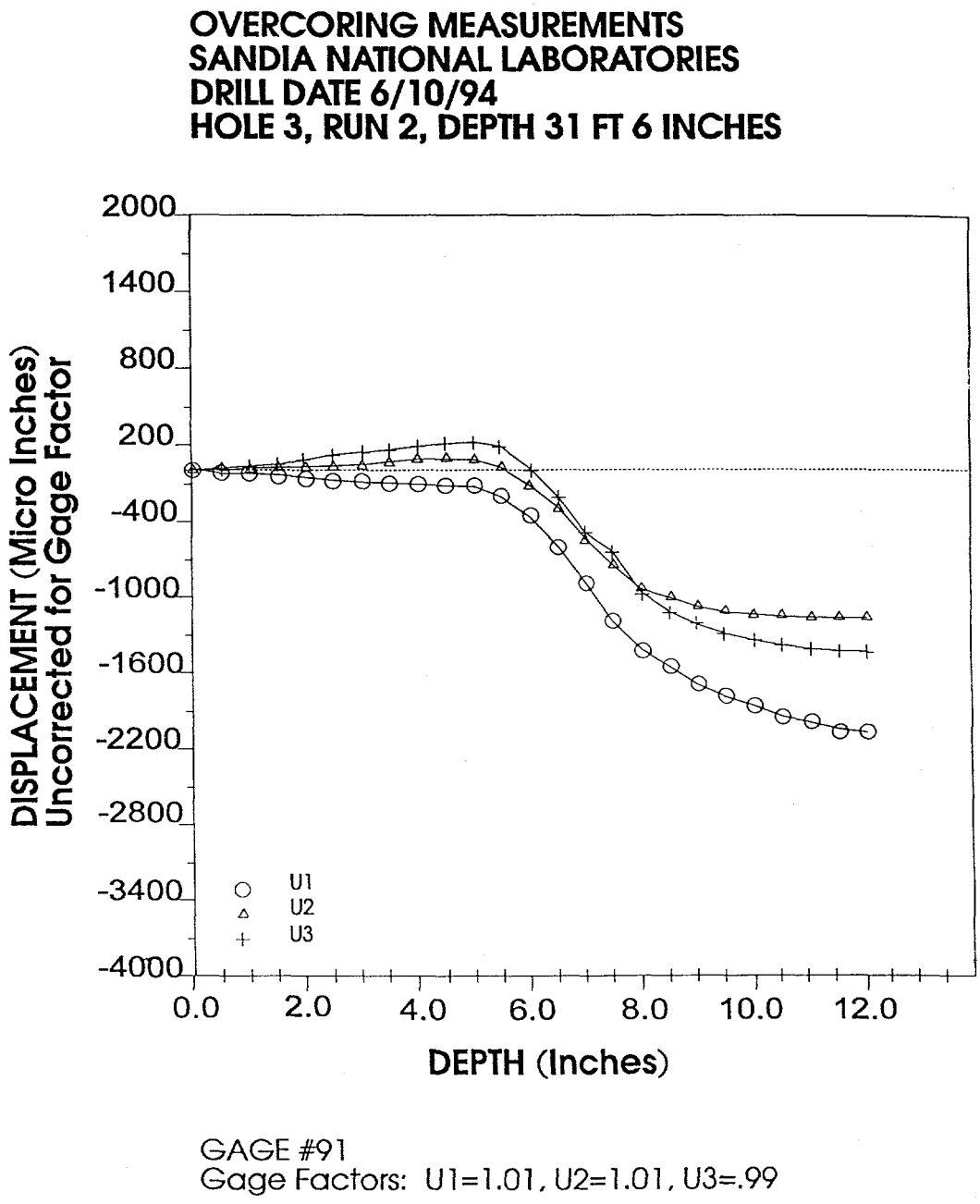

Figure 2-3. **Typical record of overcoring deformations versus drill depth from hole #3 — For DNA-UTP Test Site, Rodgers Hollow, Kentucky.**

2.2 Results of Overcoring Stress Measurements

Overcoring stress measurements were made at four locations in each of the three overcore boreholes shown in Figure 1-4. Table 2-1 lists the depths of measurements in each of the overcoring boreholes. In general, the rock from all boreholes appeared uniform.

Table 2-1. Overcore Borehole Orientations and Measurement Locations

Hole and Orientation	Measurement Depth from Borehole Collar (ft)
#1 N 60 °E Horizontal	30.5 31.5 32.5 33.5
#2 N 15 °E 135° up	30.5 32.0 34.0 35.3
#3 N 31 °W Horizontal	30.5 31.5 32.5 33.5

The three-dimensional in situ stress state was calculated using the method described by Panek (1965). In this approach, a computer program (STREL2) developed by the USBM and based on Panek (1965) was used to perform a least-squares analysis of all sets of overcoring displacements from the three holes. The method of analysis of the overcore results to the three-dimensional stress assumes that the stress field is uniform at all locations where the borehole measurements were made. In reality, the measurements are far apart (the three holes diverge) with different depths of overburden above them. The results are listed in Table 2-2 as both the principal stresses and the normal stress components aligned with North, East, and vertical-horizontal directions. The results indicate that the principal stresses are rotated out of the vertical-horizontal planes.

Table 2-2. Three-Dimensional In Situ Stress—Isotropic Assumptions

	Principal Stresses			Normal Stresses		
	σ_1	σ_2	σ_3	East	North	Vertical
Stress (psi)	373	281	176	256	234	340
Std Dev (psi)	29	26	21	26	36	20
Azimuth (deg)	63	40	137	90°	0	NA
Inclination (deg)*	146	58	79	90°	90°	180°

* 0° = vertical down; 180° = vertical up

2.2.1 Isotropic Analysis of Stress and Modulus

Results of individual displacement measurements were analyzed to determine the elastic diametral displacements, the biaxial testing displacements, and the overcore elastic modulus. The secondary principal stresses (P and Q) representing the stresses in the plane perpendicular to the borehole were then calculated using elastic equations. Table 2-3 lists the results and presents averages and standard deviations of the stress magnitudes calculated using the least-squares fit described in Duvall and Aggson (1980). U_1 represents the secondary principal strain measured during the testing. The individual measurements are generally consistent with the maximum stress oriented near vertical.

Four overcoring stress measurements were completed in hole #1 between the depths of 30.5 ft (9.3 m) and 33.5 ft (10.2 m). Biaxial compression testing of the overcores revealed that the rock was transversely isotropic with the horizontal elastic modulus as much as twice that of the vertical elastic modulus. In an attempt to better characterize the transverse isotropy, the biaxial compression tests were conducted at four different gage orientations for two overcores in hole #2 and all overcores in hole #3. The resulting characterization of the anisotropy is summarized in Table 2-4 for the two horizontal holes. Elliptical fits of the variation of elastic modulus with orientation were performed using techniques suggested by Bickel (1993). The results indicate that the maximum elastic modulus was near horizontal and the ratio of maximum to minimum elastic modulus ranged from 1.41 to 4.68, averaging 2.79 and 1.82 for the two holes, respectively.

Calculations reported by Becker and Hooker (1967) suggest that for the range of elastic moduli ratio and the magnitude of stress difference indicated by these measurements, the impact of anisotropy is low. Data analysis was therefore performed using only isotropic assumptions.

Table 2-3. Secondary Principal Stresses from Individual Overcore Measurements and Least-Square Fits of All Data in Each Hole—Isotropic Assumptions

			Secondary Principal Stresses				
Hole and	Run		P	Q	Direction of P Measured	Direction	E
Orientation	#	Depth (ft)	(psi)	(psi)	CCW from U1 (°)	of U1	(10^6 psi)
	1	30.5	392.5	217.3	-13.8	vertical	0.61
#1	2	31.5	206.7	107.8	-4.3	vertical	0.35
N60E	3	32.5	298.9	150.2	-4.2	vertical	0.58
Horizontal	4	33.5	388.3	155.5	-21	vertical	0.58
Least-Square							
Average	—	—	294	158	-10.8	—	—
St Dev	—	—	30	30	7.4	—	—
	1	30.5	190.3	150.5	16.3	NE up	0.58
#2	2	32.0	215	150.8	-17.7	NE up	
N15E	3	*Run not successful*					
135° Up*	4	34.0	236.7	152	19.6	NE up	
	5	35.3	259.1	201.9	-5.7	NE up	
Least-Square							
Average	—	—	230	179	3.2	—	0.62
St Dev	—	—	13	13	8.8	—	0.67
	1	30.5	422.6	315.3	-1.7	vertical	0.83
#3	2	31.5	472.4	321.8	-7.4	vertical	0.77
N31W	3	32.5	413.4	288.3	-12.8	vertical	0.71
Horizontal	4*	33.5	454.3	279.3	-8.2	vertical	0.89
Least-Square							
Average	—	—	459	333	-8.1	—	—
St Dev	—	—	13	13	3.6	—	—

*45° from horizontal, U1 aligned with the vertical plane
CCW = counter clockwise

Table 2-4. Anisotropic Elastic Modulus and Orientation for the Overcore Cylinders

		Strain Ellipse Axes					
Hole and Orientation	**Run #**	**A (micro in)**	**B (micro in)**	**Theta* (CCW Positive)**	**E1 (10^6 psi)**	**E2 (10^6 psi)**	**E2/E1**
	1	3396	15910	15.89	0.2436	1.1410	4.68
#1	2	4769	10690	4.64	0.2418	0.5418	2.24
N60E	3	4290	6910	-16.4	0.4674	0.7528	1.61
Horizontal	4	3530	9218	17.48	0.3504	0.9149	2.61
	Average	3996	10682	5	0.33	0.84	2.79
	St Dev	648	3817	16	0.11	0.25	1.33
	1	2145	1106	29	0.75	1.46	1.95
#3	2	2598	1292	12	0.62	1.25	2.02
N31W	3	2193	1551	5	0.74	1.04	1.41
Horizontal	4	2377	1250	2	0.68	1.29	1.90
	Average	2328	1300	12	0.70	1.26	1.82
	St Dev	206	185	12	0.06	0.17	0.28

CCW = counter clockwise
* Angle from vertical direction to direction of minimum elastic modulus in degrees

2.2.2 Miscellaneous Observations—Creep

Hysteresis was observed during testing of the cores in the biaxial chamber, suggesting that the rock was exhibiting some yielding or time-dependent behavior assumed to be due to the high loads on the contact buttons of the BDG. To confirm this, a simple creep test was performed. After overcoring, the BDG was left in the hole for approximately three hours. Data from the BDG were recorded periodically throughout the test. The results of this test are shown in Figure 2-4 and clearly indicate the presence of time-dependent creep behavior. Because the elastic deformation associated with the overcoring occurs over a very short time, no attempt to correct for the creep relaxation was performed.

2.3 Discussion of Overcoring Results

The results of the overcoring stress measurements indicate good agreement with estimates of the vertical stress due to overburden depths. The depth of cover for the test location is approximately 350 ft (107 m). The vertical stress calculated from overburden using 160 lb/ft^3 (2563 kg/m^3) unit wt. indicates a stress of about 387 psi (2.67 MPa). Comparing this calculated stress to the measured vertical stresses of 340 psi (2.34 MPa) would indicate an error of 12% based on the geophysical log from hole CB-4, which indicates a density of 160 lbs/cubic ft (2563 kg/m^3).

The intermediate and minimum principal stresses correspond well to the topography of the area and other regional measurements of stress. The general trends are similar with both maximum and intermediate principal stress oriented in the N-E direction. Other regional measurements reported by Bickel (1993) and Lindner and Halpern (1978) indicate that the maximum horizontal stress trends approximately N45E, similar to these results. The orientations are also similar to the trends of the local topographic ridges as shown in Figure 2-5. The ridge overlying the test adit is oriented at azimuth 50 60° (N50 60°E), roughly parallel to the direction of the maximum and intermediate principal stresses and perpendicular to the minimum principal stress.

The rotation of the stress field from the vertical-horizontal planes may be due to the proximity to surface and the large topographic relief indicated in the cross section in Figure 1-3.

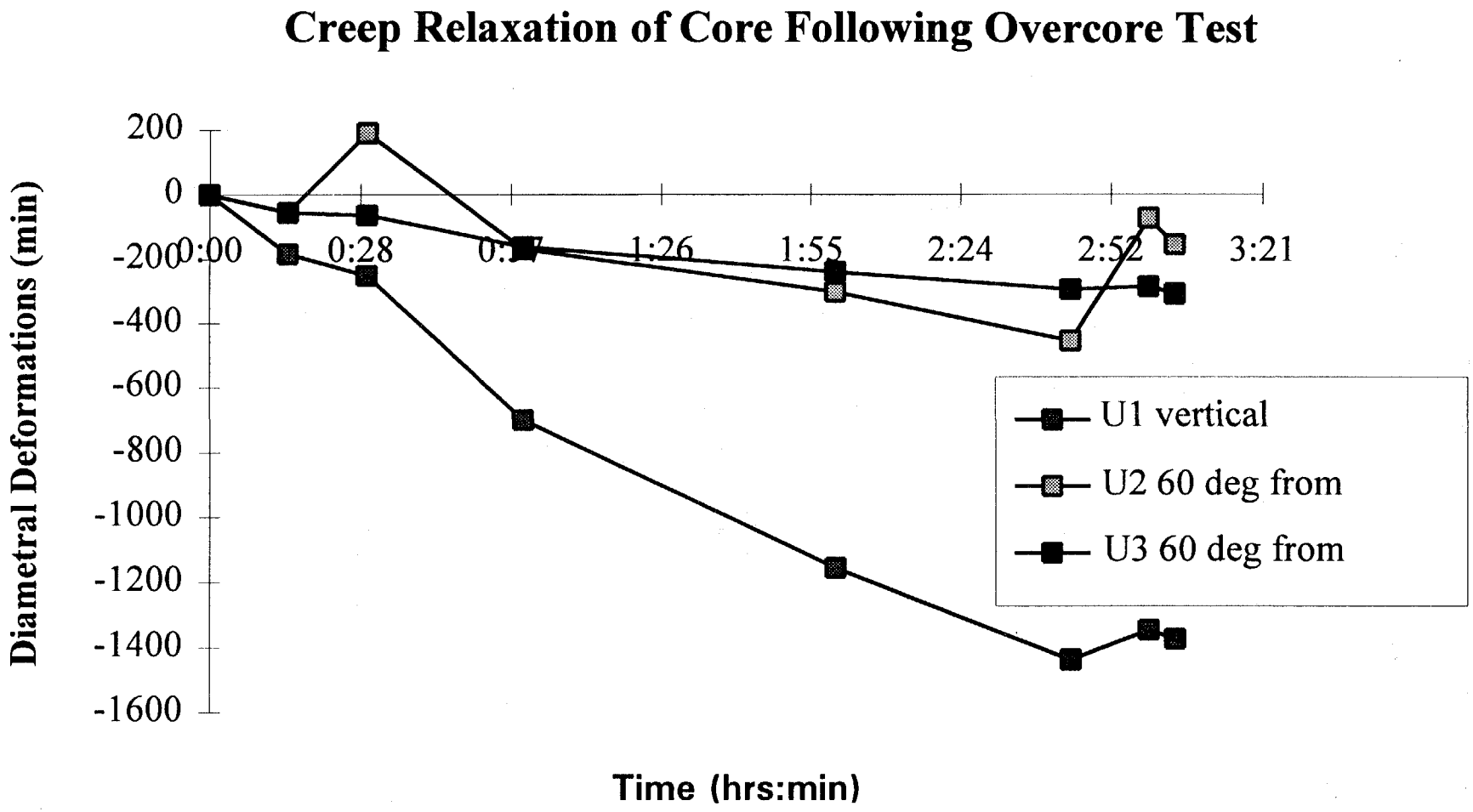

Figure 2-4. Creep deformation measured with BDG.

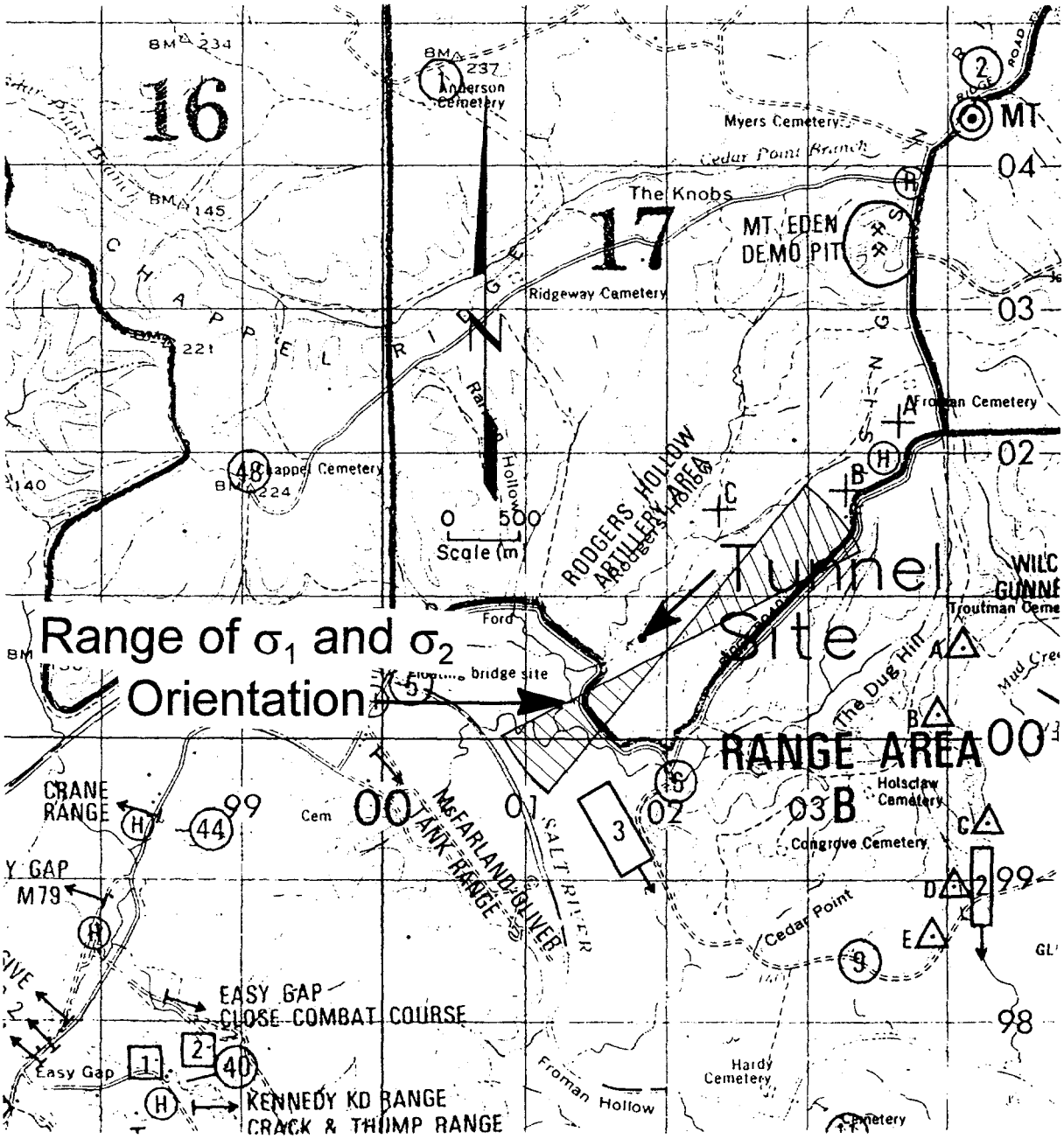

Figure 2-5. **Comparison of surface topography to orientation of intermediate and minimum principal stress.**

3.0 ASR Tests

The ASR technique is a core-based, stress-measuring technique and is described in detail in Teufel (1982). Briefly, the ASR technique consists of mounting thermally stable clip-on displacement gages on a piece of sealed, oriented core and recording the time-dependent relaxation of the core. ASR has been demonstrated by the US DOE at the Multiwell Experiment in Colorado (Warpinski and Teufel, 1989a) and is used to predict stress magnitudes and orientations for the oil and gas industries. The advantage of this technique over other core-based techniques is that measurements can be made from deep boreholes where immediate access to core is not available. For the DNA-UTP testing, ASR testing was conducted on core from one borehole drilled from the end of the test drift as shown in Figure 1-4.

3.1 ASR Test Layout/Theory

Determination of the orientation of the stress field is calculated from the principal strain orientations measured during relaxation of the core (Teufel, 1982; Teufel and Warpinski, 1984; Smith et al., 1986; Warpinski and Teufel, 1989b). Determination of the stress magnitudes is more complicated and relies on one of two models. Blanton (1983) and Warpinski and Teufel (1989b) have developed different types of viscoelastic models to explain the strain-relaxation behavior. Blanton's solution is the easier of the two to apply and yields the direct calculation of the principal stresses from the principal strains, pore pressure, and poroelastic constant, whereas the Warpinski and Teufel solution requires a least-squares fit on an entire set of strain-time data to a complex strain relaxation function, which includes dilational and distortional creep compliance. The principal stress magnitudes and orientations can theoretically be determined using the ASR technique for any rock that exhibits viscoelastic behavior.

The ASR testing was conducted on core from two depths in a single borehole oriented parallel to the axis of the test drift (see Figure 1-4). The ASR borehole was drilled approximately 1 m above one of the overcoring boreholes. Core was retrieved from depths of 13 and 30 ft (3.96 and 9.14 m) for both ASR and laboratory materials property testing. The laboratory testing results are presented in Appendix A.

After the core was removed from the borehole, it was immediately transported to the surface and then to the location where the measuring apparatus was set up. The trip time was about one hour, and another hour was required to instrument the core. To slow down dehydration of the core, each piece was wrapped in aluminum foil, and the edges of the foil were sealed with a silicone sealant (RTV).

The apparatus for measuring the strains consisted of sensitive strain sensors interfaced to a data acquisition system running on a personal computer (PC). Each strain sensor consisted of a

gage head linear variable differential transformer (LVDT) mounted in an Invar ring of a design developed by Holcomb and McNamee (1986). The ring encircled the sample and was held in place by a tapered screw on one side of the diameter to be monitored and a leaf spring contact on the other side. The LVDT was screwed into the ring in such a way that its head rested against the back of the leaf spring. This arrangement provides a stable contact between the LVDT and the sample without constraining the sample or exerting undue pressure. Because Invar has an almost zero coefficient of thermal expansion near 20°C, fluctuations in room temperature would not produce spurious strains due to changes in the dimensions of the gages. Thermal expansion coefficients for rocks are usually small enough that any temperature changes experienced during testing produce insignificant strains in the rock.

The LVDT signals were converted to DC voltages by a Schaevitz interface board. Signals were then recorded using DATAVG, a general-purpose data acquisition system used in the geomechanics laboratory (Hardy, 1993).

3.2 ASR Results

Core for the first attempt was obtained at a depth of about 13 ft (3.96 m), cored horizontal and parallel to the axis of the drift. About 2 hours passed between the time the core was cut and data recording began on two pieces of core. For the second run, core was obtained at a depth of 30 ft (9.14 m) from the same hole. Again, two adjacent pieces of core were instrumented.

To determine the complete strain tensor requires a minimum of six strain measurements on three non-coplanar planes, unless assumptions are made about isotropy and orientation of the principal stresses. For the first coring run that was instrumented, only four gages were installed on each piece of core. Three gages were installed to measure radial strains at 0, 45, and 90 degrees to vertical. The fourth gage was installed to measure strain along the axis of the core. On the second coring run, a full complement of six gages was installed on each of two core pieces. Four gages were installed in the same orientation as for the first coring run, while the fifth and sixth gages were placed so as to measure the strain at a diagonal to the core axis. The fifth gage measured along a line at 45 degrees from the vertical in the plane containing the vertical direction and the axis of the core. A sixth gage measured the strains at 45 degrees from the core axis in the horizontal plane.

Temperature fluctuations can cause problems due to expansion and contraction of the core. Figure 3-1 plots the temperature in the room during the first test, showing a range of about 2°C over the course of the test. To compensate for thermal effects, a fit was done to the later portion of the test when strains seemed to be linear with temperature. In Figure 3-2, strains (expansion is positive) observed from one of the ring gages are plotted against room temperature. For most of the test, there is little relationship, as would be expected if the strains were not simply the result of thermal expansion. At the end of the test, there did appear to be a linear

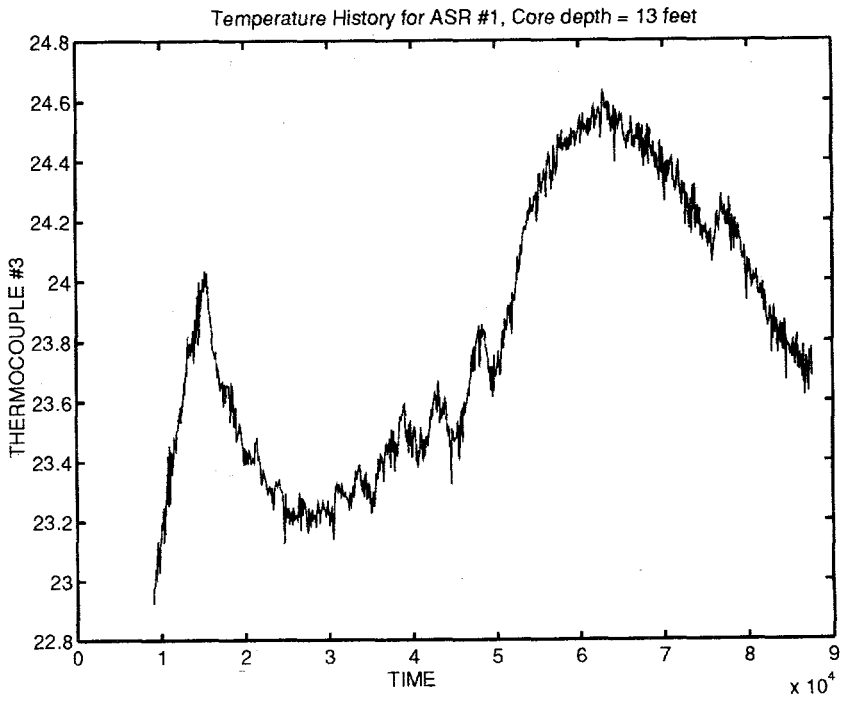

Figure 3-1. **Thermal history for the test room during the first ASR test on core from a depth of about 13 ft (3.96 m).**

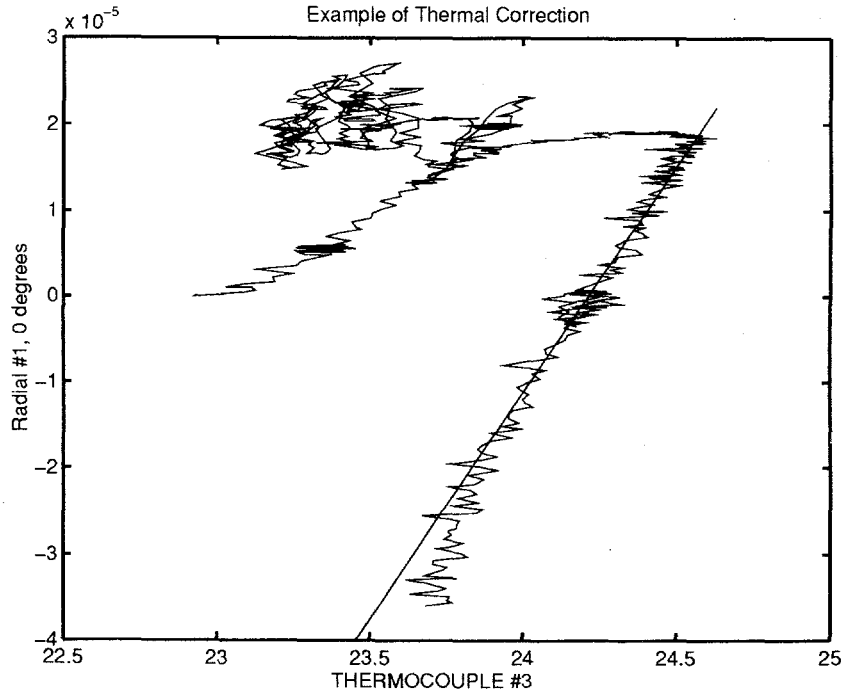

Figure 3-2. **An example of trying to remove thermal effects by a linear fit to the strain versus temperature data at the end of the test, when it is assumed that the ASR rate has diminished to zero.**

relationship between temperature and strain, and a least squares fit was done to this portion of the data. The straight line on Figure 3-2 is the strain predicted by a linear fit between temperature and strain.

Similar fits were done for each of the gages and then used to predict the strains due to temperature fluctuations earlier in the test. As a byproduct, the fits give the thermal expansion coefficient of the shale. It is surprisingly large and anisotropic (see Table 3-1).

After correction, little or no expansion was observed in the shale, as Figures 3-3 and 3-4 show. Instead the core contracted in all directions and fairly uniformly. Strains in the horizontal

Table 3-1. Thermal Expansion Coefficients α for the New Providence Shale as Inferred from a Linear Fit Between the Test Temperature and Strains During the Latter Portion of the ASR Tests.

Angle from vertical (degrees)	α ($\times 10^{-6}\ ^{\circ}C^{-1}$)	depth (ft)
Results for Run #1		
0	52	13
45	22	13
90	21	13
0	34	13
0	45	13
45	51	13
90	15	13
0	6*	13
Results for Run #2		
0	97	30
45	45	30
90	30	30
0	29	30
45	58	30
0	30	30
0	73	30
45	53	30
45	57	30
90	26	30
90	23	30

* Strain data appeared to be of low quality

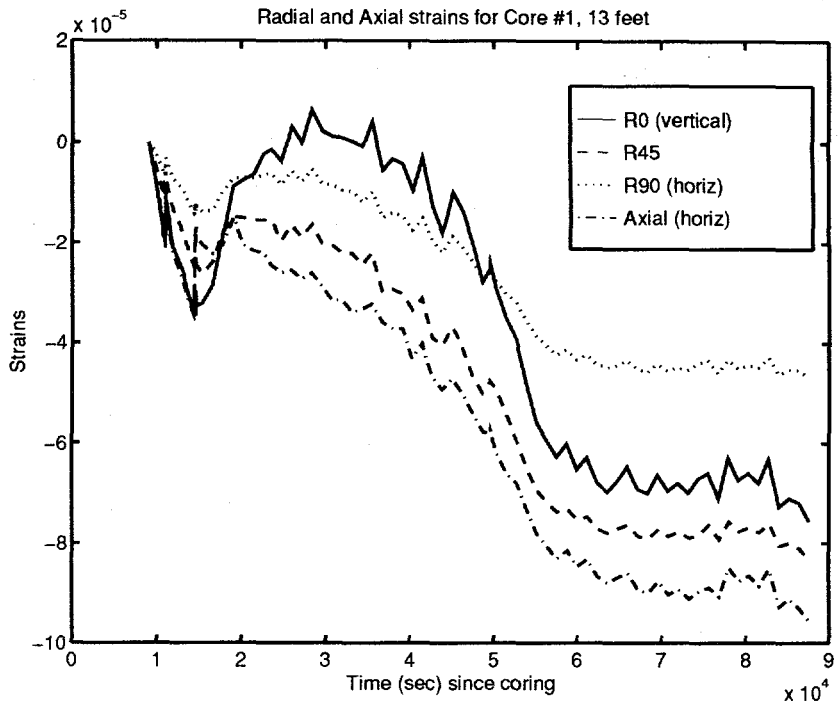

Figure 3-3. **Temperature-corrected radial and axial strains for core #1 from hole #3, at a depth of about 13 ft (3.96 m). The origin time is the time when the core was cut.**

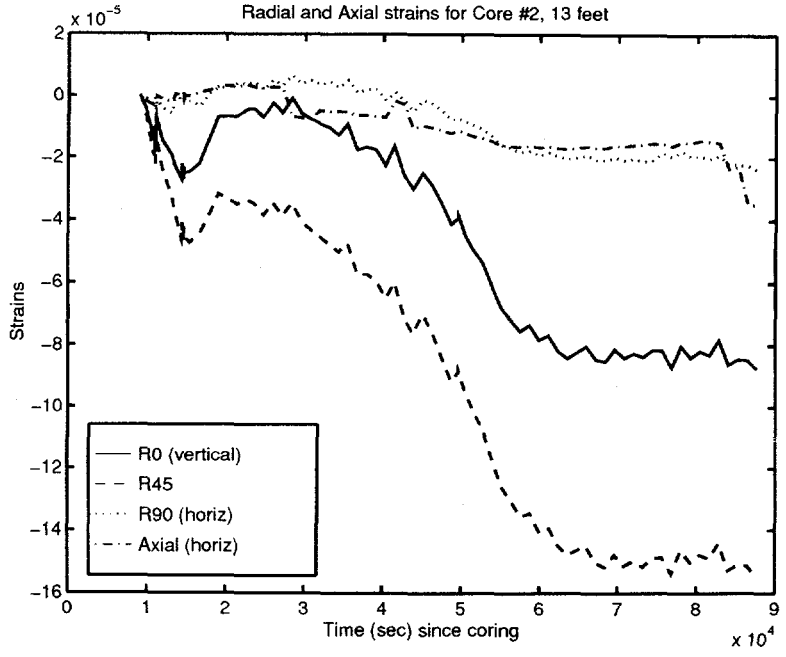

Figure 3-4. **Temperature-corrected radial and axial strains for core #2 from hole #3, at a depth of about 13 ft (3.96 m). The origin time is the time when the core was cut.**

plane seemed to be less, both for this run and the second run, which may be related to the anisotropy of the shale. Equilibrium appears to be reached at the end of the test, but that may be an illusion due to the way the temperature compensation was done. Because the last part of the test was fitted, only the non-linear strains would be observed after the linear fit was subtracted.

A second core was cut at a depth of 30 ft (9.14 m) in the same hole on the following day (Figures 3-6 through 3-9). After thermal correction, there appears to be a slight expansion of the core, abruptly followed by shrinkage. The abruptness and simultaneity of the reversal make it likely that the expansion is an artifact. As can be seen from Figure 3-5, the temperature underwent a sharp change from cooling to warming at just the time that the sense of the strain reversed. Probably, the thermal correction that was applied was slightly off and did not perfectly remove the effects of the changing temperature. At any rate, the strains are small—only a few tens of microstrains.

3.3 ASR Discussion

No convincing evidence was found for anelastic strain recovery in shale for measurements that began about 2 hours after the core was cut. Instead, the shale contracted in all directions. The contraction is surprising because it does not seem that it could be due to dehydration. The core was well sealed with aluminum foil and a silicone sealant on the seams. Another possibility is that the contractions are the result of pore fluids trapped in the low-permeability shale, slowly bleeding off over several hours. Of course, in the absence of any strain recovery, no information on stress orientation or magnitude could be obtained.

On a more positive note, the results from the overcoring tests, discussed elsewhere, indicate that shale may exhibit ASR, but on a much shorter time scale than for the sandstones customarily examined for ASR. As an experiment, after overcoring the borehole gage the core was not broken free; instead, the strains were monitored for several hours. What was observed was that the core containing the borehole gage, continued to expand. The strains were a significant percentage of the strains observed during the nominally elastic stress relief of the coring operation. If this result is true, it has implications for any geophysical technique involving cutting openings in shale. Flatjack tests (and overcoring tests in particular) could give erroneous results if a significant amount of time-dependent strain occurs.

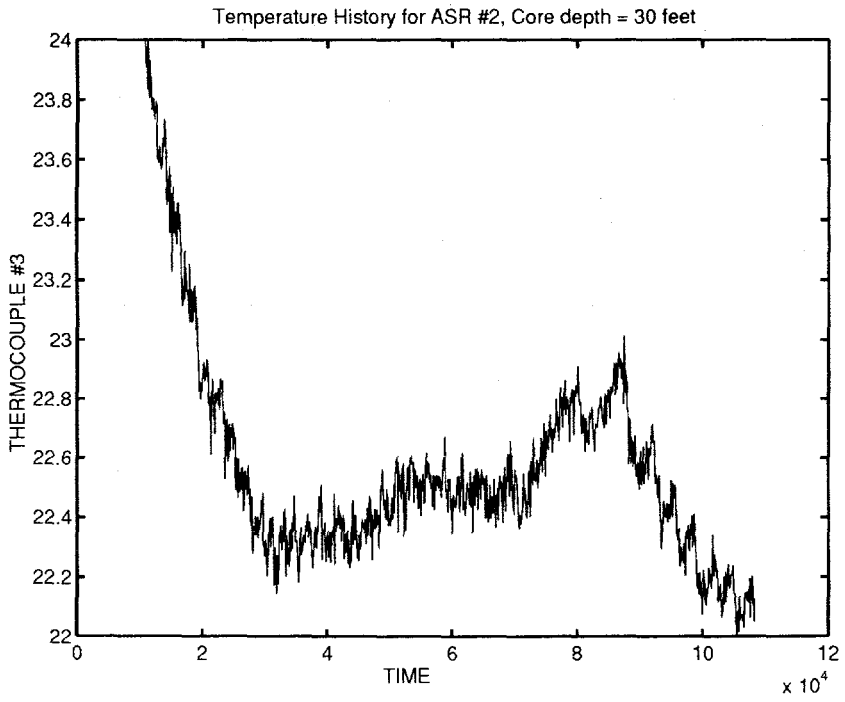

Figure 3-5. **Thermal history for the test room during the second ASR test on core from a depth of about 30 ft (9.14 m) in hole 3.**

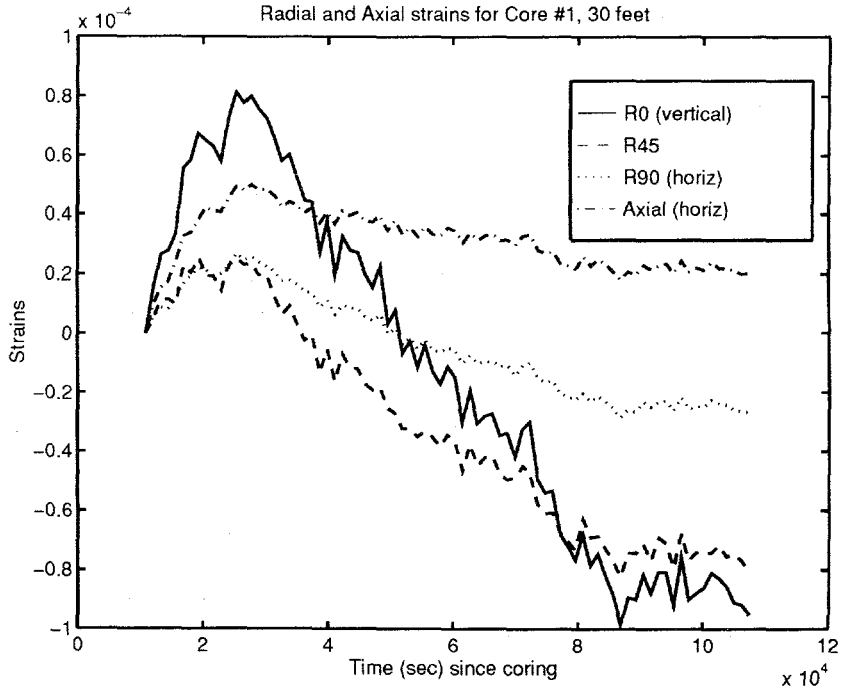

Figure 3-6. **Temperature-corrected radial and axial strains for core #1 from hole #3, at a depth of about 30 ft (9.14 m). The origin time is the time when the core was cut.**

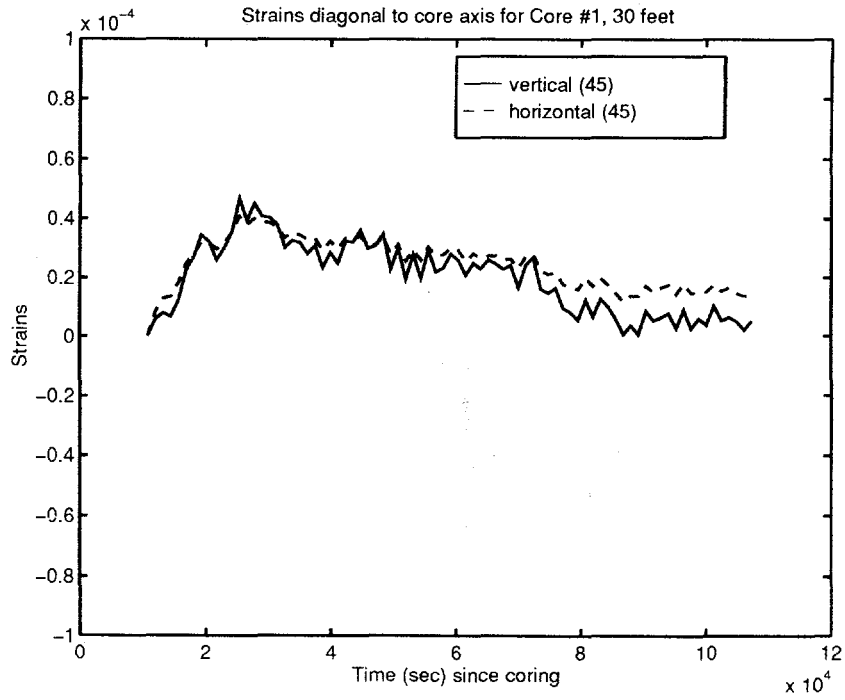

Figure 3-7. **Temperature-corrected strains along axes diagonal to the core axis, for core #1 from hole #3, at a depth of about 30 ft (9.14 m). The origin time is the time when the core was cut.**

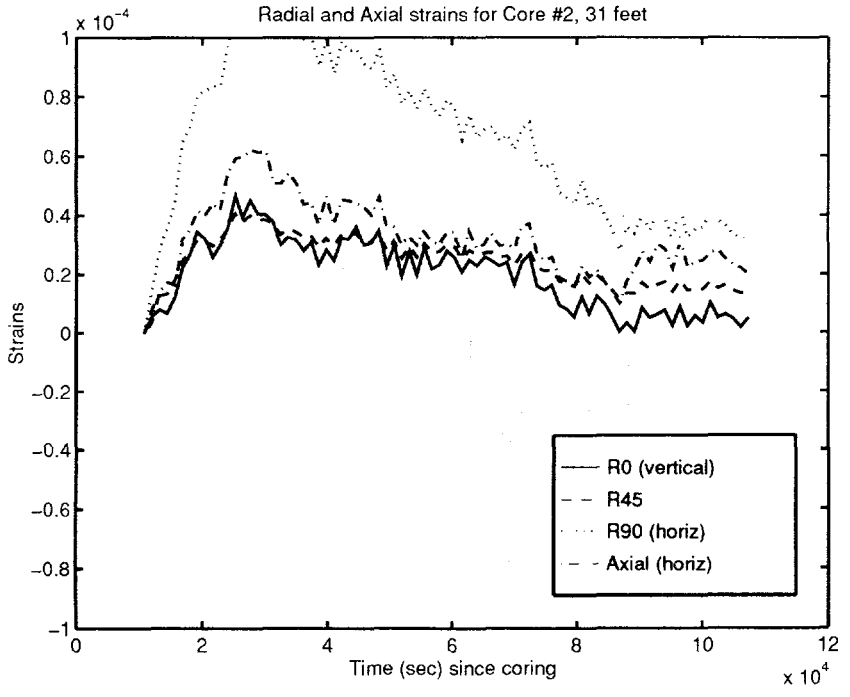

Figure 3-8. **Temperature-corrected radial and axial strains for core #2 from hole #3, at a depth of about 31 ft (9.45 m). The origin time is the time when the core was cut.**

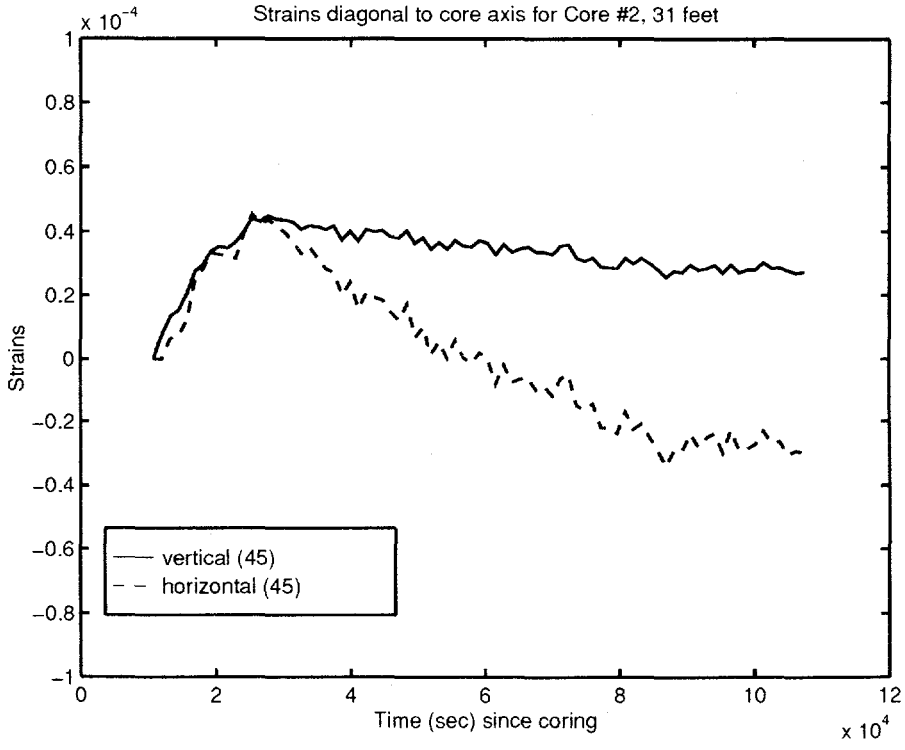

Figure 3-9. **Temperature-corrected strains along axes diagonal to the core axis, for core #2 from hole #3, at a depth of about 31 ft (9.45 m). The origin time is the time when the core was cut.**

4.0 Flatjack Tests

The pressurized slot flatjack test technique used to measure the stress near an underground opening is based on early developments by Alexander (1960), Panek (1961), Kruse (1963), Panek and Stock (1964), Rocha (1966), Rocha and da Silva (1970), and Loureiro-Pinto (1986). Over the past several years, SNL has further developed this concept as a cost-effective means of measuring rock mass properties (Zimmerman et al., 1992; Hansen et al., 1990). SNL has enhanced the original technique by developing, constructing, and demonstrating large-surface-area, high-pressure flatjacks capable of energizing large volumes of the surrounding rock, allowing a realistic estimation of the rock mass material properties surrounding underground openings. The technique essentially consists of placing stationary pins on either side of the slot to be cut, making an initial distance measurement across the slot, cutting the slot, making a second displacement measurement across the slot, and finally pressurizing the slot until the cross slot measurement corresponds with the pre-cutting dimension. The flatjack pressure necessary to restore the cross-slot dimensions is called the cancellation pressure and corresponds in principle to the stress acting normal to the plane of the slot at that location. Measurement of the rock mass deformability is usually accomplished by a series of increasing load-unload cycles of the flatjack accompanied with rock mass deformation measurements. The pressure/deformation history is then evaluated to determine rock mass deformation modulus.

4.1 Test Theory/Layout

4.1.1 Theoretical Background

The history of measurement of stress using pressurized flatjacks in thin slots is described in Jaeger and Cook (1979). In its simplest form, the pressure required on the entire slot surface to "cancel" the closure caused by slot cutting should be equal to the original stress normal to the slot.

The theory behind the measurement of stress using flatjacks was initially developed by Tincelin (1951) and equations developed by Alexander (1960). Alexander used elasticity theory to describe the displacements of a pressurized slot. Assumptions for this analysis are 1) the slot can be considered a flat ellipse in plane stress, and 2) the slot is unaffected by shear stress parallel to it (the slot is located in a local principal stress plane). The test essentially involves 1) establishing measurement pins, 2) measuring initial distance between pins (y), 3) cutting the slot, 4) measuring pin displacement due to slot closure (dv), 5) pressurizing the flatjack to "cancel" pin displacement (p_c), and optionally, 6) conducting load unload cycles at successively higher pressures to evaluate rock mass deformability. In reality, the flatjack does not occupy the entire slot, and during pressurization the original flatjack dimension is reduced. Therefore, Jaeger and Cook (1979) recommend that a correction factor be used to approximate the actual loaded

area during the flatjack pressurization. This correction factor is simply the ratio of flatjack area divided by the slot area.

The "measured" stress represents the stress normal to the slot in the region surrounding the underground opening. These measured stresses therefore, do not represent the far-field principal stresses, but rather represent local stresses acting around the tunnel at the location of the flatjack tests. The slot normal stress is simply the product of the measured flatjack pressure and the correction factor. Loureiro-Pinto (1986) recommends that tests should preferably be run in several orientations (tests in nonparallel slots) to allow for the study of rock mass anisotropy. Typically, slots are cut vertically and horizontally in the ribs of underground openings. The far-field stress acting on the plane perpendicular to the drift at the slot location can be estimated from the measured slot normal stresses by performing a reverse stress concentration analysis using numerical stress analyses. Simulation of slot deformation was performed using JAC (Biffle, 1984) to assist in determining the area of influence of the flatjack. These simulations used rock material properties from the overcoring testing.

The evaluation of rock mass deformability from in situ flatjack testing is complex. Typically, analytic/empirical methods (e.g., Zimmerman et al., 1992; Loureiro-Pinto, 1986) are used to determine deformation modulus from in situ measurements. Alternatively, elastic analyses, non-linear continuum analyses, or discrete-block analyses (e.g., Chen, 1991; Jung, 1991) using finite-element or discrete-element methods can be used to evaluate rock mass properties using flatjack pressure displacement histories. The analyses described for the DNA-UTP testing has focused on analytical/empirical methods, although finite-element techniques have also been used to gain insight into the rock mass response. Modulus of deformation can theoretically be determined from load or unloading histories.

Various analytical solutions have been proposed for determination of the deformation modulus using pressurized flatjacks. These analytical solutions generally assume that the slot is regarded as a flat ellipse in plane stress and that displacement of the surface of the slot is affected only by the normal stress across it. Alexander (1960) proposed that both modulus of deformation and Poisson's ratio could be determined from the slot closure due to cutting the slot if measurements across two or more distances were made. The Alexander (1960) test geometry included a thin square flatjack typically grouted into a thin square slot of slightly larger dimensions. In this case, the loaded area is of the same approximate size as the slot. The analyses also assume that the flatjack occupies the complete depth of the slot and shear stress is developed between the flatjack and rock during loading. These assumptions differ from the flatjack slot geometry for the DNA testing in which the slot is large relative to the flatjack.

The Alexander (1960) equation for in situ modulus is:

$$E = \frac{c\sigma_n}{\delta v}\left\{(1-v)\left[\left(1+\frac{y^2}{c^2}\right)^{1/2} - \frac{y}{c}\right] + (1+v)\left(1+\frac{y^2}{c^2}\right)^{-1/2}\right\} \quad (1)$$

where

E = deformation modulus
ν = Poisson's ratio
$\delta\nu$ = 1/2 measured slot deformation due to slot cutting
c = 1/2 slot length
σ_n = slot normal stress (from the cancellation test)
y = distance of measuring pin from slot centerline.

Alexander (1960) also suggested that two corrections must be applied to the above equation to account for the effect of the finite width of the slot and the effects of stress parallel to the plane of the slot. As noted in Jaeger and Cook (1979) these corrections tend to cancel one another. Therefore, for the initial slot closure, the original Alexander equation can be used as a first order estimate of the modulus of deformation of the rock mass if accurate measurements of the slot closure are made and Poisson's ratio can be assumed.

Alternate approaches to estimating the modulus of deformation from load/unload cycles can be made using a modification of the Loureiro-Pinto (1986) analysis or by simply using foundation engineering settlement equations. Of particular interest is the settlement of a flexible square footing on an elastic half-space due to uniform loading. The flatjack represents such a uniformly loaded flexible footing. The settlement equation is from Bowles (1982):

$$E_s = PBI_w(1-\nu^2)/d \quad (2)$$

where

E_s = elastic modulus

d = average displacement or displacement at the center of the flatjack due to the uniform load

P = flatjack pressure

B = least side dimension of the flatjack

I_w = Influence factor based on shape of the loaded area and rigidity

ν = Poisson's ratio.

For a square flexible loaded area, the influence factor I_w is equal to 0.95 (Bowles, 1982). This influence factor is representative of the average displacement under the loaded area which corresponds to d. A different I_w will apply if a displacement d is defined such as edge or center displacements. The use of the settlement equation presumes that the flatjack/slot geometry can be represented approximately by an elastic half-space. The measured cross-slot displacement due to the flatjack loading is equal to twice the displacement used in the settlement equation. The elastic half-space assumption may be a reasonable assumption for the case where relatively soft rock is loaded by a flatjack that occupies a relatively small space within the slot. Obviously, the edge effects of the slot proximity to the drift are neglected.

Loureiro-Pinto (1986) presented an approach to determine rock mass modulus using instrumented flatjacks. The analysis considers the location of the deformation gages within the flatjacks, the slot geometry, the flatjack shape, and the depth of the crack that is formed as the flatjacks are pressurized. Louriero-Pinto (1986) presented design charts along with the following equation for deformation modulus:

$$E_i = k_i(1-\nu^2)P/d_i \qquad (3)$$

where

E_i = modulus of deformability

k_i = coefficient depending on the stiffness, shape, arrangement and number of flatjacks, location of the measuring points, on the shape of the test chamber (tunnel), and on the depth of the crack formed during pressurization.

ν = Poisson's ratio

P = flatjack pressure

d_i = slot deformation at the i^{th} measuring location.

Loureiro-Pinto's approach is to evaluate the deformations from each of four deformeters placed within the flatjacks. The locations and displacements of the deformeters are "corrected" using the k coefficient. Unknowns in the above equation include the crack depth formed upon flatjack pressurization. The design charts presented in Loureiro-Pinto (1986) suggest, for the geometries tested, that the k coefficient should be about 200 (cm) for the slot dimension of about 6.6 ft (2 m). For this simplified analysis, we have assumed that crack propagation does not occur until macroscopic failure of the rock is seen. We have also averaged all four of the deformeter locations to correspond to the singular measurement point, which is the average of the Nova gage outputs for each load/unload cycle.

4.1.2 Slot and Instrumentation Layout

Flatjack testing for the DNA-UTP program consisted of two distinct phases: phase 1 involved determination of the slot normal stress, and phase 2 involved evaluation of the rock mass deformability. Evaluation of the slot normal stress includes one flatjack pressurization

sequence up to the cancellation pressure. The rock mass deformability measurements include increasing load-unload cycling coupled with deformation measurements until rock mass failure.

The layout for the flatjack tests is shown in Figures 4-1 and 4-2. A vertical slot in the left rib is shown in Figure 4-1; a horizontal slot in the right rib is shown in Figure 4-2. The slots were cut using a custom built rock saw developed by SNL and J.F.T. Agapito and Associates (Carlisle and Brechtel, 1991). The saw consists of a hydraulic power and control system, a frame, and a cutter bar (similar to a chain saw bar) that uses a diamond-abrasive impregnated belt to cut the rock. The cutter bar and belt system are commercial products developed for cutting limestone and other quarry rocks. Figure 4-3 shows the saw setup for the vertical slot; Figure 4-4 shows the saw setup for the horizontal slot. The flatjacks are made from thin sheets of 304 stainless steel butt welded to one-half tubes of the same material. The dimensions of the flatjacks prior to pressurization measure 32 in by 32 in (0.81 by 0.81 m) and are 3/8-in (0.95 cm) thick. The flatjacks are designed for 8,000 psi (55 MPa) maximum pressure.

Measurements of rock deformation due to flatjack pressurization were made across each slot along five parallel lines as shown in Figures 4-1 and 4-2. Three lines (Nova-1, Nova-2, and Nova-3) captured the rock displacements within about 9 in (0.22 m) of both sides of the slot. Two additional cross-slot measurements (HSI-1 and HSI-2) were made to evaluate displacements of the rock mass within about 18 in (0.46 m) of the slot. Both ends of the central cross-slot measurements (Nova-1) were referenced to far-field anchors perpendicular (HSI-5 and HSI-6) and parallel (HSI-3 and HSI-4) to the slot, and to anchors across the drift (HSI-7 and HSI-8). These far-field anchors are intended to evaluate gross movement of the measurement pins due to flatjack pressurization. Flatjack pressure was also monitored during the testing.

The various gages illustrated in Figures 4-1 and 4-2 actually measure the relative displacement between the two pins to which they are attached. For instance, the Nova pins measure the relative displacement of pins on either side of the slot due to slot closure and slot expansion. Likewise, the HSI gages measure longer gage-distance relative-displacement across the slot, from the fair-field, and across the drift. The six pins associated with the Nova gages and the four pins associated with gages HSI-1 and HSI-2 were anchored at a nominal depth of about 26 in from the face of the underground opening. Anchoring the pins at this depth was necessary to minimize potential surface displacements associated with surface mounted pins. This anchor depth also corresponds with locations near the center of the flatjack loaded area and thereby should be better able to represent rock displacements caused by flatjack loading.

Two different types of gages were used to measure displacements during flatjack pressurization. The close slot measurements were made using spring loaded captured plunger-type linear potentiometric gages (Nova gages), and longer gage displacements were measured using wire-actuated linear potentiometric gages (HSI gages). The accuracy and precision of both types of gages is 0.0001 in (2.5μm) ± 0.00005 in (1.3 μm). Additional manual displacement measurements were made across the slot, using a digital vernier caliper with an accuracy of 0.0001 in (2.5 μm). This digital vernier was used to measure the close-in pin dimensions before

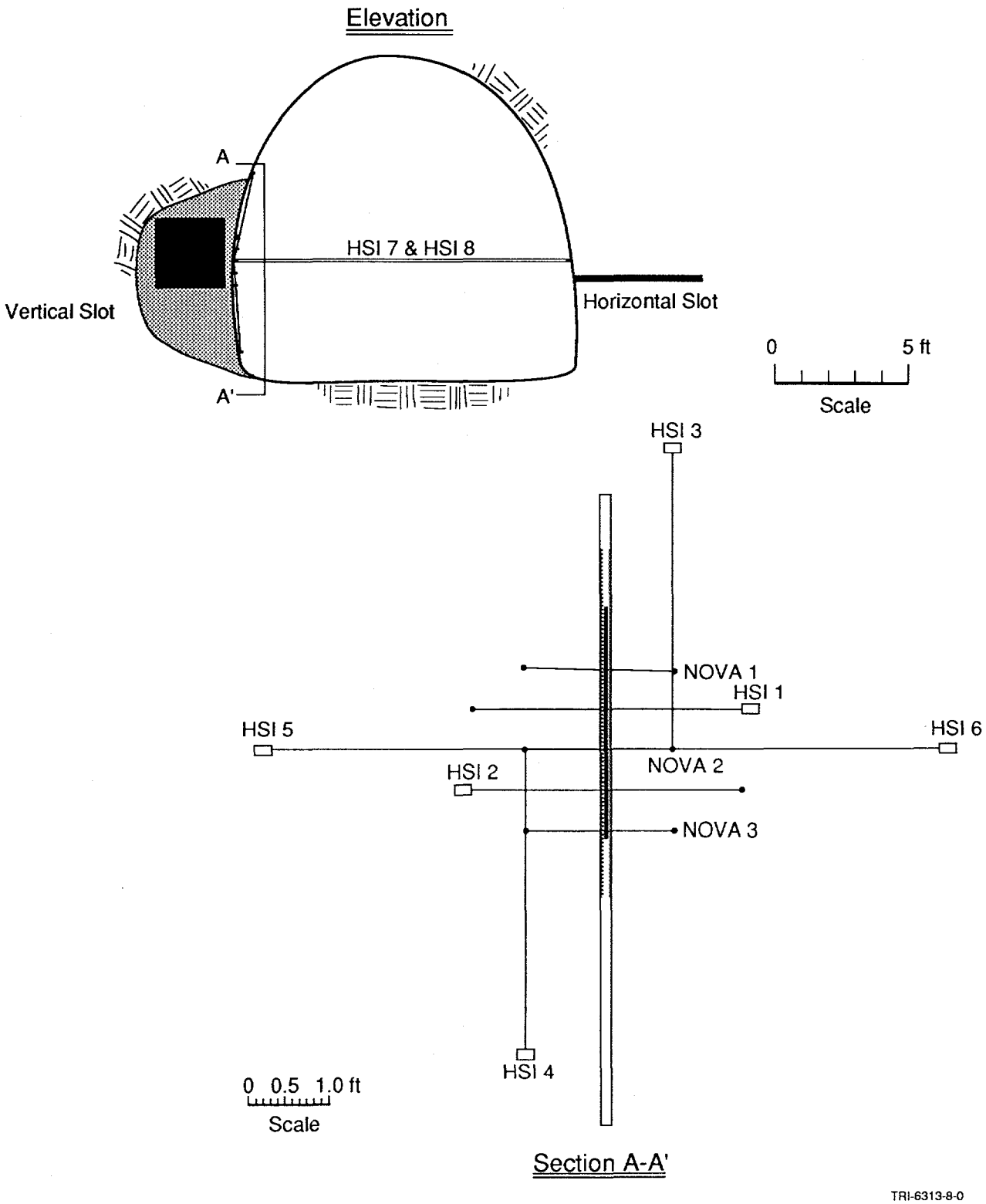

Figure 4-1. Test drift showing vertical flatjack test setup.

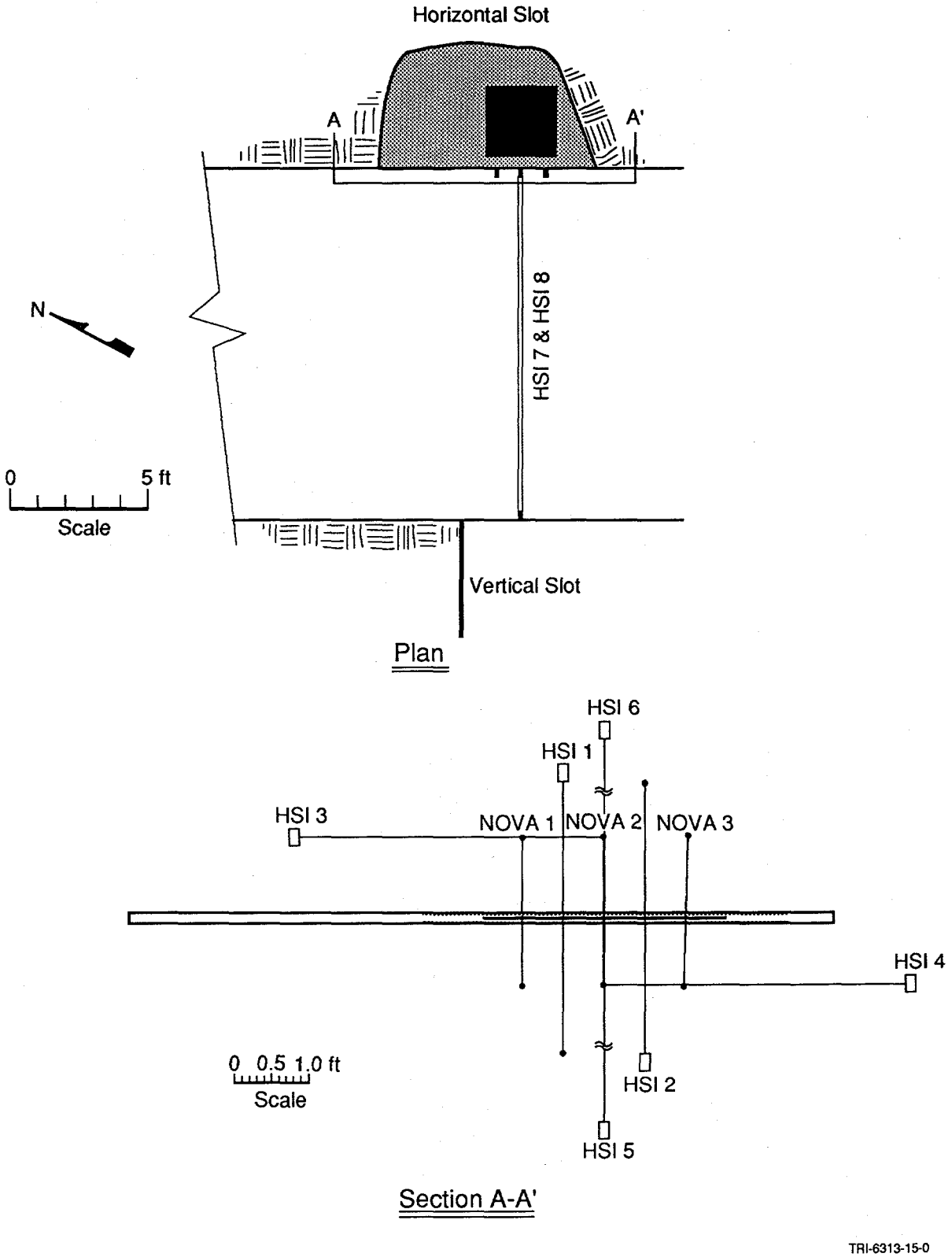

Figure 4-2. Test drift showing horizontal flatjack test setup.

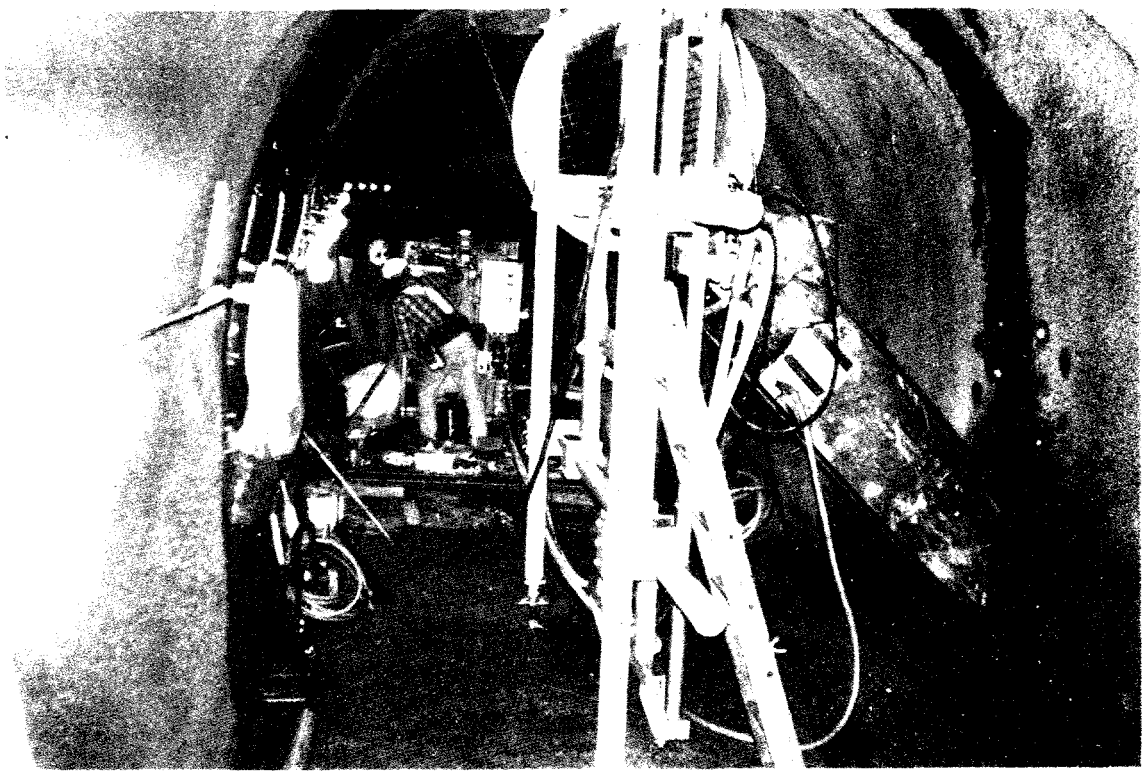

Figure 4-3. Rock saw setup—vertical slot.

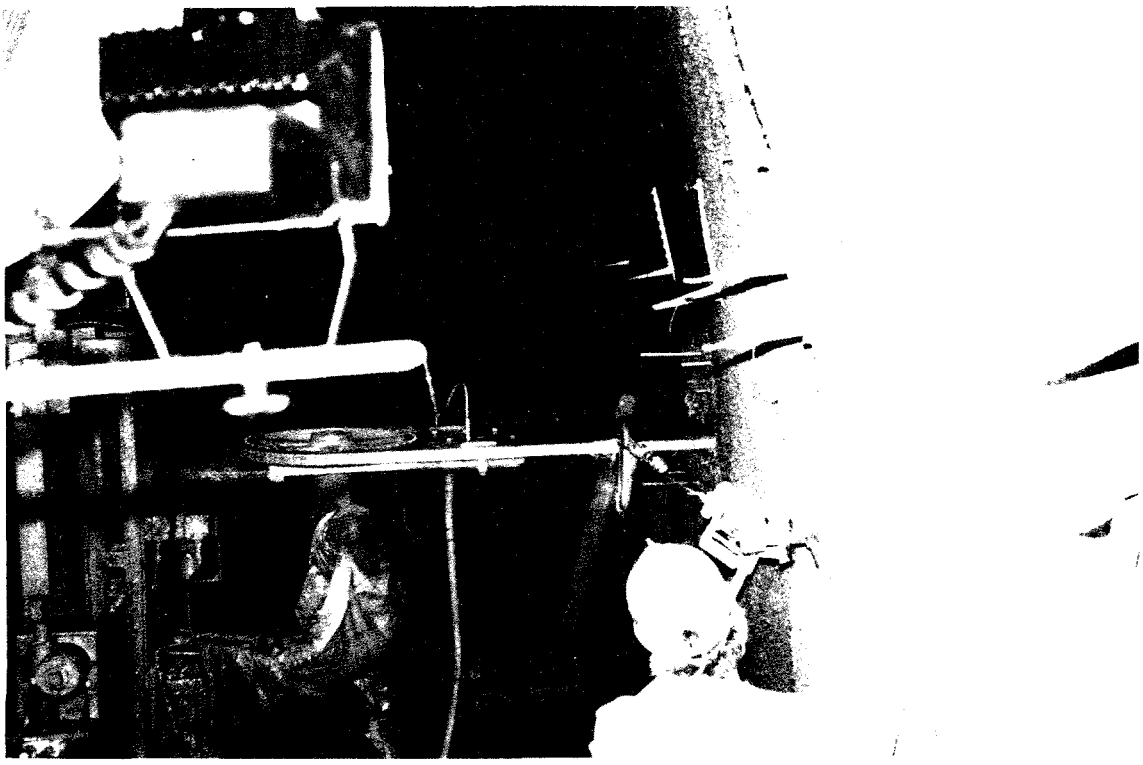

Figure 4-4. Rock saw setup—horiozntal slot

and immediately after cutting the slot. The difference between these two measurements is the cancellation displacement used during the flatjack pressurization to measure cancellation pressure. Digital data including Nova gages, HSI gages, and flatjack pressure transducer data were collected using a PC-based data acquisition system that included a digital voltmeter, HP3497A data acquisition unit, and IBM-386 PC. Other manual data were collected and recorded in engineering notebooks. Figure 4-2 shows the near-field instrumentation to the horizontal flatjack test.

4.2 Test Results

The test results are presented in two parts: first the evaluation of the slot normal stress is presented, then an evaluation of the deformation modulus based on the flatjack load/unload cycles is presented.

4.2.1 Slot Normal Stress

The slot normal stress was calculated based on the analyses presented in Section 4.1. Measurement pins corresponding to Nova-1, Nova-2, and Nova-3 were first set, and the initial distance between pins was measured. The slot was then cut, and the distance between pins measured again. The difference between each set of measurements corresponds to the closure due to cutting the slot. This closure is then "canceled" by the pressurization of the flatjack. To calculate the "corrected" slot normal stress, the flatjack loaded area, the flatjack pressure, and the "affected" slot area must be known or estimated. As discussed in Section 4.1.1, the "corrected" slot normal stress is simply the product of the flatjack pressure at cancellation and the ratio of pressurized area and slot area as given below

$$\sigma_n = P_c\left(\frac{A_F}{A_S}\right) \tag{4}$$

where

σ_n = "corrected" slot normal stress
P_c = flatjack pressure at cancellation
A_F = area of the flatjack
A_S = area of the slot "affected" by the flatjack.

The original equations for determining "corrected" slot normal stress as presented in Jaeger and Cook (1979) presumed that the slot area was only slightly larger than the flatjack area. This is clearly not the case for the DNA flatjack testing in which the slots were approximately four times the flatjack area. Under these circumstances, and with relatively weak surrounding rock, it became necessary to further qualify the slot area as that which is significantly affected by the flatjack pressurization. Therefore, empirical comparisons between the numerical simulations

presented in Section 4.2.3 were made to better estimate the "affected" slot area. From the deformed meshes developed for the 3D numerical simulations of the horizontal slot, it was estimated that not all of the slot was affected by the flatjack pressurization. A conservative estimate of the "affected" slot area was made based on these comparisons and used to calculate the "corrected" slot normal stress. A detailed discussion of the numerical modeling is presented in Section 4.2.3.

Table 4-1 lists the results of the slot closure and cancellation pressure for both the vertical and horizontal slots. The "affected" slot areas were determined as previously described. Differences between "affected" slot areas for the two slots are due to slightly different test geometries. For the vertical slot, only the cancellation pressure for the Nova-2 gage is presented. Cancellation pressures for all three Nova gages are presented for the horizontal slot to allow for comparisons with the numerical simulations described in Section 4.2.3.

Figures 4-5 and 4-6 show flatjack pressure histories for each of the vertical and horizontal slot tests. The initial load cycles were intended to "cancel" the slot closure caused by cutting the slot.

Table 4-1 Slot Closure and Cancellation Pressure

Gage	Vertical Slot	Horizontal Slot
Closure Nova-1 (in)*	0.154	0.027
Closure Nova-2 (in)*	0.0405	0.011
Closure Nova-3 (in)*	0.064	0.009
Average Closure (in)	0.0862	0.0157
Cancellation Pressure (psi)	500	1370 Nova-1 1100 Nova-2 1960 Nova-3
Flatjack Area (in^2)	1,024	1,024
Affected Slot Area (in^2)	~3,300	~3,700
Corrected Slot Normal Stress (psi)	155 (Nova-2)	304 (Nova-2)

* closures measured before and after slot cutting using manual digital vernier

The corrected slot normal stresses measured using the flatjack cancellation technique are lower than those calculated assuming gravitational loading and are also lower than those measured using the overcoring technique. The corrected slot normal stress for the vertical slot corresponds to the stress acting parallel to the test drift at that location. The corrected slot normal stress presented in Table 4-1 for the horizontal slot represents the stress concentrated around the underground opening.

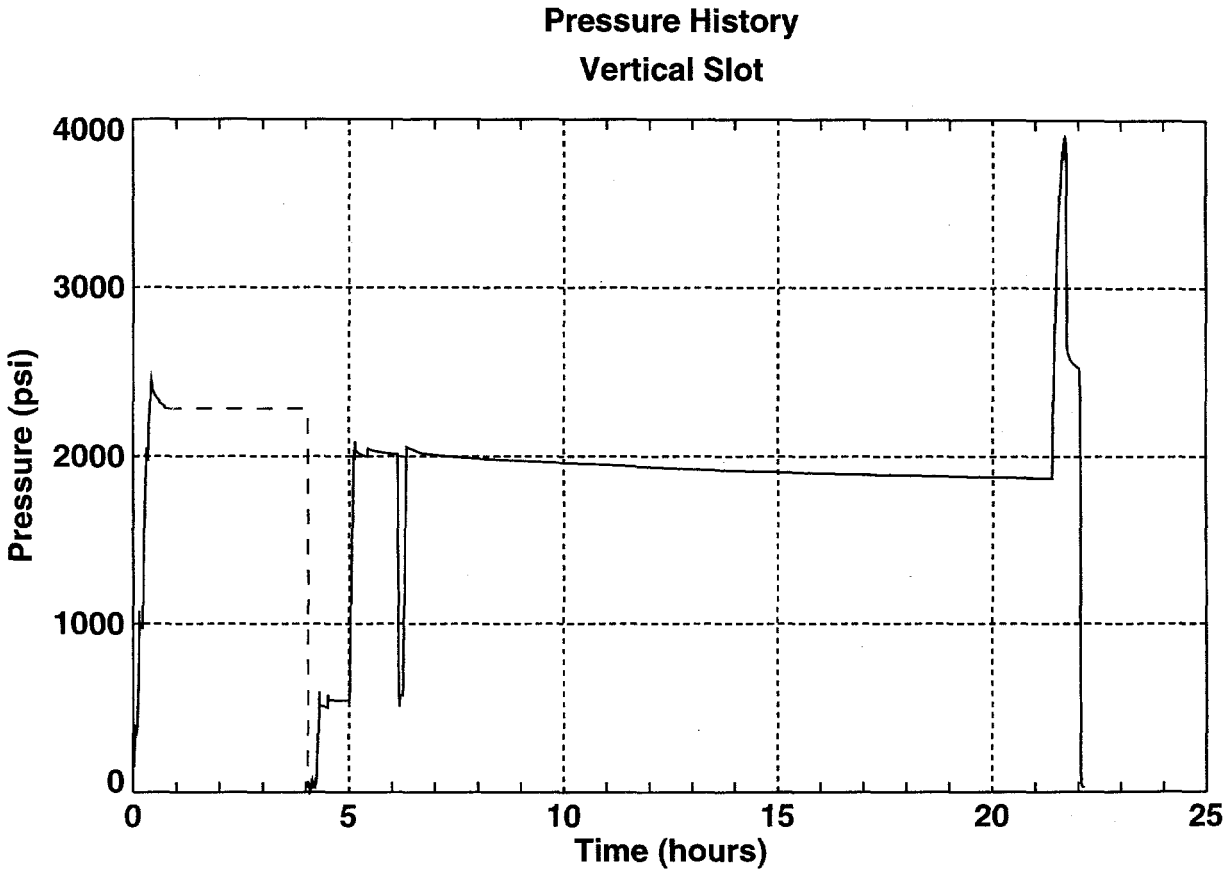

Figure 4-5. Flatjack pressure history for vertical slot test.

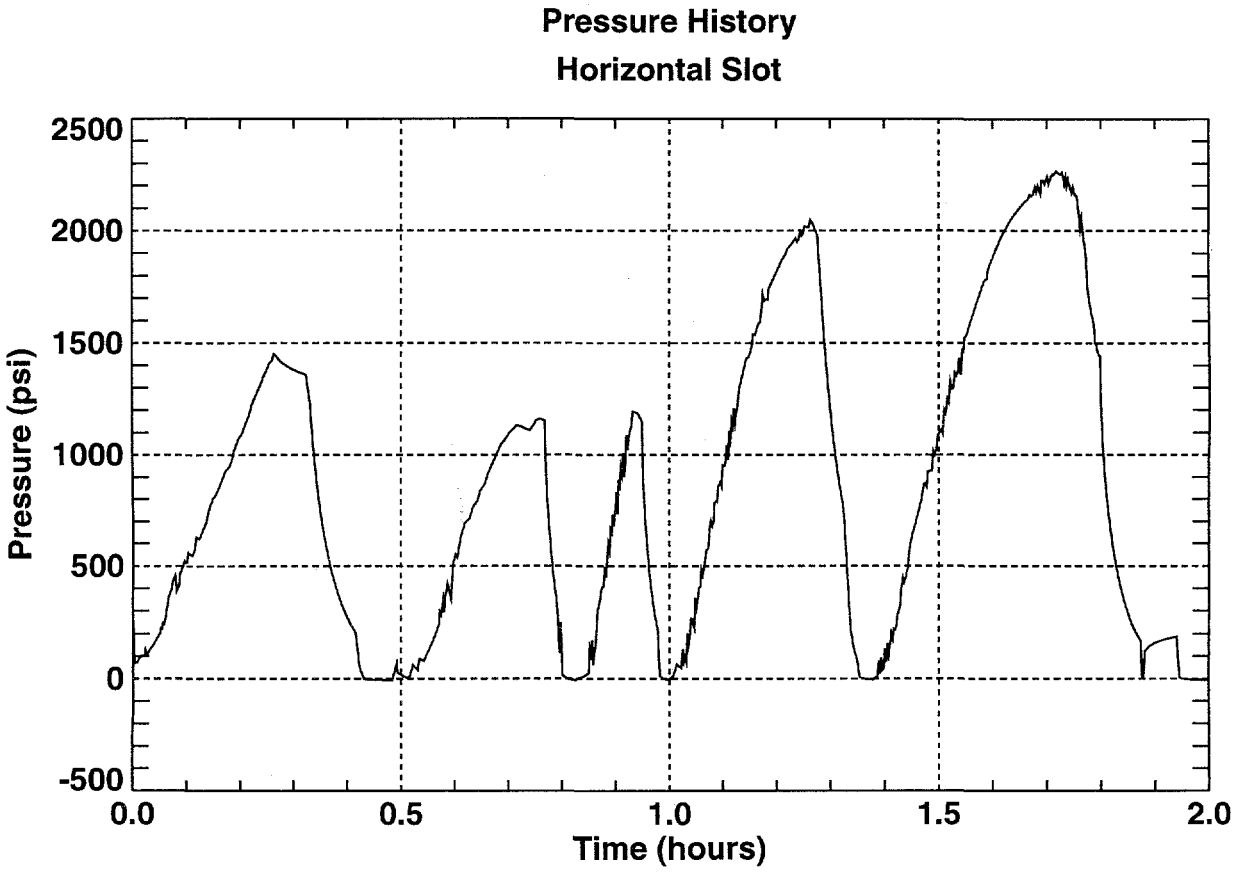

Figure 4-6. Flatjack pressure history for horizontal slot test.

4.2.2 Deformation Modulus Determination Using Analytical Techniques

The deformation modulus was calculated using each of three simplified analytical models described in Section 4.1. Figures 4-7 and 4-8 show the pressure/displacement histories for the vertical and horizontal flatjack tests, respectively, for the central cross-slot measuring pins Nova 2 (see Figures 4-1 and 4-2). Both Figures show very little response of the rock mass until flatjack pressures neared the cancellation pressures. For the vertical flatjack test, only two load cycles were performed prior to failure of the rock. The horizontal test included five load-unload cycles to failure of the rock. In both tests, the failure of the shale exhibited behavior similar to punch tests on soils in which general or local shear failure of the material outside the loaded area occurs. In the flatjack tests the failed rock around the flatjack bulged into the open slot. The calculated modulus of deformation using the analytical methods described in Section 4.1 are presented in Table 4.2. Complete plots of pressure/deformation data for all gages are presented in Appendix B.

The calculated moduli using a range of Poisons Ratio are presented in Table 4-2. A range of Poisson's ratios is presented because of variability in the laboratory data presented in Appendix A. The results using the Alexander (1960) analysis predicts the modulus using the initial slot closure data and does not consider the load/deformation history of the flatjack. For the Bowles (1982) and Loureiro-Pinto (1986) analyses, the next-to-last unloading cycle was used for the horizontal slot. The slot closure data for the horizontal slot produced excessively high modulus values when used in the Alexander (1960) analysis and are not presented. The load/unload history for the vertical slot produced excessively high modulus values when used in the Bowles (1982) and Loureiro-Pinto (1986) analyses; these modulus values are likewise not presented. A discussion of the flatjack testing results is presented in Section 4.3. The Bowles (1982) and Loureiro-Pinto (1986) analyses for the horizontal slot appear reasonable and are within the bounds of the laboratory and overcoring results.

4.2.3 Numerical Analysis of the Horizontal Flatjack Test

Analyses of the horizontal flatjack tests were conducted to simulate the response of an elastic rock mass surrounding the flatjack and to compare the simulation with the measured deformations. Numerical simulations were conducted using two-dimensional (2D) finite-element analyses and three-dimensional (3D) displacement discontinuity analyses. The computer code JAC (Biffle, 1984) was used for the 2D plane-strain analyses and program EXPAREA (St. John, 1978) for the 3D modeling.

A 2D analysis of the test drift was conducted to estimate the preexisting stress at the slot horizon. The 2D analysis of the slot was conducted as an interim step to gain a better understanding of the slot closures due to the relatively small flatjack located off the center of the slot. A 3D EXPAREA analysis provided a better approximation of the slot geometry and therefore was conducted to evaluate the deformations as a result of pressurization of the flatjack.

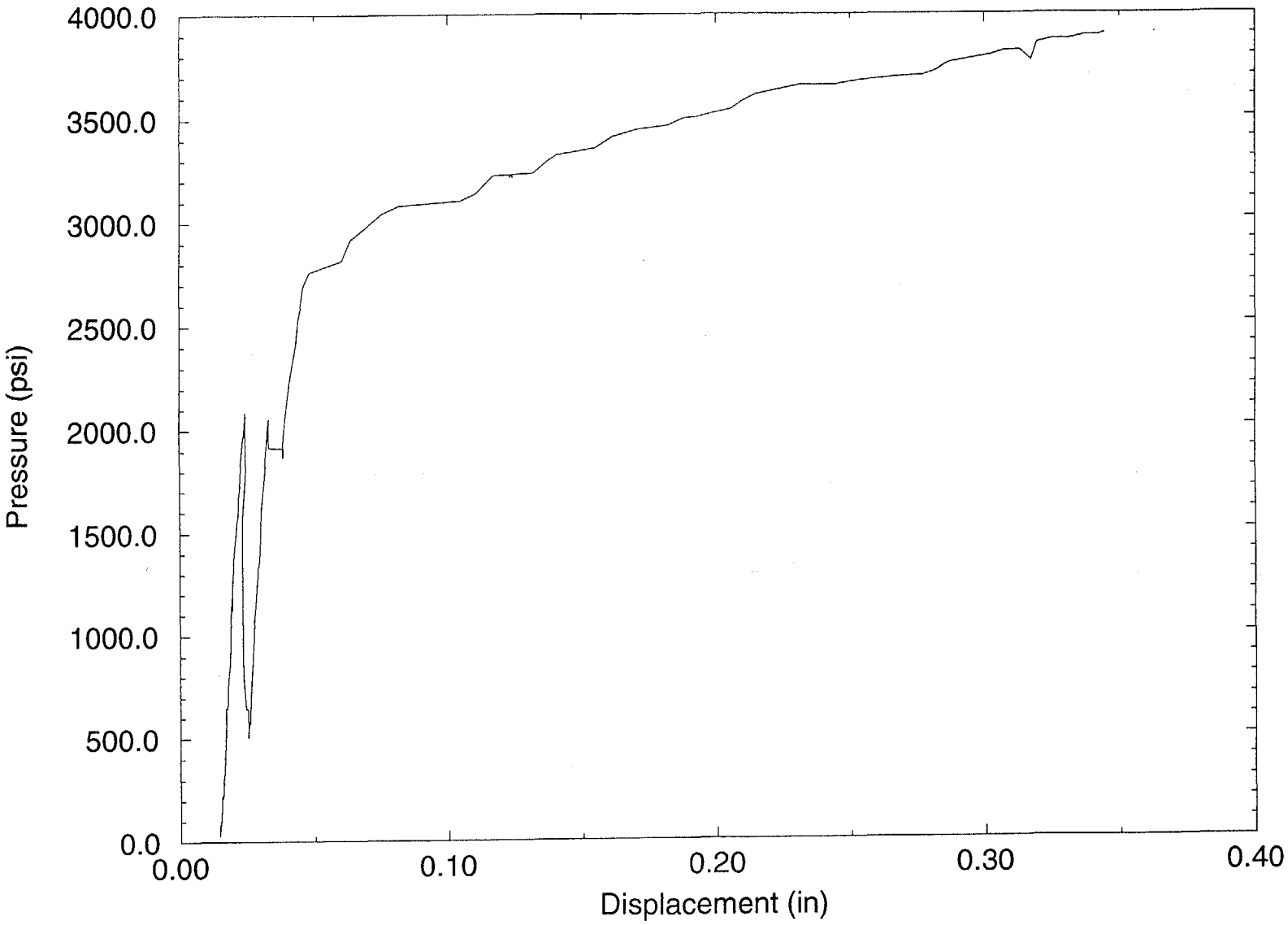

Figure 4-7. Pressure/displacement history-vertical slot—Nova 2 center cross-slot measurements.

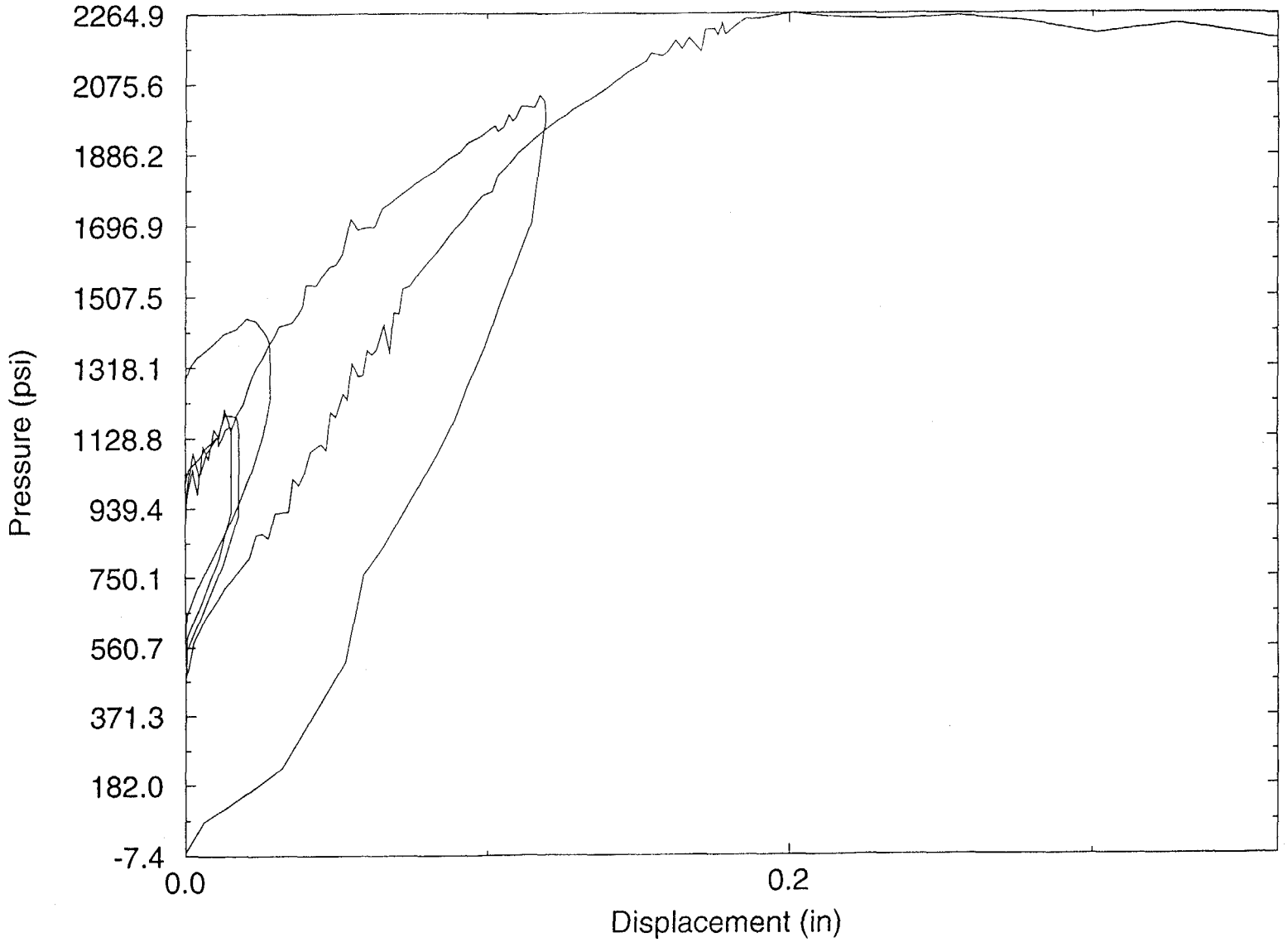

Figure 4-8. Pressure/displacement history-horizontal slot—Nova 2 center cross-slot measurements.

Table 4.2. Modulus of Deformation Estimates for DNA Flatjack Tests

Alexander (1960)*		Foundation Settlement Eq.** (Bowles, 1982)		Loureiro-Pinto (1986)**	
$E=c\sigma_n/\delta v\{(1-\nu)[(1+y^2/c^2)^{1/2}-y/c]+(1+\nu)(1+y^2/c^2)^{-1/2}\}$		$E=(PB/\delta)(1-\nu^2)I_w$		$E_i=k_i(1-\nu^2)P/d_i$	
Vertical slot)		Horizontal slot		Horizontal slot	
Deformation Modulus (psi)	ν	Deformation Modulus (psi)	ν	Deformation Modulus (psi)	ν
$.44 \times 10^6$	0.1	1.14×10^6	0.1	1.47×10^6	0.1
$.45 \times 10^6$	0.2	1.10×10^6	0.2	1.43×10^6	0.2
$.45 \times 10^6$	0.3	1.04×10^6	0.3	1.35×10^6	0.3
$.45 \times 10^6$	0.4	0.96×10^6	0.4	1.25×10^6	0.4
$.45 \times 10^6$	0.5	0.86×10^6	0.5	1.11×10^6	0.5

* slot closure data only

** unloading portion of next-to-last loading cycle

The horizontal slot was located in the rib of the test drift approximately 4 ft above the floor as shown in Figure 4-1. A plan view of the horizontal slot is shown in Figure 4-9. The maximum depth of the slot was approximately 58 in., and the slot thickness was 1.5 in.

All of the numerical analyses were conducted assuming that the rock mass behaved as a linear elastic and isotropic material. The deformation modulus used was 700,000 psi (4.8 GPa), based on the mean vertical modulus derived from cylindrical pressurization of the overcore samples. Poisson's ratio was assumed to be 0.25.

The in situ stress field used in the analyses of the flatjack tests was derived from overcore measurements taken near the flatjack test slots. For both the 2D and 3D analyses, it was necessary to rotate the stress components into the local coordinate system adopted for the analyses as shown in Figure 4-10.

Table 4-3 gives the measured principal stress tensor and rotated components. The horizontal plane is defined by the x'y' plane with the x' coordinate axis oriented normal to the axis of the drift. The z' coordinate axis is oriented vertically up. The drift axis in the area of the flatjack tests was oriented N31°W with a dip of 0°.

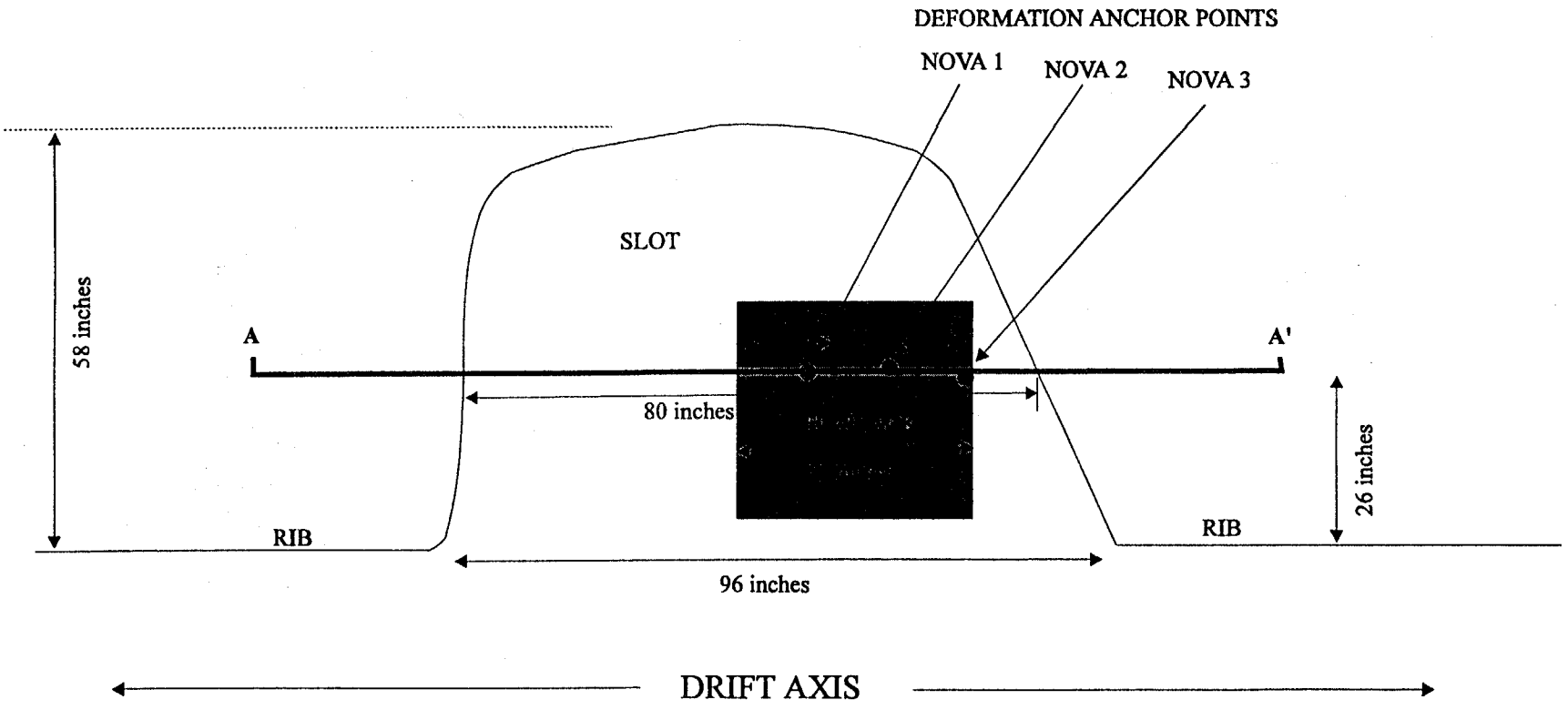

Figure 4-9. Plan view of the horizontal slot showing approximate flatjack location and dimensions.

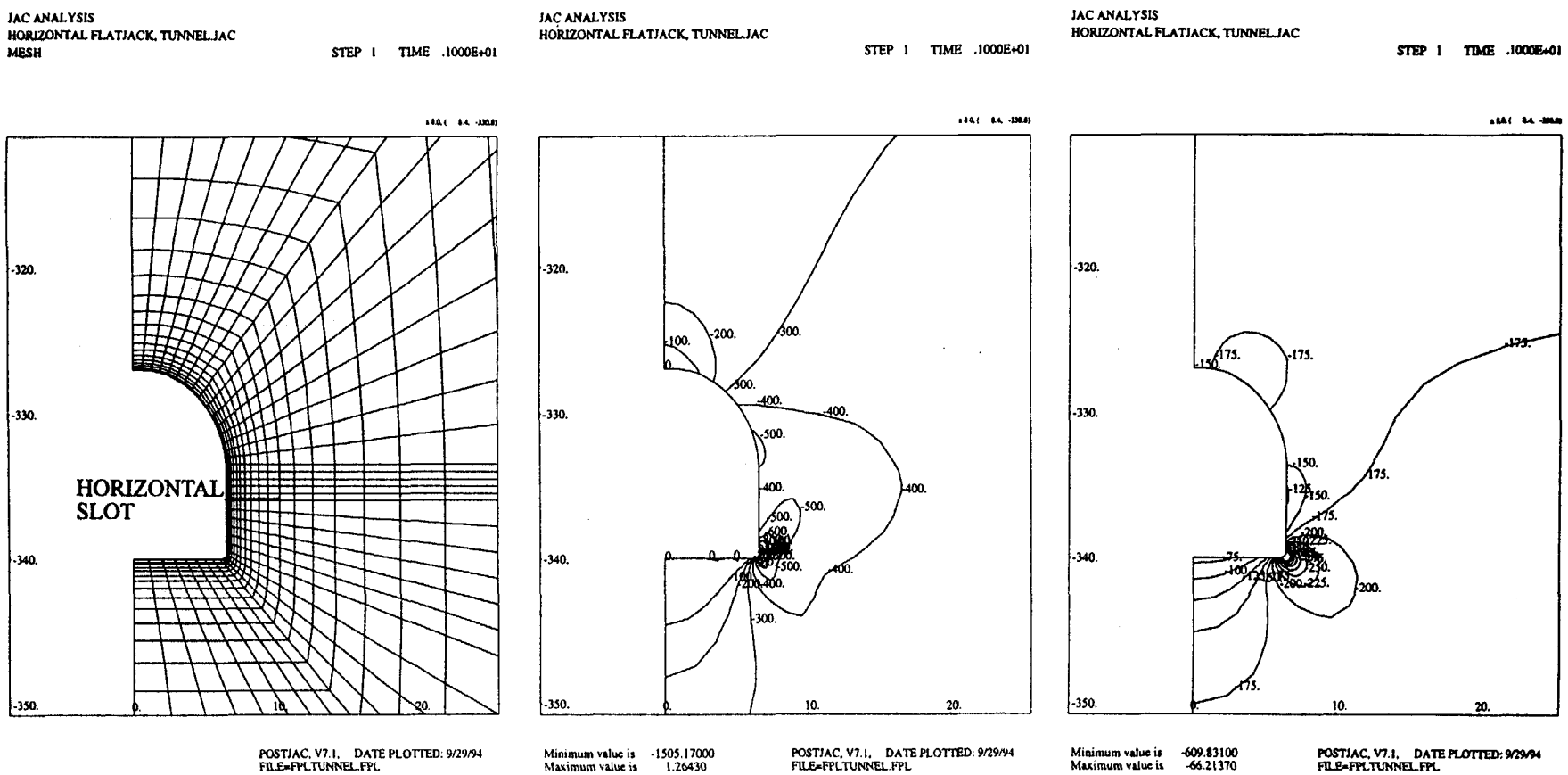

Figure 4-10. Two-dimensional finite-element mesh and vertical and axial stress contours form the drift analysis.

Table 4-3. Premining Stress Field in the Area of the Flatjack Test

		Azimuth (degrees)	Inclination (degrees)*	Stress (psi)**
Maximum Principal Stress		63	146	-373
Intermediate Principal Stress		40	58	-281
Minimum Principal Stress		137	79	-176
Syy'	Horizontal Stress Parallel to the Drift Axis	-	-	-185
Sxx'	Horizontal Stress Normal to the Drift Axis	-	-	-305
Szz'	Vertical Stress	-	-	-340
Sxy'	Shear Stress in the Horizontal Plane	-	-	-19
Syz'	Shear Stress in the Vertical Plane Parallel to the Drift	-	-	23
Sxz'	Shear Stress in the Vertical Plane Normal to the Drift	-	-	-47

* 0 degrees is oriented down
** Compression negative

4.2.3.1 2D Analysis of the Horizontal Flatjack Test

Two numerical models were prepared for the 2D analysis of the horizontal flatjack test. The first analysis was conducted to calculate the stress field at the slot horizon prior to cutting. The second analysis was a simulation of a long horizontal slot developed along A-A' in Figure 4-9. The calculated stresses at the slot horizon from the drift model were applied as the boundary condition for the model.

The finite-element mesh and contour plots of the vertical and axial stress results from the drift analysis are shown in Figure 4-10. The calculated vertical and axial (parallel to the drift and slot) stress distributions along the slot are tabulated and plotted in Figure 4-11.

The average vertical stress along the slot horizon was -478 psi (-3.3 MPa) (compressive), or 141% of the in situ vertical stress component of -340 psi (-2.3 MPa). The maximum vertical stress along the slot occurred approximately 27 in (0.69 m) from the rib and had a magnitude of -501 psi (3.45 MPa). The minimum vertical stress of -400 psi (2.76 MPa) occurred at the rib.

NODE NUMBER	COORDINATE (ft)	DISTANCE FROM RIB (inches)	VERTICAL STRESS (psi)	AXIAL STRESS (psi)
469	6.5	0	400	124
470	6.589	1.068	405	125
471	6.699	2.388	416	128
472	6.838	4.056	430	131
473	7.011	6.132	444	136
474	7.228	8.736	460	141
475	7.498	11.976	475	146
476	7.836	16.032	489	152
477	8.259	21.108	498	159
478	8.787	27.444	501	165
479	9.448	35.376	496	171
480	10.273	45.276	482	175
481	11.305	57.66	463	179
LENGTH WEIGHTED MEAN			478	161

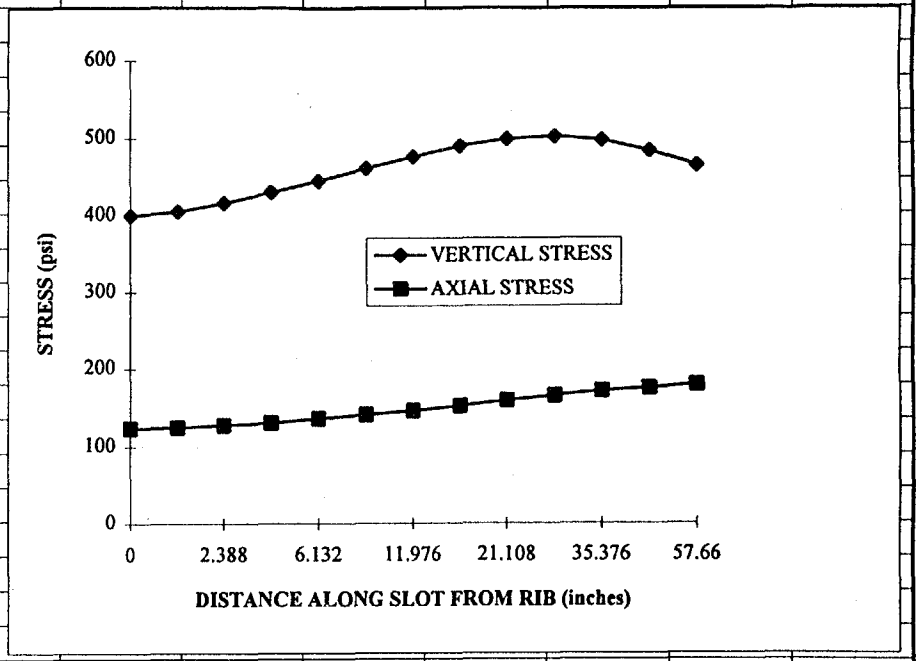

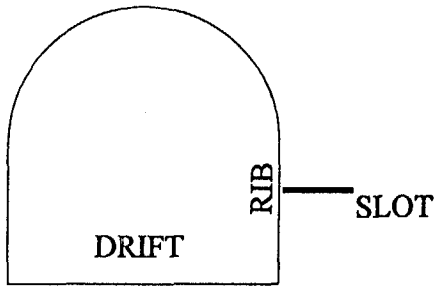

Figure 4-11. Two-dimensional finite-element mesh results from the drift analysis showing vertical and axial stress distribution at the location of the horizontal slot prior to cutting.

The average axial stress along the slot horizon was -161 psi (1.11 MPa) (compressive) or 87% of the in situ component of -185 psi (1.28 MPa). As shown in Figure 4-11, the axial stress increases in a relatively uniform manner away from the rib. The minimum axial stress was -124 psi (0.85 MPa), and the maximum value was -179 psi (1.23 MPa).

The average shear stress along the slot horizon in the plane of the analysis ranged from -0.3 to -45 psi (0.002 to 0.31 MPa). The mean shear stress along the slot horizon was -29 psi (0.2 MPa). The distribution increased fairly uniformly from the rib to the slot end. The magnitude of the shear stress indicates that the vertical stress is near a principal stress direction in the vicinity of the slot.

The finite-element mesh used for the second numerical model representation of the horizontal slot is shown in the left diagram in Figure 4-12, where only the top half of the slot is meshed by assuming a horizontal plane of symmetry through the center. The length of the slot modeled was 80 in (2. m) consistent with the vicinity of the deformation monitoring points shown in Figure 4-9. Line A-A' in Figure 4-9 indicates the location of the vertical plane modeled, located approximately 26 in (0.6 m) from the rib.

The stress field from the drift analysis with a vertical stress of 478 psi (3.3 MPa) was applied to the slot mesh as the initial stress. Deformation of the mesh due to excavating the slot was calculated in the first step and incremental pressure boundaries were then applied to the mesh to simulate the flatjack load. Figure 4-12 illustrates the deformed mesh due to slot excavation and subsequent flatjack pressurization to 2,000 psi (13.8 MPa).

Predicted slot closures due to the cutting of the slot were -0.092, -0.077, and -0.045 in (-2.34, -1.96, and -1.14 mm) at locations Nova 1, Nova 2 and Nova 3, respectively (see Figure 4-9). As would be expected, the smallest closure occurred at the location nearest to the slot edge (Nova 3). The largest closure of the three measured locations occurred at Nova 1, which was located nearest the center of the slot and furthest from the rock edge.

The results of the simulation of the flatjack pressurization are presented in Figure 4-13 and indicate that the slot stiffness was greatest at the Nova 3 measurement location. The slot stiffnesses at the Nova 2 location was slightly greater than at the Nova 1 location because the Nova 1 location is closer to the center of the slot.

The slot closures due to excavation at the locations Nova 1, Nova 2, and Nova 3 were recovered when the flatjack pressure reached approximately 750 psi (5.2 MPa) as shown in Figure 4-13. Deformation of the slot not in contact with the flatjack was very small.

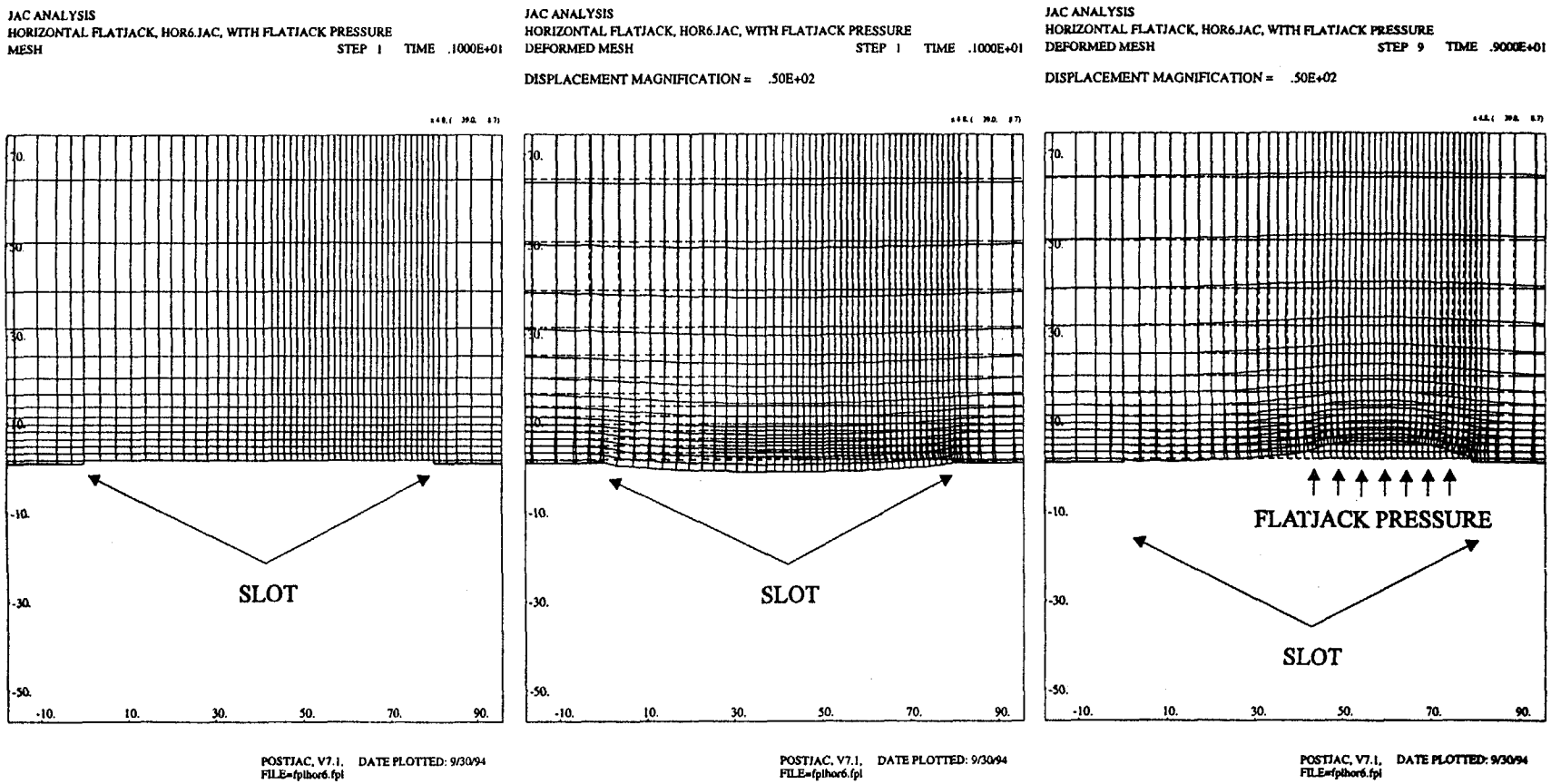

Finite Element Mesh | **Deformed Mesh after Slot Cutting** | **Deformed Mesh with 2000 psi Pressure in Flatjack**

Figure 4-12. Finite-element mesh and deformed shapes from the two-dimensional analysis of the horizontal slot.

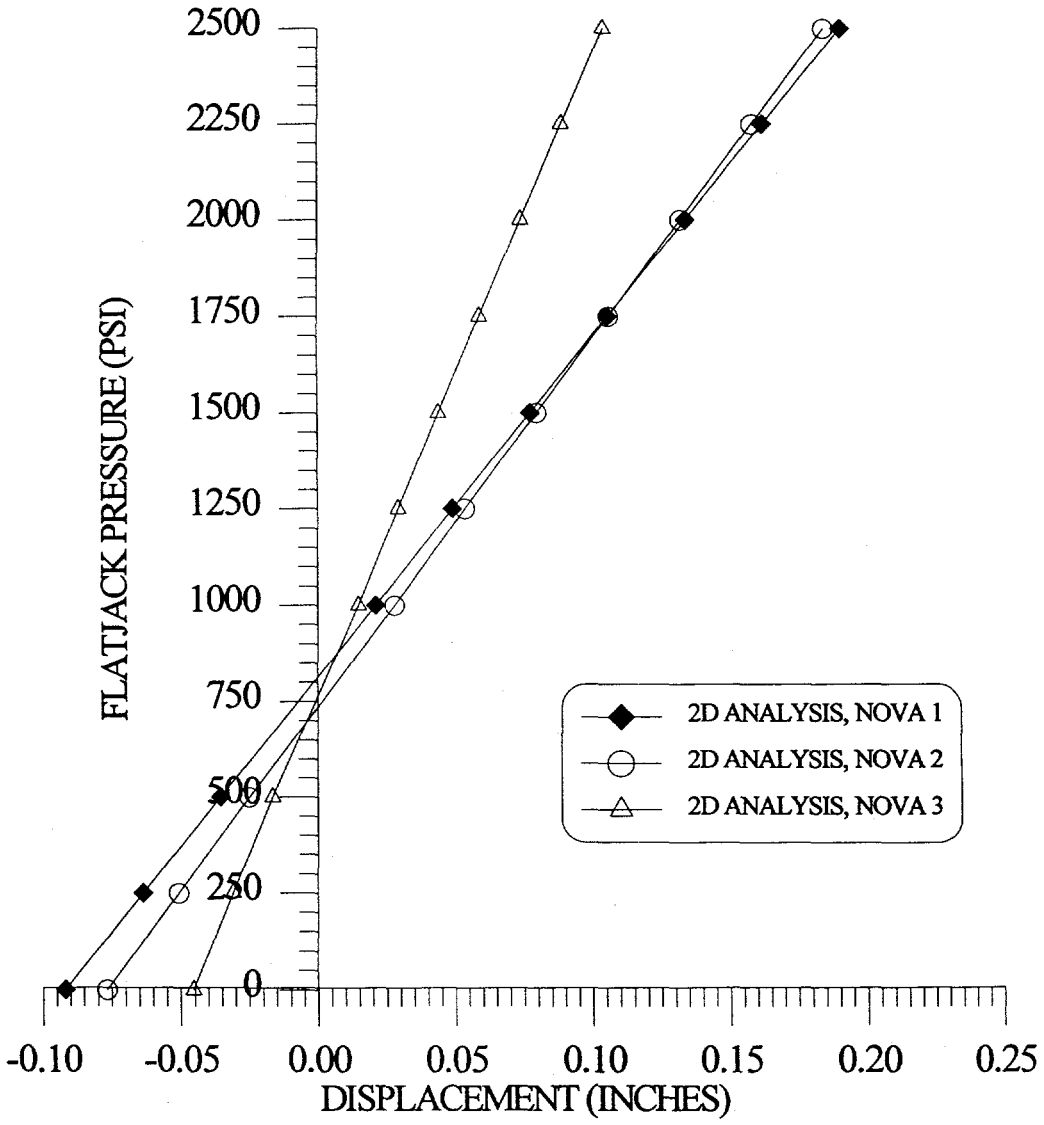

Figure 4-13. Computed deformations from the 2-D analysis due to the pressurization of the flatjack.

4.2.3.2 3D Analysis of the Horizontal Flatjack Test

The 3D representation of the horizontal flatjack test using the displacement discontinuity method is illustrated by the mesh shown in Figure 4-14. The slot is simulated as a thin, tabular excavation. The geometric representation of the slot is quite good using this method, but it requires that the drift geometry be generalized to be a long, wide slot. This representation of the drift is judged adequate for this analysis because the drift excavation is only required in the model to approximate the stress redistribution onto the slot region.

The mesh represents a plan view of the drift, the horizontal slot, and the flatjack. The region shown in the mesh in Figure 4-14 was discretized with 2-in.-square elements represented by the individual x's. The drift width was 13 ft as shown in Figures 4-1 and 4-2. The slot dimensions are shown in Figure 4-9.

The stress field in the vicinity of the slot was computed in the model by imposing the in situ vertical stress over the entire mesh. Based on the overcore measurements in this area, the in situ vertical stress was 340 psi (2.34 MPa); shear stresses are not considered.

Slot deformation results from the 3D analysis are shown in Figures 4-15 through 4-17. Figure 4-15 shows contours and a 3D surface of the slot closure after excavation of the slot but prior to pressurization of the flatjack. In Figure 4-16, the flatjack has been pressurized to 500 psi (3.45 MPa), predicting the reduction in the total closure in the vicinity of the pressurized flatjack. Figure 4-17 shows the arithmetic difference between the deformations due to the excavation of the slot and the deformations in the slot after pressurization of the flatjack to 500 psi (3.45 MPa).

Predicted slot closures from the 3D analysis due to the cutting of the slot (no pressurization) were -0.074, -0.065, and -0.049 in (-1.88, -1.65, and -1.24 mm) at locations Nova 1, Nova 2 and Nova 3, respectively. As expected, the smallest closure occurred at the location nearest to the slot edge (Nova 3). The largest closure of the three measured locations occurred at Nova 1, which was located nearest the center of the slot and furthest from the rock edge.

The computed deformations due to pressurization of the flatjack from the 3D analysis are shown graphically in Figure 4-18. The computed deformation for gage locations Nova 1 and Nova 2 indicate that the slot deformed more at the Nova 1 gage upon excavation. Subsequent deformations at the Nova 1 and Nova 2 gages due to pressurization were parallel.

The results of the 3D pressurization analysis indicate that the slot closures at the locations Nova 1, Nova 2 and Nova 3 due to the excavation of the slot were recovered when the flatjack pressure reached approximately 1,000 psi (6.9 MPa).

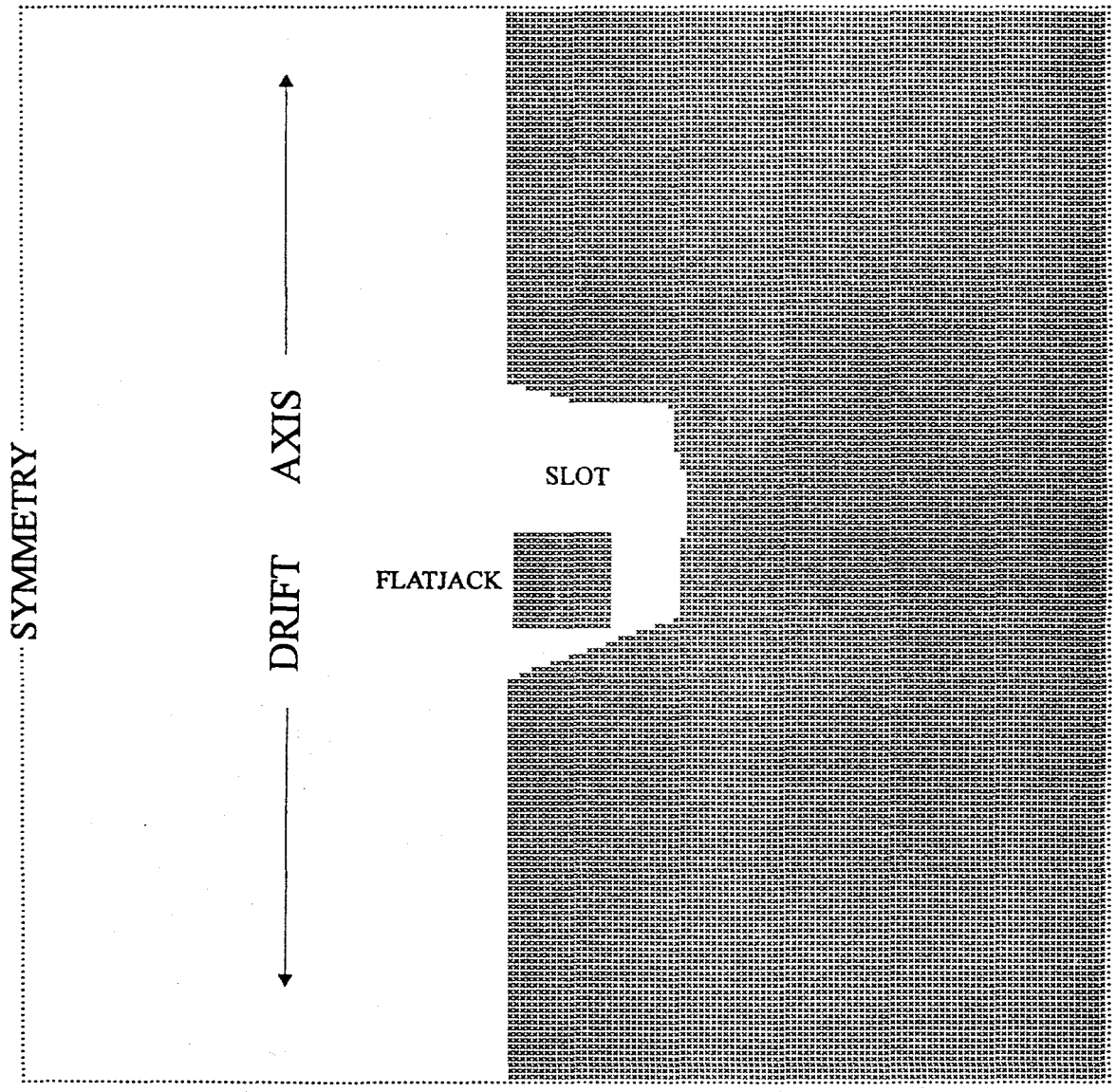

Figure 4-14. Mesh used for the 3D analysis of the flatjack pressurization test.

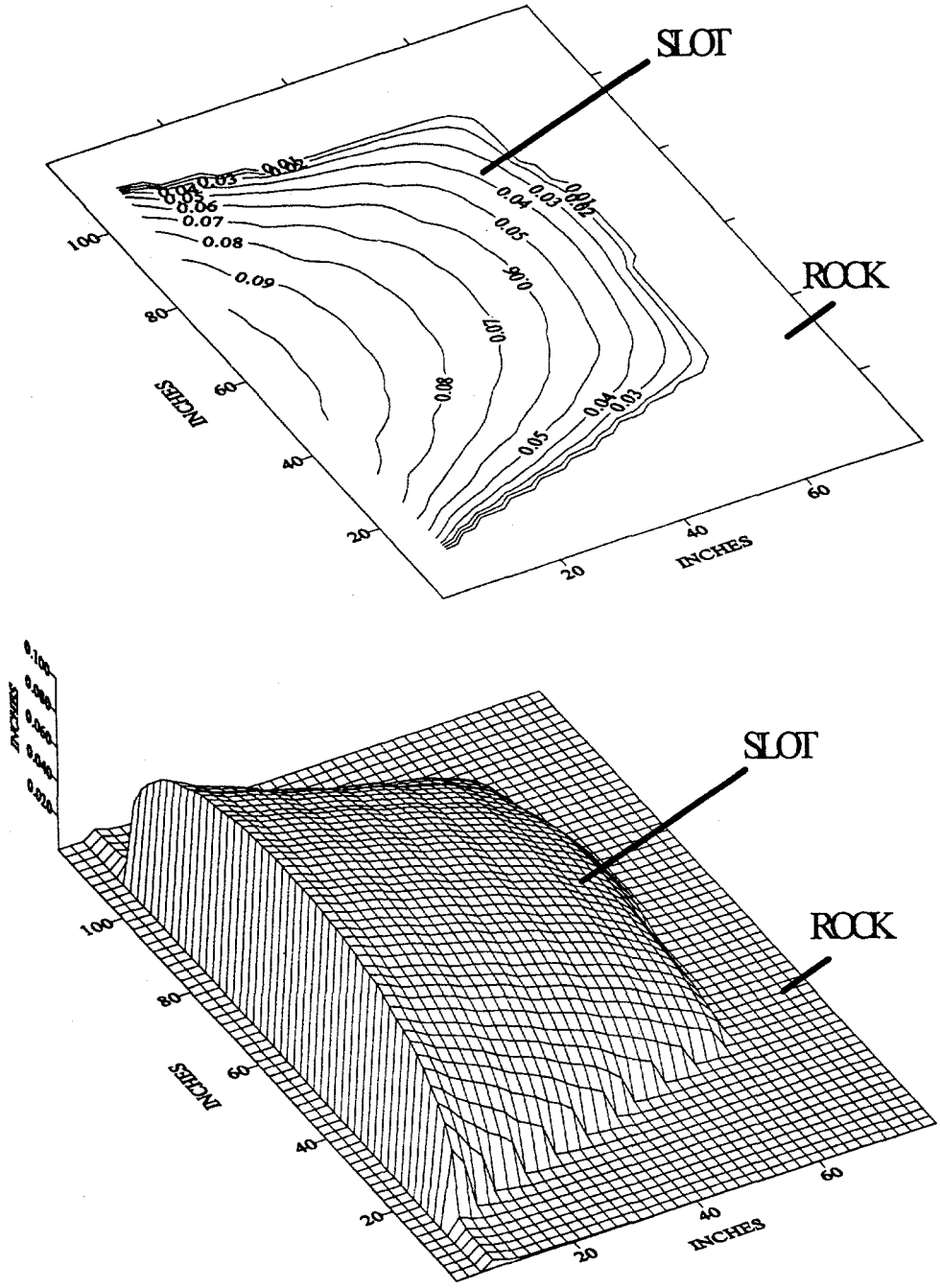

Figure 4-15. **Distribution of the computed deformations from the 3D analysis due to the excavation of the slot.**

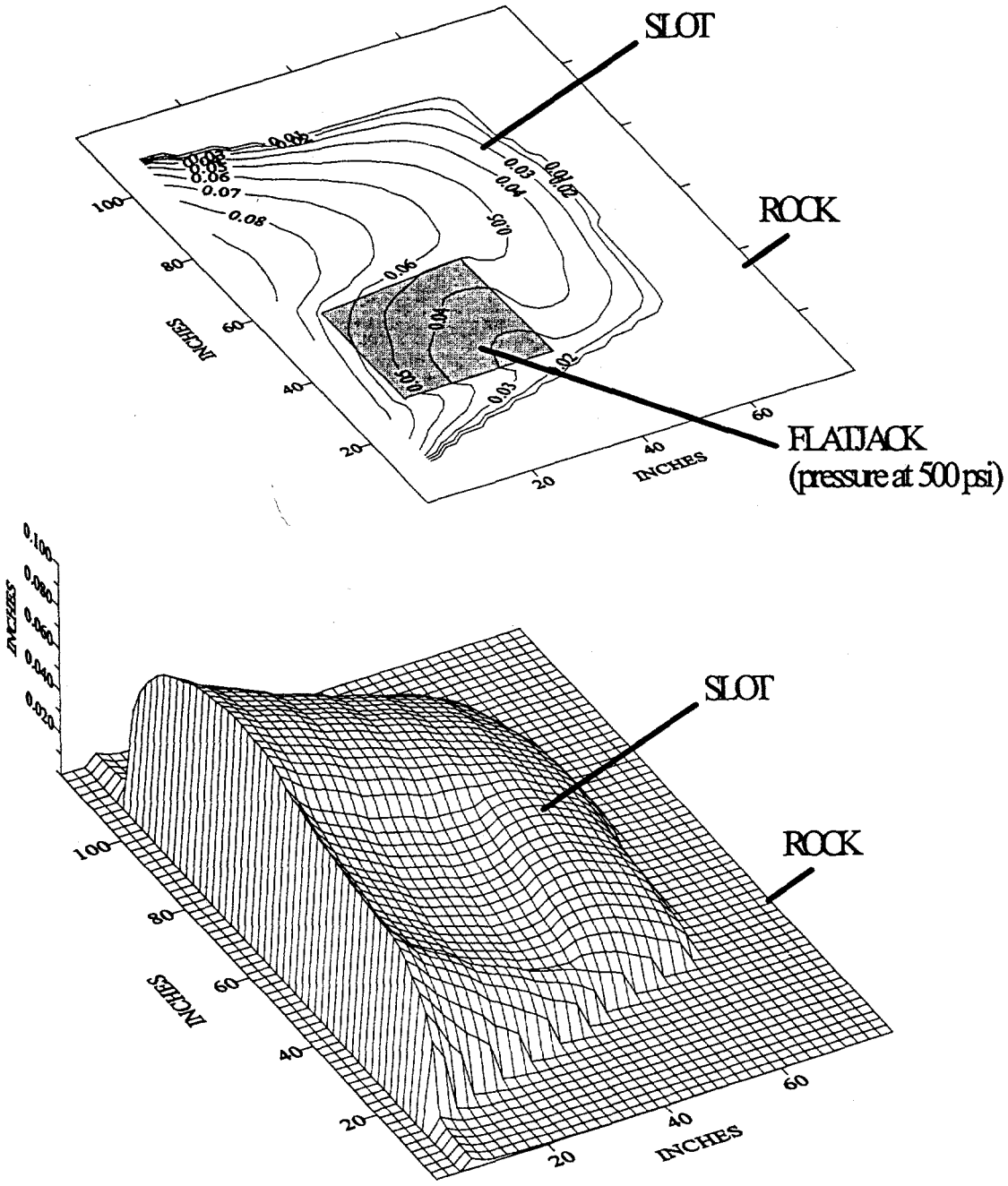

Figure 4-16. Distribution of the computed deformations from the 3D analysis due to the slot excavation and flatjack pressurization to 500 psi.

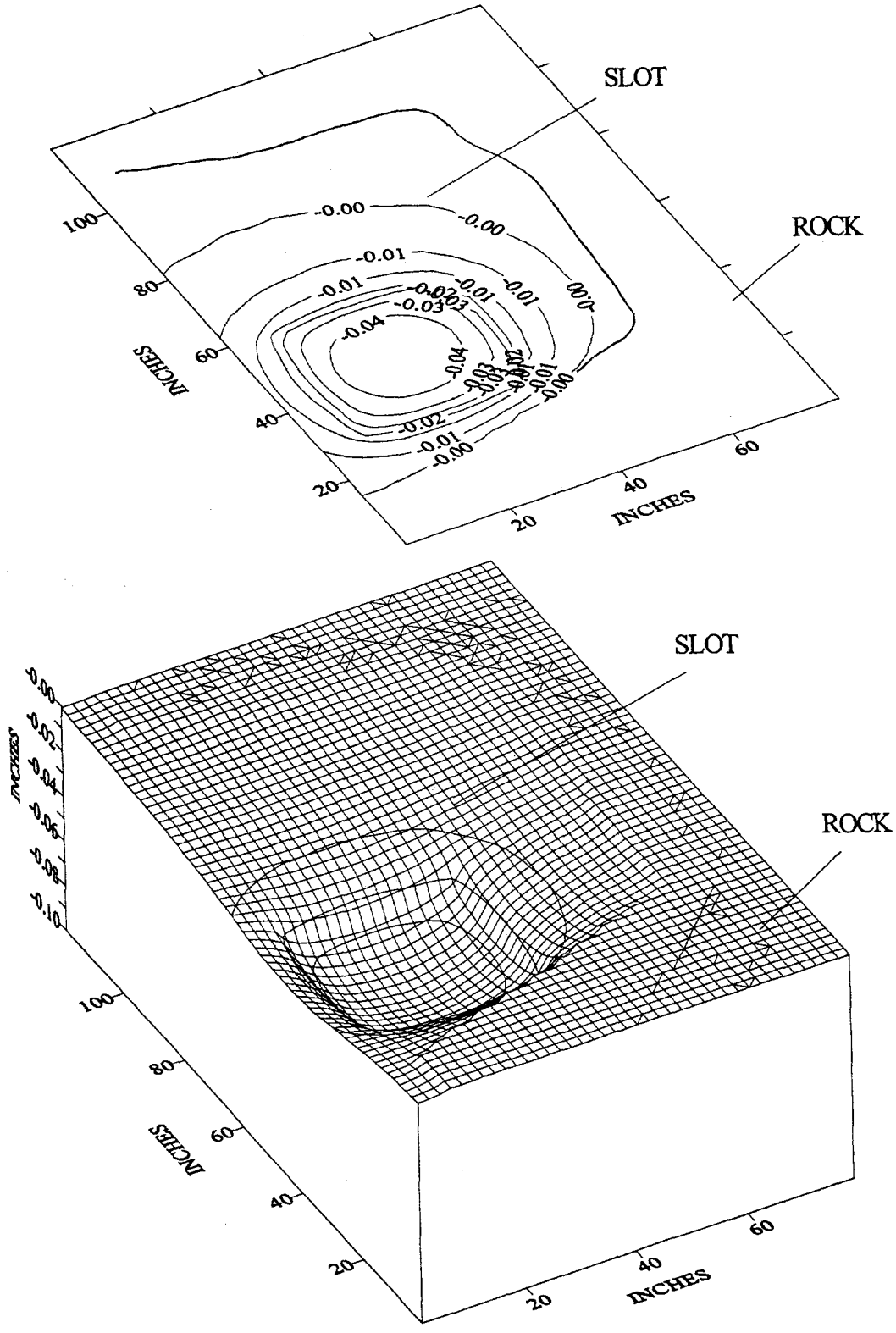

Figure 4-17. Distribution of the induced deformations from the 3D analysis. Values plotted here are the arithmetic differences between values plotted in 4-15 and 4-16.

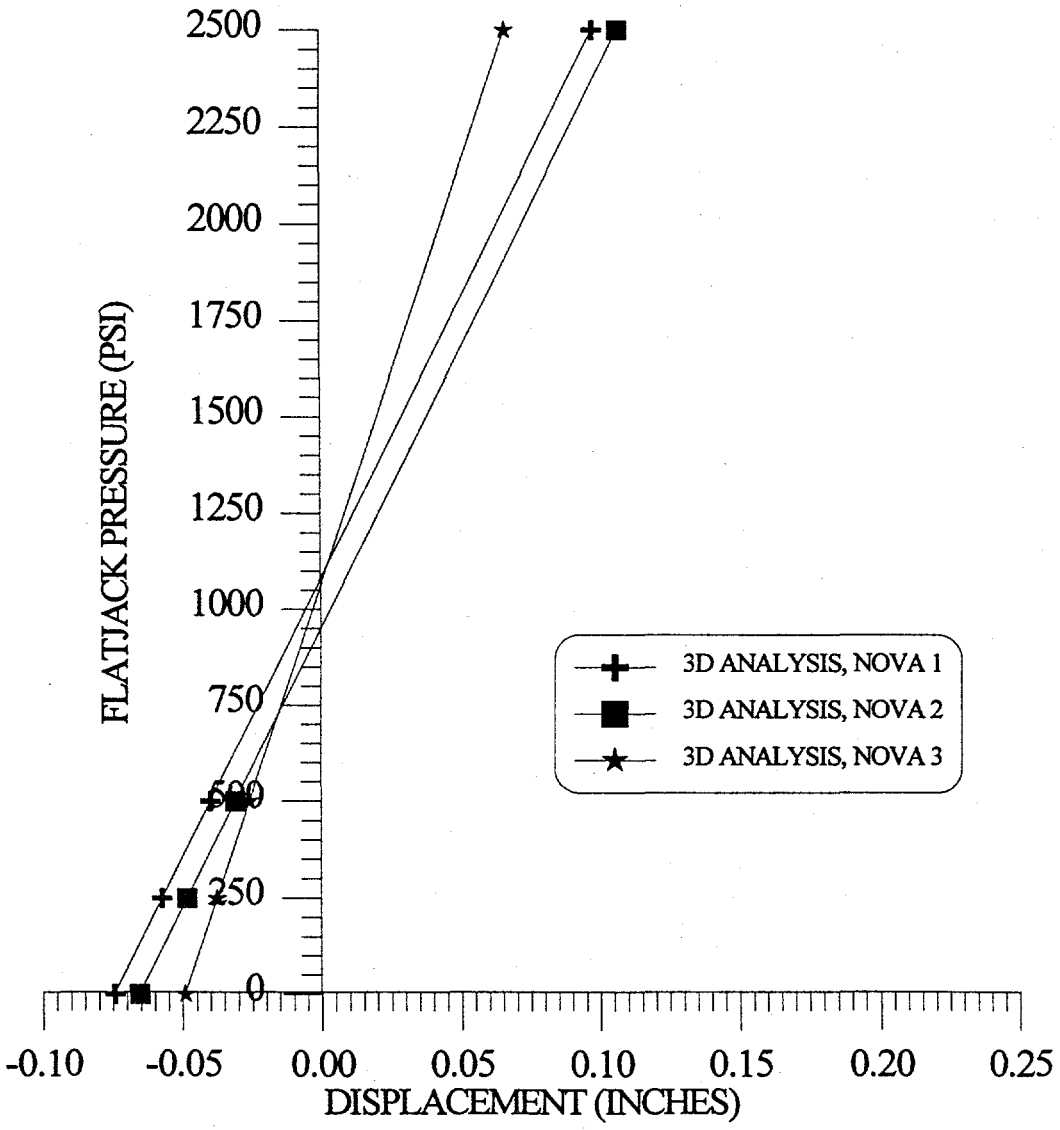

Figure 4-18. Computed deformations from the 3D analysis due to pressurization of the flatjack.

4.3 Discussion of Flatjack Tests and Results

The flatjack testing conducted at the DNA-UTP site produced complex and sometimes contradictory results. Several explanations can be offered for these results. First, the rock clearly exhibits nonlinear behavior and the geometry of the loading and instrumentation was not ideal. The nonlinear behavior is difficult to account for in the complex geometries of the flatjack tests and the simplified analytic models, which assume linearly elastic behavior. Second, measurement of cross-slot deformations by the use of anchored pins is a technique not ideally suited to "soft" materials, which exhibit large displacements upon loading and low strength. These types of pins are prone to rotation when the rock does not translate uniformly on loading. The Nova pin response during the initial load cycles is possibly a result of such rotation. The Nova gages were initialized to measure only extension during flatjack pressurization and were unable to measure any gage length shortening due to rotation of the Nova pins toward the slot. Figure 4-8, in particular, shows that the Nova 2 gage for the horizontal test was not responsive at low flatjack pressures and responded significantly only as pressures exceeded about 1,000 psi (6.9 MPa). It is suspected that displacements were controlled at lower pressures by rotation of the pins toward the slot and were only affected by translation at higher flatjack pressures. Third, flatjack techniques are particularly susceptible to rock mass disturbance as these tests are conducted very close to mined openings and can be affected by damage to the rock during the mining process. Damage during mining could cause a relaxation of stress surrounding the openings, which would result in lower slot normal stress as measured using flatjacks. Figures 4-16 and 4-17 show deformed meshes for the horizontal flatjack tests. Note the significant distortional displacements in the near field around the flatjack. Note also that the influence of the pressurized flatjack is limited to a small portion of the slot and that a large portion of the left part of the slot is largely undisturbed. Figure 4-17 in particular was used to assist in estimating the affected slot area in Table 4-1 for the slot-normal stress calculations.

A comparison of the JAC and EXPAREA results with the actual horizontal slot test data is presented in Figures 4-19 and 4-20. Both figures clearly show the lack of gage response at low flatjack pressure. In particular, Nova 3 does not register displacement until flatjack pressure reaches about 1,700 psi (11.7 MPa). The elastic modulus used for these analyses was 700,000 psi (4.86 GPa).

Although the early time low pressure data are questionable, it is interesting to note that the slopes of the Nova 2 and Nova 1 data compare favorably with the JAC results. This similarity suggests that the modulus used for these analyses may be consistent with the actual measured response of the rock mass.

The deformation in the 2D and 3D simulations that correspond to the anchor points of the field tests are compared in Table 4-4.

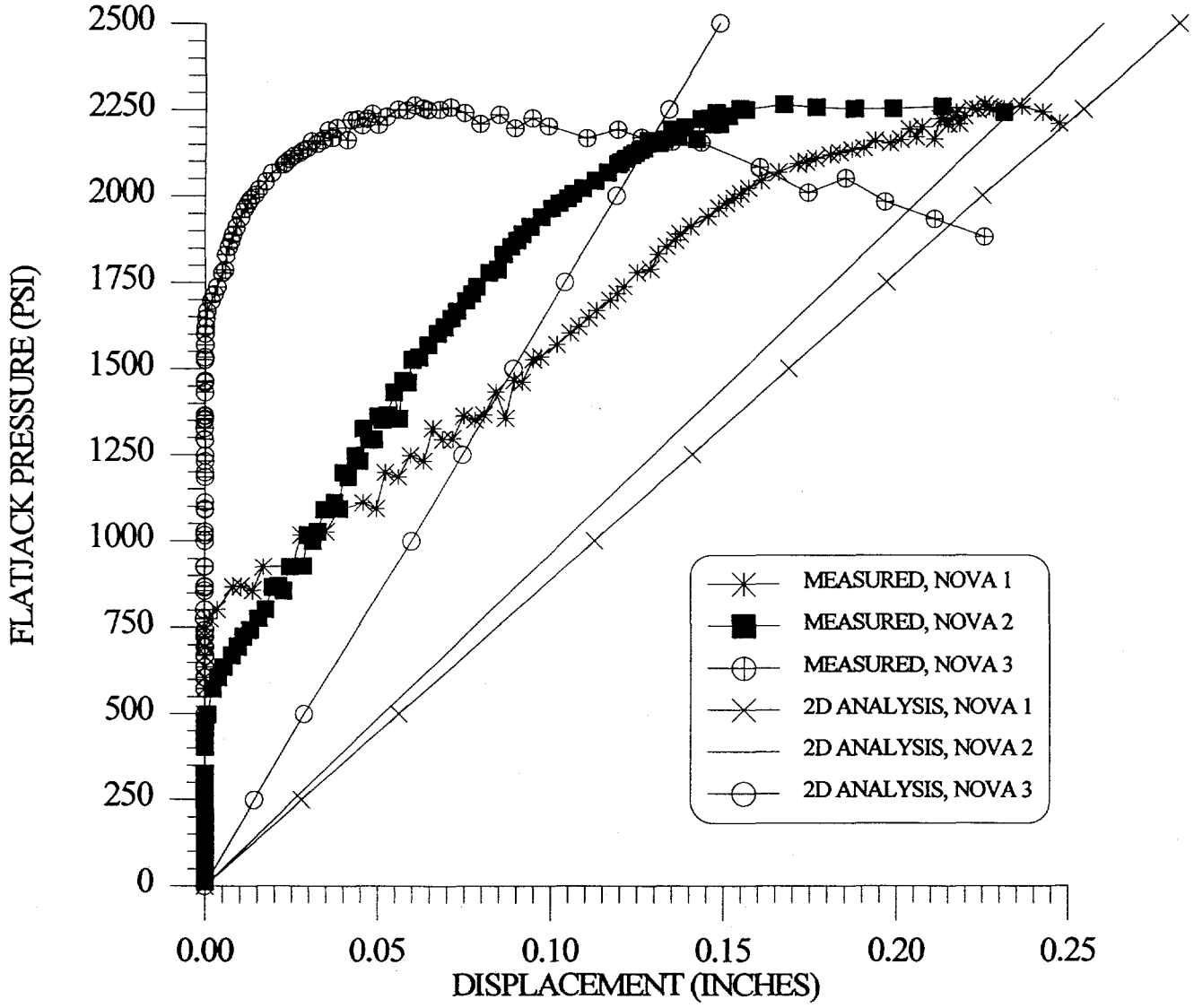

Figure 4-19. Measured deformations due to flatjack pressurization and computed results from 2D analysis (JAC).

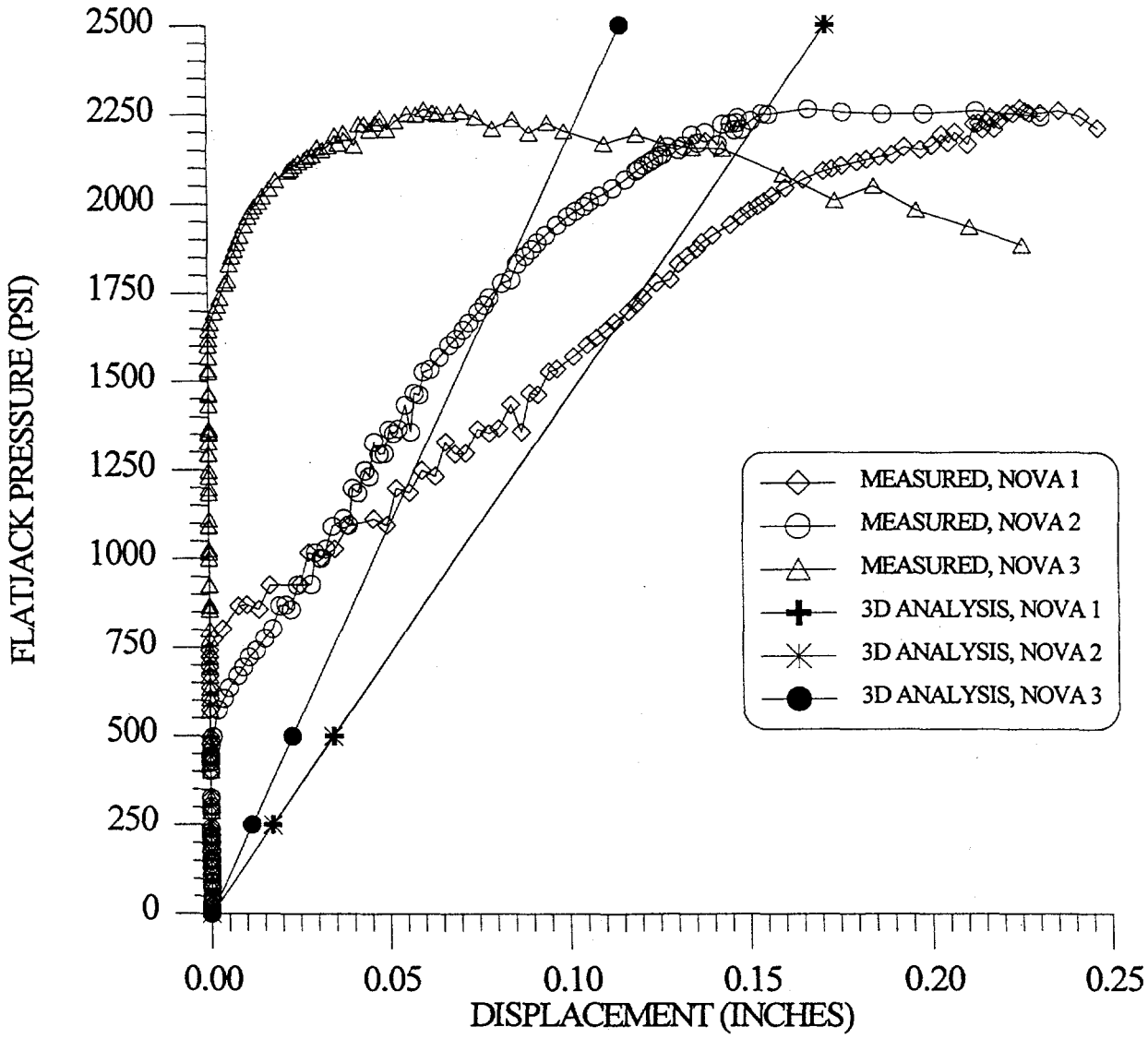

Figure 4-20. **Measured deformations due to flatjack pressurization and computed results from the 3D analysis (EXPEREA).**

Table 4-4. Measured and Calculated Slot Closure Due to the Excavation of the Horizontal Slot

Analysis		NOVA 1	NOVA 2	NOVA 3
2D	Measured (inches)	0.027	0.011	0.009
	Calculated (inches)	0.092	0.077	0.045
	Ratio (%)	29.4	14.3	20.0
3D	Measured (inches)	0.027	0.011	0.009
	Calculated (inches)	0.074	0.065	0.049
	Ratio (%)	36.5	16.9	18.4

The ratio of the measured to the calculated relaxation of the slot expressed as a percentage ranged between 14 and 37% of the calculated displacements. The largest difference occurred for the Nova 2 gage. The scatter in the ratio of measured to calculated closure suggests that the mismatch is not simply due to the difference between elastic modulus of the overcoring and rock mass scales. Applying an average correction for the 3D analysis would require increasing the elastic modulus to 2.3×10^6 psi (15.9 GPa), which exceeds the highest value measured in overcoring by a factor of 3.1 (see Table 4-2).

The pressure-deformation response of the slots is compared to the analysis results in two forms: first, the magnitudes of the pressures required to cancel the slot closure due to excavation are compared in Table 4-5; second, the pressure-deformation records for the slot tests are compared in Figures 4-19 and 4-20 for the 2D and 3D analyses, respectively.

Table 4-5. Comparison of Measured and Calculated Cancellation Pressure for the Horizontal Slot (psi)

Analysis		NOVA 1	NOVA 2	NOVA 3
2D	Measured	1370	1100	1960
	Calculated	820	710	820
	Ratio (%)	59.9	64.5	41.8
3D	Measured	1370	1100	1960
	Calculated	1090	950	1070
	Ratio (%)	79.6	86.4	54.6

In Table 4-5, the ratio of the calculated to the measured cancellation pressures expressed as a percentage ranged between 42 and 86%. The relative magnitudes of the cancellation pressure ratios are much greater than for the slot closure ratios presented in Table 4-4. The 3D results presented in Table 4-5 show significantly better agreement with the measured data than do the 2D results.

5.0 Summary

It is clear from the previous discussions that only the overcoring technique produced results that are repeatable and consistent with predictions of in situ stress based on gravitational loading. The overcoring results showed principal stress magnitudes and orientations as follows:

σ_1 = 373 psi (2.57 MPa) at 34°N 63°E
σ_2 = 281 psi (1.94 MPa) at 122°N 40°E
σ_3 = 176 psi (1.21 MPa) at 101°N 137°E

inclination is measured as 0° = vertical down and 180° = vertical up.

These values are consistent in magnitude and orientation to those expected due to gravitational loading and topographic effects. Measurement of modulus using the biaxial cell yielded moduli from 340,000 to 1,270,000 psi (2.36 to 8.76 GPa) with a modulus anisotropy of up to about 4 with horizontal modulus being the higher. This modulus anisotropy is consistent with other laboratory results presented in Appendix A.

The ASR testing did not produce reasonable results. In fact, the core tested contracted rather than expanded during the measurements. This complex behavior could be due to pore fluids in the shale, slowly bleeding off over time. Additional testing with immediate application of the strain gages may eliminate some of the testing problems. However, the rock's complex anelastic response could still confuse the results.

The flatjack testing results are perhaps the most complex of all. Stresses measured using the flatjacks were consistently lower than what would be expected based on the overcoring results. The ranges of moduli estimated using standard analytical techniques are extreme, with the upper values very much in question. A comparison of results from numerical modeling with data from the horizontal flatjack test suggest a rock mass modulus of about 700,000 psi (4.86 GPa) normal to the horizontal slot. This is consistent with the analytical analysis of the flatjack load/unload histories (Bowles, 1982; Loureiro-Pinto, 1986) that suggest rock mass modulus between 870,000 and 1,450,000 psi (6 and 10 GPa). It is thought that most of the difficulty encountered in interpreting the flatjack results can be attributed to the complex nonlinear behavior of the rock mass, the complex test geometry, and difficulties due to possible pin rotations. Much of the test related problems could be resolved by reconfiguring the instrumentation to make primary slot deformation measurements from within the slot. This is especially important for materials of low stiffness and strength where significant distortion can occur in the rock at the edge of the flatjack.

6.0 References

Alexander, L.G. 1960. "Field and Laboratory Tests in Rock Mechanics," *Proceedings of the 3rd Australian-New Zealand Conference on Soil Mechanics and Foundation Engineering.* 161-168.

Baumeister, T. 1978. *Mark's Standard Handbook for Mechanical Engineers.* 8th ed. New York, NY: McGraw-Hill.

Becker, R.M., and V.E. Hooker. 1967. *Some Anisotropic Considerations in Rock Stress Determinations*, RI 6965. Washington, DC: U.S. Department of the Interior, Bureau of Mines.

Bickel, D.L. 1985. Overcoring Equipment and Techniques Used in Rock Stress Determination. (Bureau of Mines Information Circular 9013, an update of IC 8618).

Bickel, D.L. 1993. *Rock Stress Determinations from Overcoring: An Overview.* Bulletin 694 E2X, S2X, Washington, DC: U.S. Department of the Interior, Bureau of Mines.

Biffle, J.H. 1984. *JAC-A Two-Dimensional Finite Element Computer Program for the Non-Linear Quasistatic Response of Solids with the Conjugate Gradient Method.* SAND80-0998. Albuquerque, NM: Sandia National Laboratories.

Blanton, T.L. 1983. "Relation Between Recovery Deformation and In-Situ Stress Magnitudes," *Proceedings, 1983 SPE/DOE Joint Symposium of Low Permeability Reservoirs, Denver, CO, March 13-16, 1983.* SPE 11624. Dallas, TX: Society of Petroleum Engineers of AIME.

Bowles, J.E. 1982. *Foundation Analysis and Design.* 3rd ed. New York, NY: McGraw-Hill.

Carlisle, S.P., and C.E. Brechtel. 1991. "Development of a Rock Cutting Saw System for Preparing In Situ Tests in Welded Tuff." SLTR91-4003. Albuquerque, NM: Sandia National Laboratories.

Chen, E.P. 1991. "Analysis of G-Tunnel High-Pressure Flatjack Development Test." SLTR90-4004. Albuquerque, NM: Sandia National Laboratories.

Duvall, W.I., and J.R. Aggson. 1980. *Least Squares Calculation of Horizontal Stresses from More Than Three Diametral Deformations in Vertical Boreholes.* RI 8414. Washington, DC: U.S. Department of the Interior, Bureau of Mines.

Goodman, R.E. 1980. *Introduction to Rock Mechanics.* New York, NY: John Wiley & Sons.

Hansen, F.D., R.E. Finley, and J.T. George. 1990. "Rock-Mass Experiments on Jointed Welded Tuff," *Proceedings of the International Conference on Mechanics of Jointed and Faulted Rock, Institute of Mechanics, University of Vienna, Austria, April 18-20, 1990.* Rotterdam: A.A. Balkema. 961-968.

Hardy, R.D. 1993. Event Triggered Data Acquisition in the Rock Mechanics Laboratory. SAND93-0256. Albuquerque, NM: Sandia National Laboratories.

Holcomb, D.J., and M.J. McNamee. 1986. "A Displacement Gage for Rock-Mechanics Laboratory," *Experimental Mechanics*. Vol. 26, no. 3, 217-223.

Jaeger, J.C., and N.G.W. Cook. 1979. *Fundamentals of Rock Mechanics*. 3rd ed. New York, NY: John Wiley & Sons.

Jung, J. 1991. "Three-Dimensional Analysis of the G-Tunnel High-Pressure Flatjack Development Test." SLTR91-4002. Albuquerque, NM: Sandia National Laboratories.

Kruse, G. 1963. *Static Stress Determinations at Oroville Underground Powerhouse (flatjack and borehole technique)*. California Dept. Water Resources, Rock Mechanics Report No. 4.

Lindner, E.N., and J.A. Halpern. 1978. "In-Situ Stress in North America: A Compilation," *International Journal of Rock Mechanics and Mining Sciences & Geomechanics Abstracts*. Vol. 15, no. 4, 183-203.

Loureiro-Pinto, J. 1986. "Suggested Method for Deformability Determination Using a Large Flat Jack Technique," *International Journal of Rock Mechanics and Mining Sciences & Geomechanical Abstracts*. Vol. 23, no. 2, 131-140.

Merrill, R.H., and J. Peterson. 1961. *Deformation of a Borehole in Rock.* RI 5881. U.S. Department of the Interior, Bureau of Mines.

Panek, L.A. 1961. "Measurement of Rock Pressure with a Hydraulic Cell," *Transactions of the American Institute of Mining, Metallurgical, and Petroleum Engineers*. Vol. 220, 287-290.

Panek, L.A., and J.A. Stock. 1964. *Development of a Rock Stress Monitoring Station Based on the Flat Slot Method of Measuring Existing Rock Stress*. RI-6537. College Park, MN: U.S. Department of the Interior, Bureau of Mines.

Panek, L.A. 1965. *Calculation of the Average Ground Stress Components from Measurements of the Diametral Deformation of a Drill Hole*. RI 6732. Washington, DC: U.S. Department of the Interior, Bureau of Mines.

Rocha, M. 1966. "Rock Mechanics in Portugal," *1st Congress of the International Society of Rock Mechanics, Lisbon, Portugal, September 25-October 1, 1966*. Vol. 3, 121-141.

Rocha, M., and J.N. da Silva. 1970. "A New Method for the Determination of Deformability in Rock Masses," *Proceedings of the Second Congress of the International Society for Rock Mechanics, Belgrade, Yugoslavia, September 21-26, 1970.* Belgrade: Institute for Development of Water Resources. Vol. 1, no. 2-21, 423-437.

Smith, M.B., N.K. Ren, G.G. Sorrels, and L.W. Teufel. 1986. "A Comprehensive Fracture Diagnostics Experiment: Comparison of Seven Fracture Azimuth Measurements," *SPE Production Engineering.* Vol. 2, 423-432.

St. John, C.M. 1978. EXPAREA: *A Computer Code for Analysis of Test Scale Underground Excavations for Disposal of Radioactive Waste in Bedded Salt Deposits*, Y/OWI/SUB-7118/2. Oak Ridge, TN: Office of Waste Isolation.

Teufel, L.W. 1982. "Prediction of Hydraulic Fracture Azimuth from Anelastic Strain Recovery Measurements of Oriented Core," *Issues in Rock Mechanics, Proceedings of the 23rd Symposium on Rock Mechanics, University of California, Berkeley, CA, August 25-27, 1982.* Eds. R.E. Goodman and F.E. Heuze. New York, NY: Society of Mining Engineers of the American Institute of Mining, Metallurgical and Petroleum Engineers. Vol. 23, 238-245.

Teufel, L.W., and N.R. Warpinski. 1984. "Determination of In Situ Stress from Anelastic Strain Recovery Measurements of Oriented Core: Comparison to Hydraulic Fractures Stress Measurements in the Rolling Sandstone, Piceance Basin, Colorado," *Rock Mechanics in Productivity and Protection, Proceedings Twenty-Fifth Symposium on Rock Mechanics, Northwestern University, Evanston, IL, June 25-27, 1984.* Ed. C.H. Dowding and M.M. Singh. New York: Society of Mining Engineers of the American Institute of Mining, Metallurgical and Petroleum Engineers. 176-185.

Tincelin, E. 1951. "Research on Rock Pressure in the Iron-Mines of Lorraine (France)," *Proc. 1st Int. Conference on Rock Pressure and Support in Workings, Liege, France.*

Underground Technology Program (UTP). 1991. *Geotechnical Design Summary Report, Volume 2 - Appendices B&C.*"

Warpinski, N.R., and L.W. Teufel. 1989a. "In-Situ Stresses in Low-Permeability, Nonmarine Rocks," *JPT, Journal of Petroleum Technology.* Vol. 41, no. 4, 405-414.

Warpinski, N.R., and L.W. Teufel. 1989b. "Viscoelastic Constitutive Model for Determining In-Situ Stress Magnitudes from Inelastic Strain Recover of Core," *SPE Production Engineering.* Vol. 4, no. 3, 272-280.

Zimmerman, R.M., K.L. Mann, R.A. Bellman, Jr., Steven Luker, and D.J. Dodds. 1991. *G-Tunnel Pressurized Slot-Testing Evaluations.* SAND87-2778. Albuquerque, NM: Sandia National Laboratories.

APPENDIX A

Supporting Laboratory Mechanical Properties Testing and Observations

Sandia National Laboratories
Albuquerque, New Mexico 87185-0751
Geomechanics Department

date: July 7, 1994

to: L. S. Costin, 6313 MS1326

Robert Hardy

from: R. D. Hardy, 6117 MS0751

subject: Mechanical Properties of New Providence Shale.

We received one piece of core from Hole #3 at the Rodgers Hollow Site on the Fort Knox Military Reservation.

We removed two sub-cores, NPS1 and NPS2, two inches diameter by five inches long for testing. Sub-cores were parallel to the main core. Both samples were centerless ground on their OD, then end ground to produce parallel ends normal to the core axis. Sample material was stored in water between machining operations and until final test assembly was begun. Test specimens were coated with bees wax for testing. The tested samples were preserved by dipping in bees wax after removal of gauges and end caps.

After machining, dimensions were measured with results entered on Test Data Report forms. There were surface blemishes made by the grinder which are noted on the test report (copies attached).

Acoustic wave velocities were measured in three axes on the velocity bench. Both compressional and shear wave velocities were measured with shear in two orthogonal directions on each axis. When the shear particle motion is parallel to the bedding plane, the compressional wave is attenuated. It would seem that this material channels shear waves along the bedding plane. All readings were made using shear transducers which allow us to get both shear and compressional wave velocities simultaneously. Results are shown in Table 1.

The original core came from a horizontal hole parallel to the drift. In the following discussion, axial is parallel to the drift in a horizontal plane and lateral is transverse to the drift in a horizontal plane, (see Figure 1).

There were a total of six readings made in different orientations as follows:

1) P-wave axial through the sample and the S-wave polarized in the vertical direction, (P_{11}, S_{13}).

2) P-wave axial through the sample and the S-wave polarized in the horizontal direction, (P_{11}, S_{12}).

3) P-wave in the vertical direction and the S-wave polarized in the axial direction, (P_{33}, S_{31}).

4) P-wave in the vertical direction and the S-wave polarized in the horizontal lateral direction, (P_{33}, S_{32}).

5) P-wave in the horizontal direction and the S-wave polarized axial to the sample, (P_{22}, S_{21}).

6) P-wave in the horizontal direction and the S-wave polarized in the vertical direction, (P_{22}, S_{23}).

NOTE: For NPS1 reading #1 the S-wave arrival is detectable at two times. This can be explained by the fact that the shale is birefringent. If the transducers are aligned a few degrees off of the

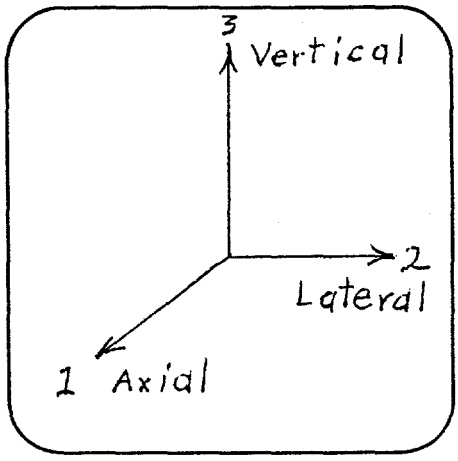

Figure 1: Orientation of Compressional and Shear waves.

Velocity (mm / μsec)						
			NPS1		NPS2	
Reading #	Wave Orientation		P-wave	S-wave	P-wave	S-wave
1	P_{11}	S_{13}	3.69	2.04/1.16	3.77	1.93
2	P_{11}	S_{12}	–	1.96	2.84	2.04
3	P_{33}	S_{31}	2.90	1.24	–	1.26
4	P_{33}	S_{32}	2.88	1.17	2.28	1.19
5	P_{22}	S_{21}	3.70	1.99	3.73	2.04
6	P_{22}	S_{23}	3.62	1.17	3.81	1.16

Table 1: P & S Wave velocities. The P-wave arrival is very difficult to pick in the P_{11} and P_{22} directions. It could not be located in NPS1 reading two and NPS2 reading three.

bedding plane the S-wave will be split into fast and slow components which were detectable in this case. The first arrival yielded a velocity of 2.04 mm / μsec. The second arrival yielded a velocity of 1.16 mm / μsec. By symmetry, the shear velocity from the first, third, fourth and sixth readings should be identical. This symetry was observed in the slow wave arrival on NPS1 but was not observed on NPS2.

After measuring wave velocities the samples were prepared for uniaxial compression testing. Steel end caps 0.5 inches thick were applied with scotch tape around their periphery and the assembly was then dipped in bees wax to seal the surface. The wax was removed from the end cap face. Rings were attached to mount LVDT displacement transducers. The rings mount on three points which bear against the sample surface through the bees wax. Wax was applied around the mounting points to seal and secure them, (see sketch on the test report).

Two tests were conducted with load applied parallel to the bedding plane. Displacement was measured parallel and transverse to the load. In the first test, lateral displacement was measured normal to the bedding plane, (vertical). In the second test lateral displacement was measured parallel to bedding, (horizontal). As might be expected, the lateral strain was quite different in the two orientations. The properties are tabulated in Table 2 and displayed in the attached figures.

Mechanical Properties			
Sample	Peak Stress	Young's Modulus	Poisson's Ratio
NPS1	17.92 MPa	4.84 GPa	0.824
NPS2	14.96 MPa	5.56 GPa	0.124

Table 2: Mechanical Properties of New Providence Shale as Measured in the Rock Mechanics Laboratory

Attachments:

Test Data Packages for both tests.
Disk containing DATAVG and MATLAB files for both tests, (Costin only).

Copy to:

J. T. George, MS1326
R. E. Finley, MS1326
D. J. Holcomb, MS0751
W. R. Wawersik, MS0751
6117 file, MS0751

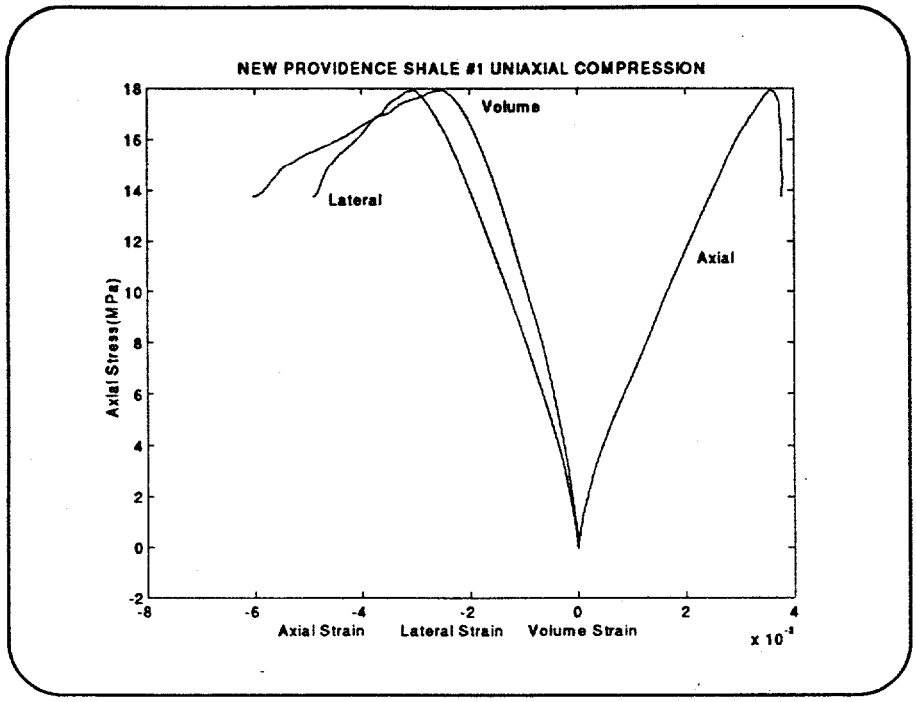

Figure 2:

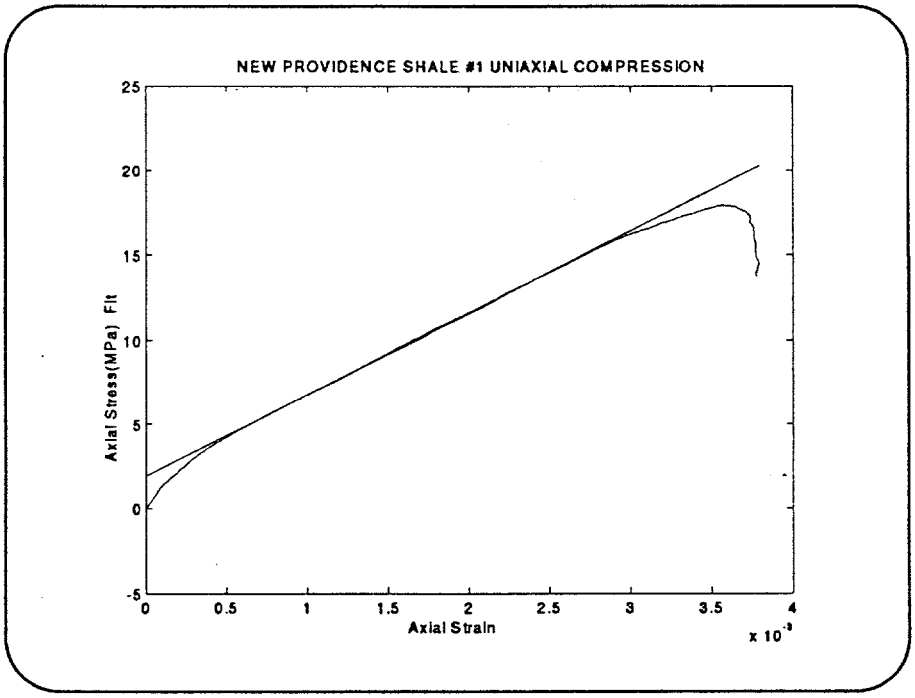

Figure 3:

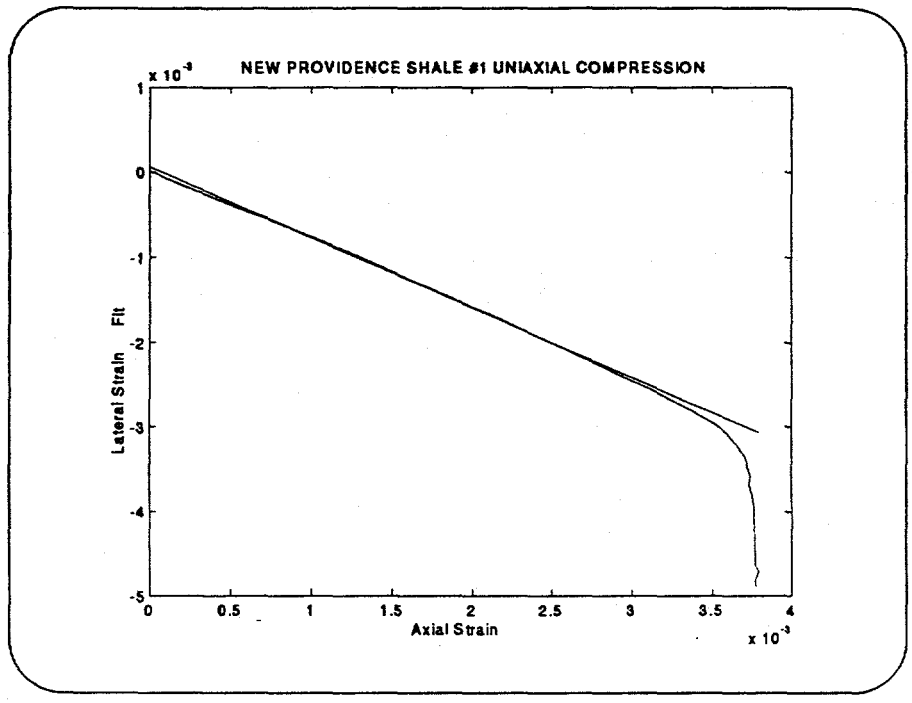

Figure 4:

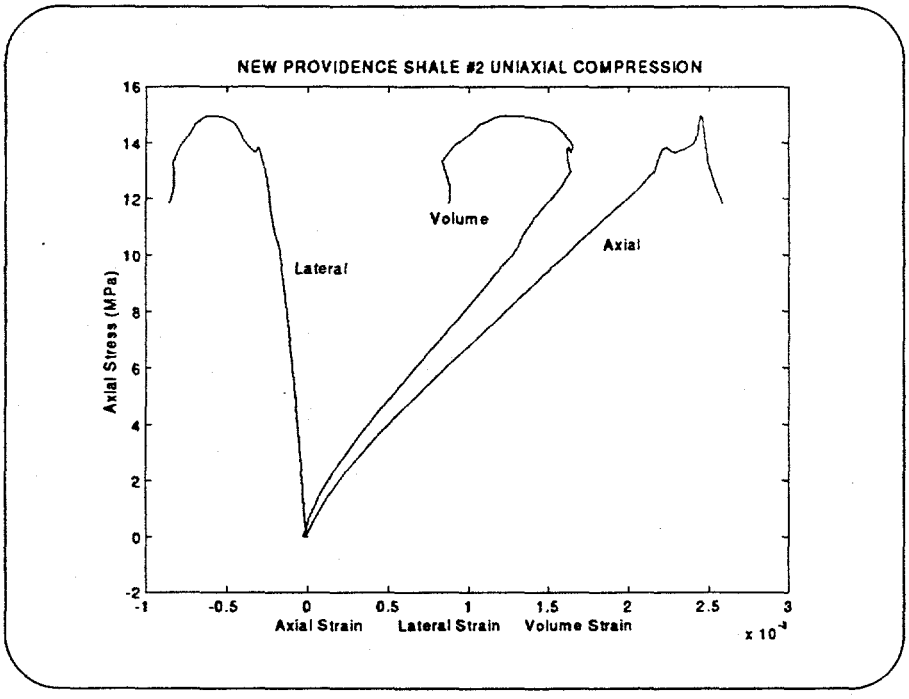

Figure 5:

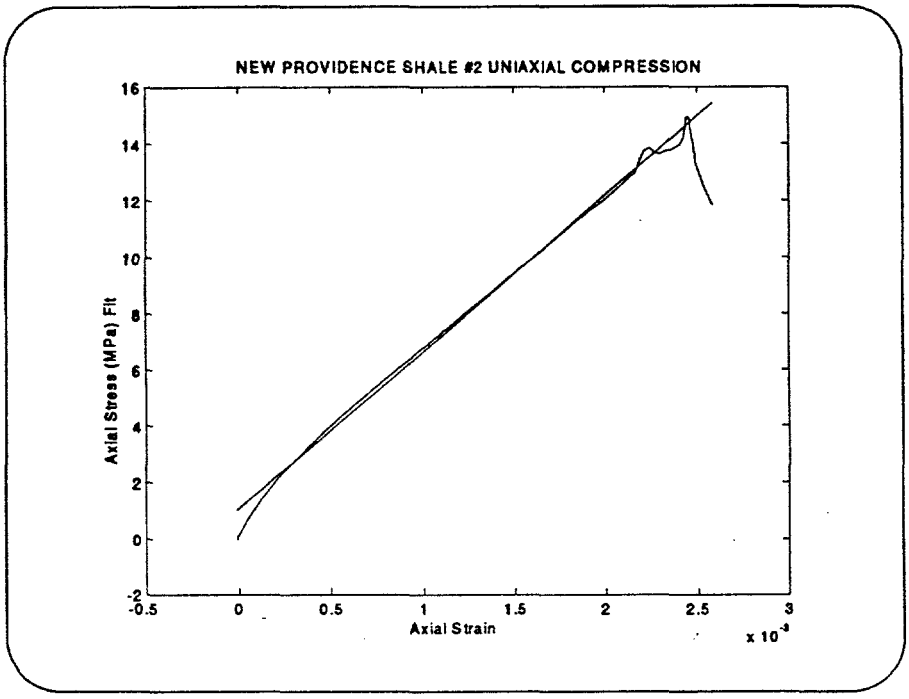

Figure 6:

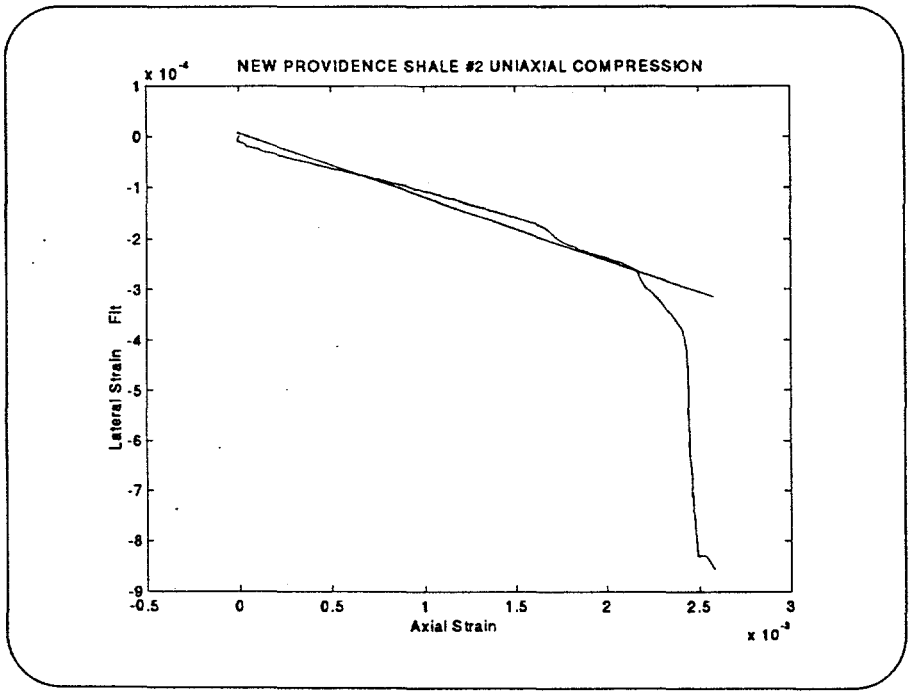

Figure 7:

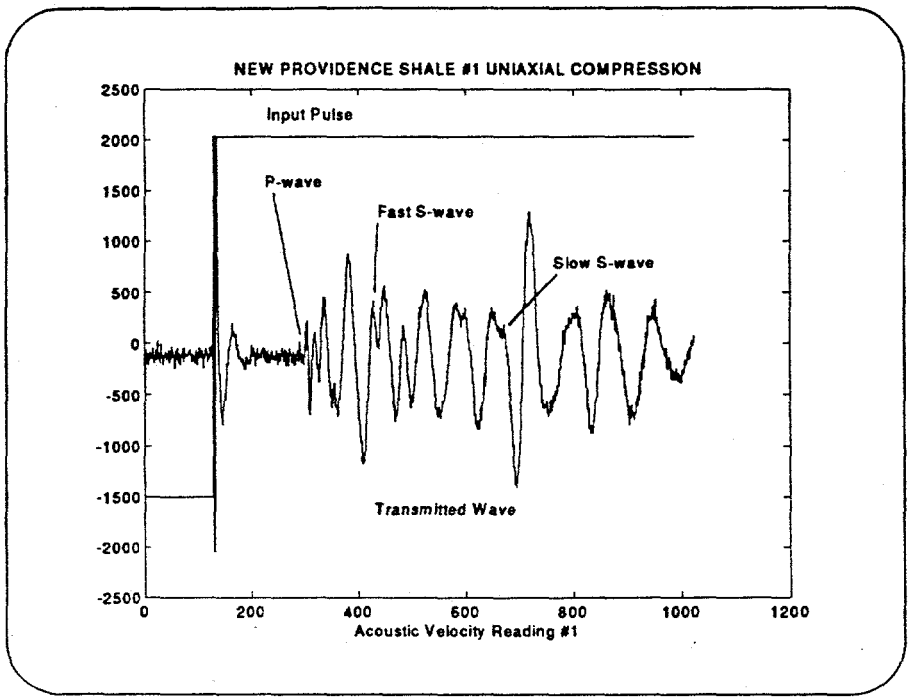

Figure 8:

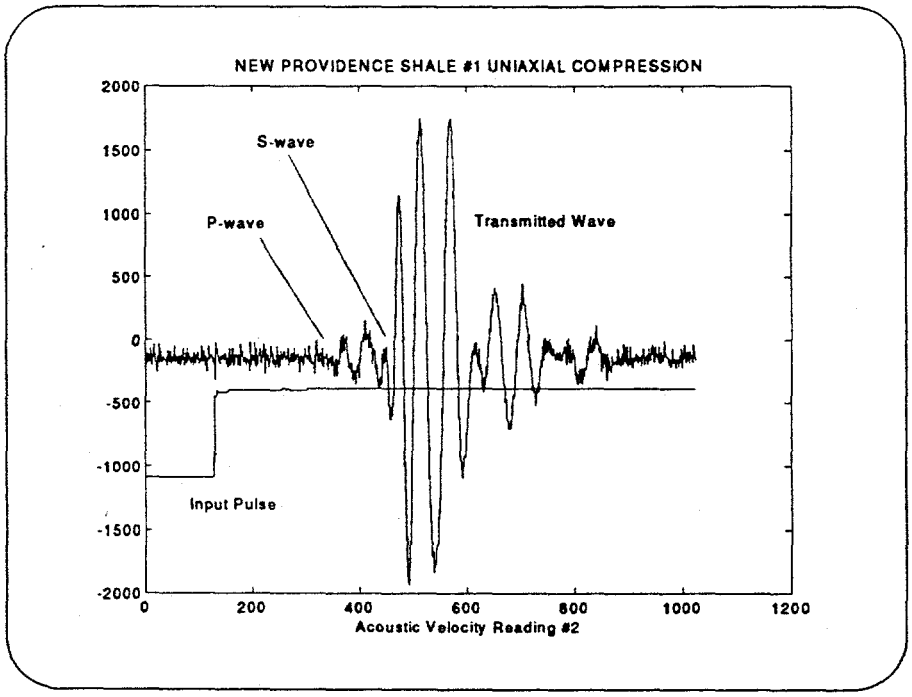

Figure 9:

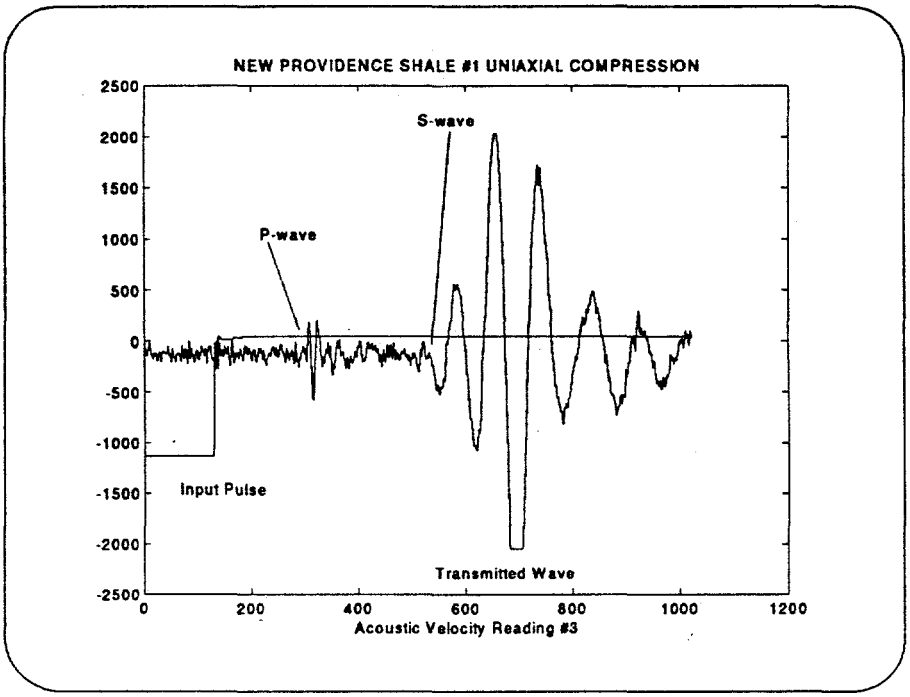

Figure 10:

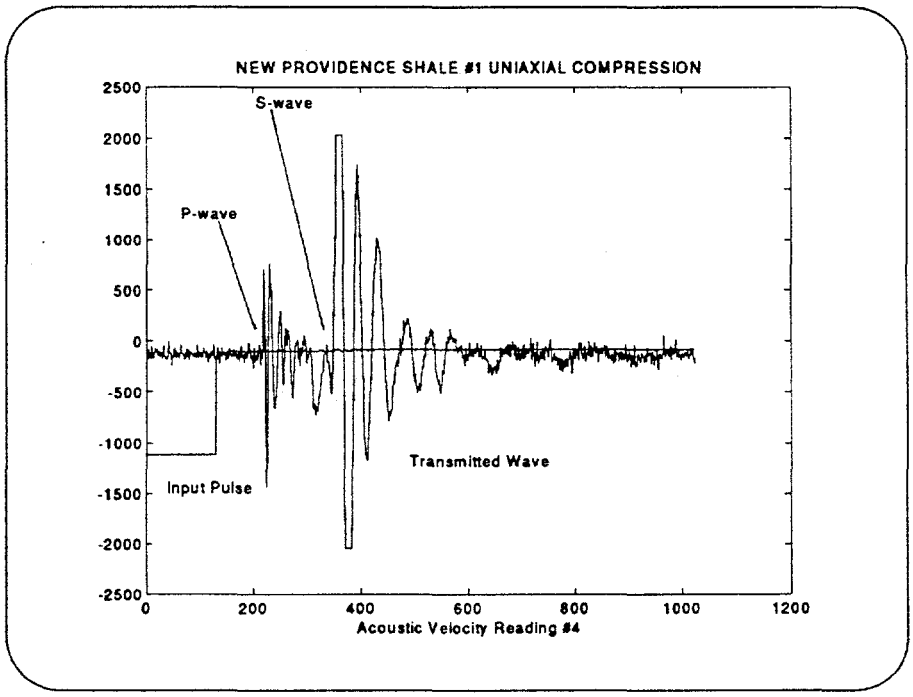

Figure 11:

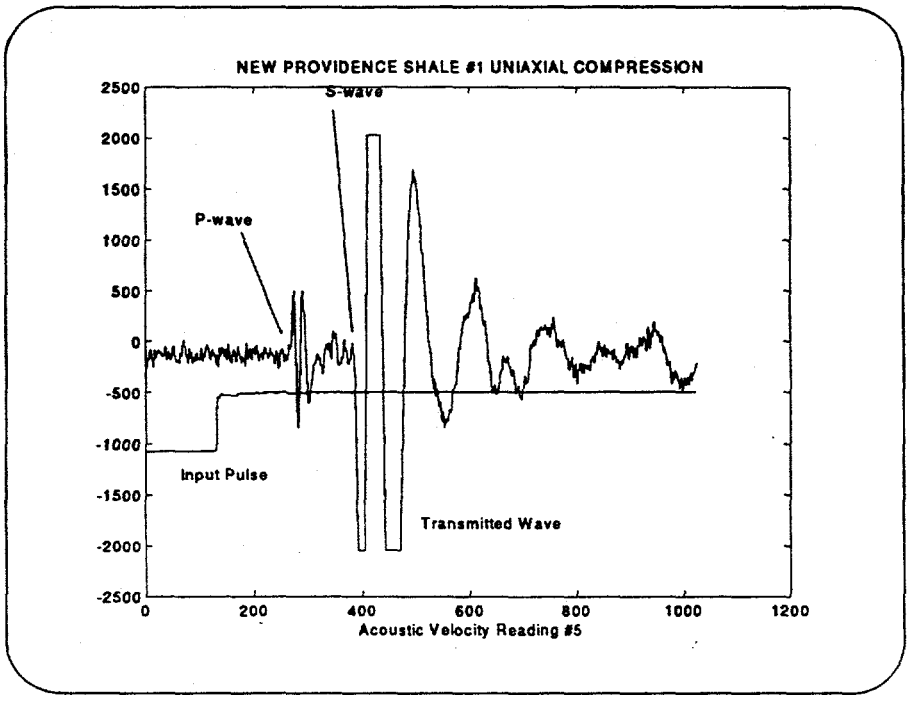

Figure 12:

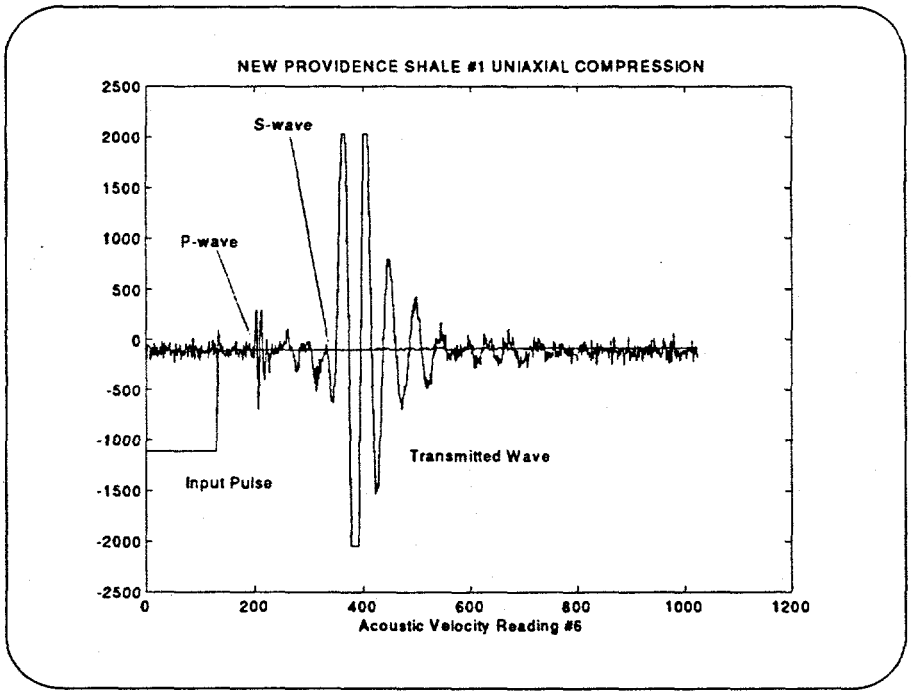

Figure 13:

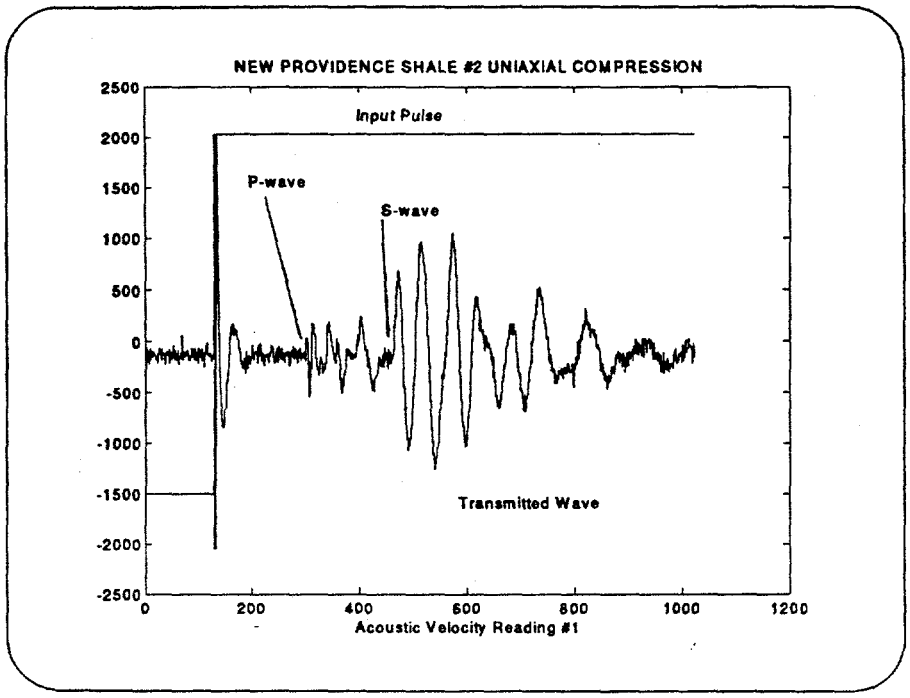

Figure 14:

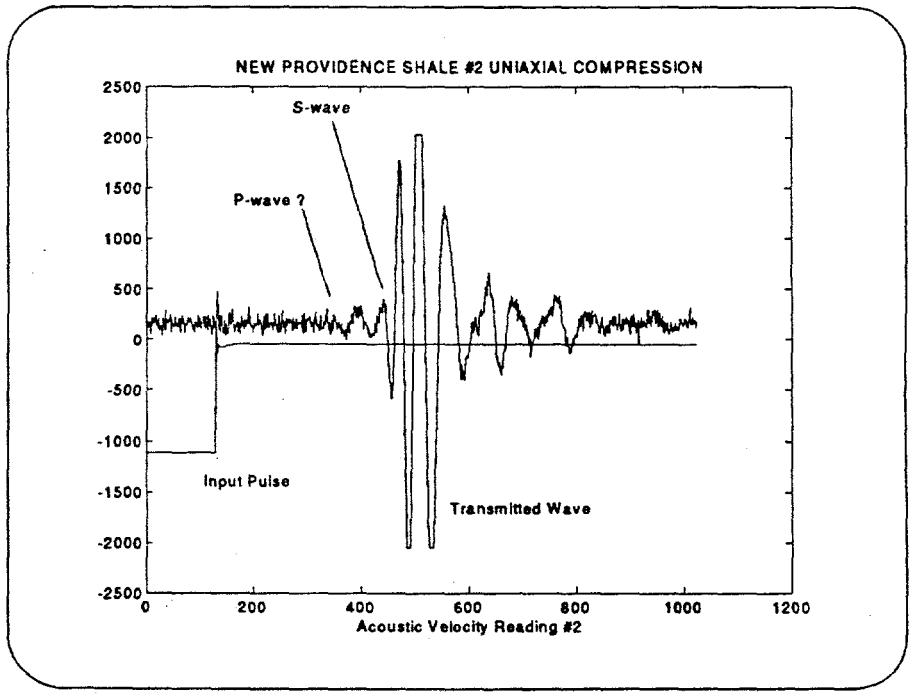

Figure 15:

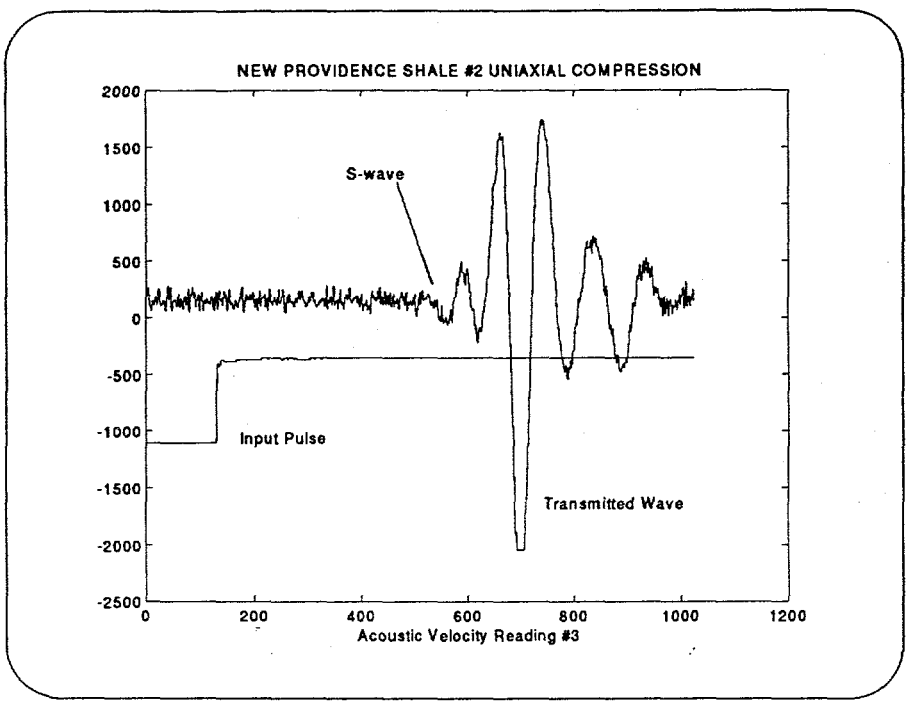

Figure 16:

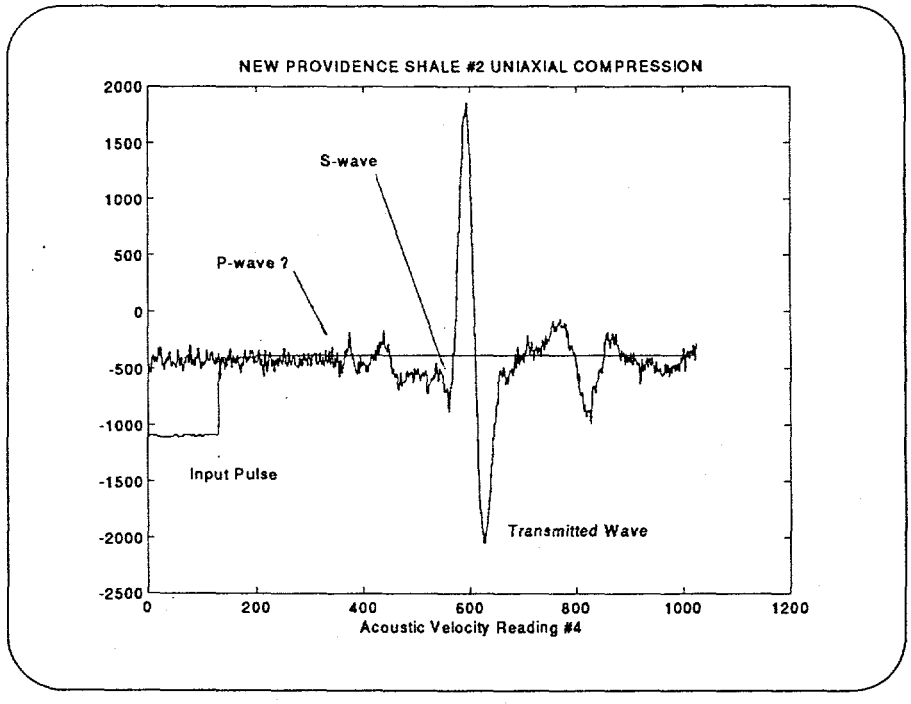

Figure 17:

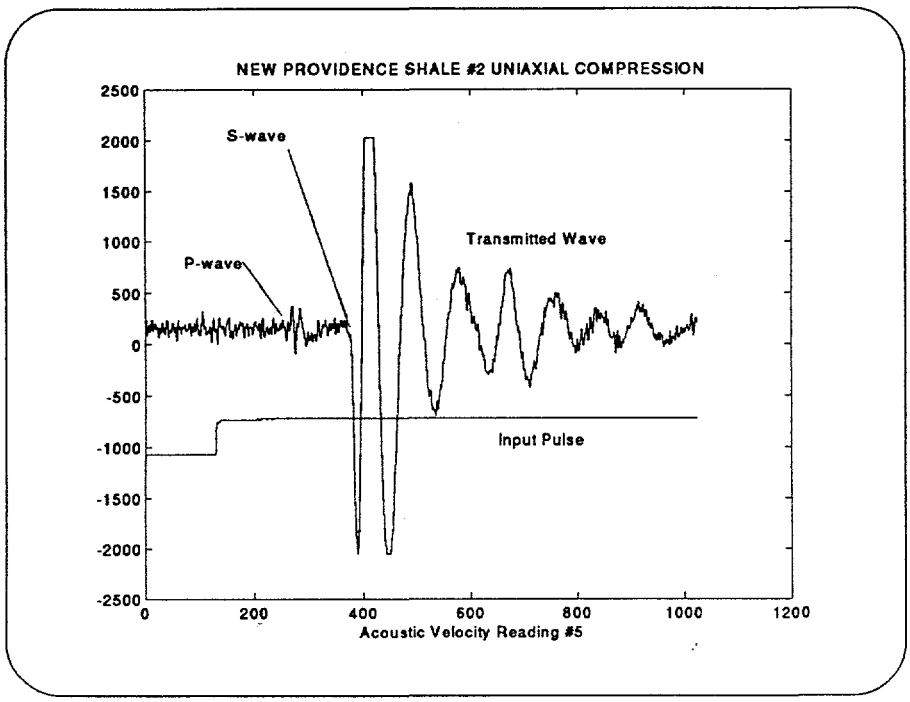

Figure 18:

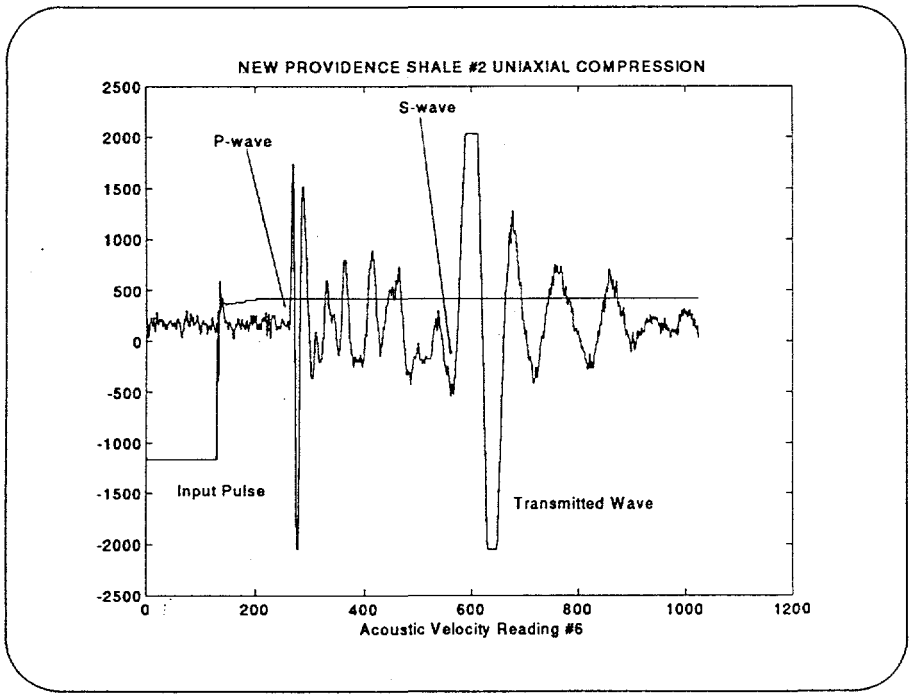

Figure 19:

RML3-1 March 8, 1994

Page: _____ Of: _____

Date: 6/28/94

Initials: RDV

Rock Mechanics Laboratory Test Check List

Test ID: NPS1

Requester: J. Holcomb

Case Number: 4274.000

Mark those items present and indicate the number of each.

☒ Test Request Form: Pages 1

☒ Test Data Report Form: Pages 3

☐ Data Disk(s): Number 1

☒ Calibration Data: Pages 2

☒ Plots: Pages 3

☒ Additional Notes: Pages 1 [illegible]

☐ Analysis Notes: Pages _____

☐ Other: _____ Pages _____

☐ Other: _____ Pages _____

☐ Other: _____ Pages _____

☐ Other: _____ Pages _____

Notes:

Unused spaces intentionally left blank.

RML1-1, February 16, 1994

Page: _____ Of: _____

Date: 6/28/94

Initials: RDH

Rock Mechanics Laboratory Test Request Form

(Use to collect and organize your thoughts when planning a test.)

Test ID: NPS 1

Requester: D. Holcomb

Case Number: 4274.000

Type of Test: Uniaxial Compression

Confining Pressure: 0

Due Date: _____

Objectives: (Why are we doing this test.) _____

Sample Material: (Specify control number if needed.) #1 New Providence shale

Sample Shape and Dimensions: (Specify units.)

☒ Cylinder: Diameter: 2"

Length: 5"

☐ Prism: Width: _____ Height: _____ Thickness: _____

Preparation Details: (Finish, Cautions, etc.)

Core & grind. Keep in water until coating is applied.

Instrumentation: (Location and Type. Attach sketch if you feel it will help.)

Axial & Lateral LVDTs. Make P & S velocity readings axial, vertical & Horizontal

Special Instructions:

Sample Disposition: Coat & bag

Data Disposition: _____

Other: _____

Test Control:

Axis:	Control Variable:	Units Desired:	Ramp Rate:
Load		Kn	
Stroke		mm	
Pressure			
Axial Strain	x	m m	10^{-5} strain rate
Lateral Strain		m m	

Neatness Counts! If your instructions cannot be read, the test may be delayed.
Unused spaces intentionally left blank.
*** Attach continuation pages as needed. ***

RML2-1(April 8, 1994)

Page: _____ Of: _____

Date: 6/25/94

Initials: RDT

Rock Mechanics Laboratory Test Data Report

Sample Preparation Details

Test ID: NPS 1

Requester: D. Holcomb

Case Number: 4274.000

Technician(s): Hardy

Sample Material: (Specify control number if needed.) #1 New providence shale

Diameter: 1.977" Length: 4.969" Width: _____ Height: _____

Mass: 657.6 g Coating: Bees Wax Other: _____

Sketch: (Include Dimensions & add continuation pages as needed.)

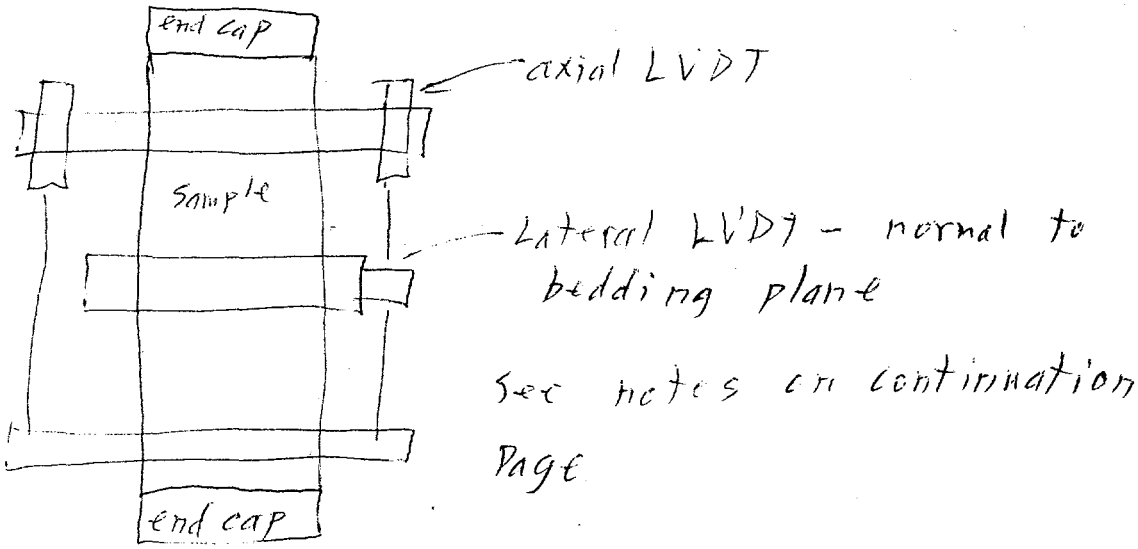

Preparation Details: Material was cored from original sample then ground all surfaces. Sample was kept in water between operations. Tap water used as a coolant for all machining. End caps secured with scotch tape and sample coated (continu

Instrumentation:

Type & Serial No.		(Check Calibration Dates) Gage Length, etc.	Location on Sample
Load Cell 161.31k.cc	211		Machine Load
Stroke LVDT	124		Machine Stroke
Pressure Transducer			Control Pressure
Axial LVDT	1124/1209	75 mm	Axial
Lateral LVDT	3515	50.7 mm	Lateral

Unused spaces intentionally left blank.

Date: 6/28/94

Initials: JDH

Rock Mechanics Laboratory Test Data Report

Continuation Page

Test ID: NPS1

Requester: D. Holcomb

Prep. continued.
with bees wax before installing gauge rings

Notes:

This material is soft. while end grinding the fixture made groves on the original Top & bottom surfaces. The sample is not perfectly round. It is 1.993" in the vertical direction and 2.001" in the horizontal direction. The groves are about 0.014" deep.

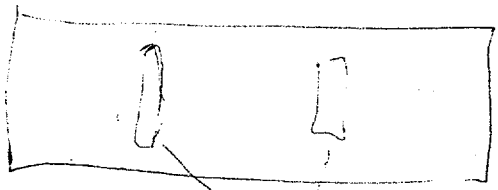

RML2-2 March 10, 1994

Page: ______ Of: ______

Date: 6/29/94

Initials: RDT

Rock Mechanics Laboratory Test Data Report

Data Recording Information

Test ID: NPS 1

Requester: D. Holcomb

Machine Used: 220 KIP

Controller Type: 458

Requested Confining Pressure: 0

Controller Settings:

Function Generator Settings:

Variable:	Range Full Scale:	Span %	Rate:	Time:
Load	450 Kn			
Stroke	10 mm			
Control Pres.	———			
Ax. strain	± 0.1 in	100	0.00075 mm/sec	
Lat. strain	± 0.05 in			

Attach printout of setup if desired.

Variables Recorded:	Scale Factors:	Shunt Cal. (V)
Load	45.0 KS ~~45.505~~ Kn/V	~~3.644~~ 8.577
Stroke	1.000 mm/V	NA
Control Pressure	———	———
Ax. strain	0.2574 mm/V	———
Lat. Strain	0.125 mm/V	———

Data Storage:

File Names:	Contents:
NPS 1 .SET	Setup File
NPS 1 .DAT	Data File
NPS 1 .HDR	Header File
1TRACK01	Axial, Shear Vert
1TRACK02	Axial, Shear Horiz
1TRACK03	Vertical, Shear axial
1TRACK04	Vertical, shear lateral
1TRACK05	Horizontal, Shear axial
1TRACK06	Horizontal, shear lateral

Comments:

At end of test I switched to stroke control a little fast + crumbled the sample.

Unused spaces intentionally left blank.

*** Attach continuation pages as needed. ***

Setup Data
Transducer Calibration on 220 KIP, by R. D. HARDY, Thu Mar 10 11:52:23 1994
Standard transducer: SCHAEVITZ, Model PCA-220-100., Serial # 5195
Conditioner: MTS, Model 458.13, Serial No. 135567
Range .100 IN, Gain NA, Zero NA
Transducer Type LVDT PAIR, Transducer Serial No. 1124/1209
Excitation Voltage: NA, Shunt Cal. Output: NA
Reciprocal of Slope is 0.010135 IN./V +/- 0.000002 IN./V (95% Confidence)

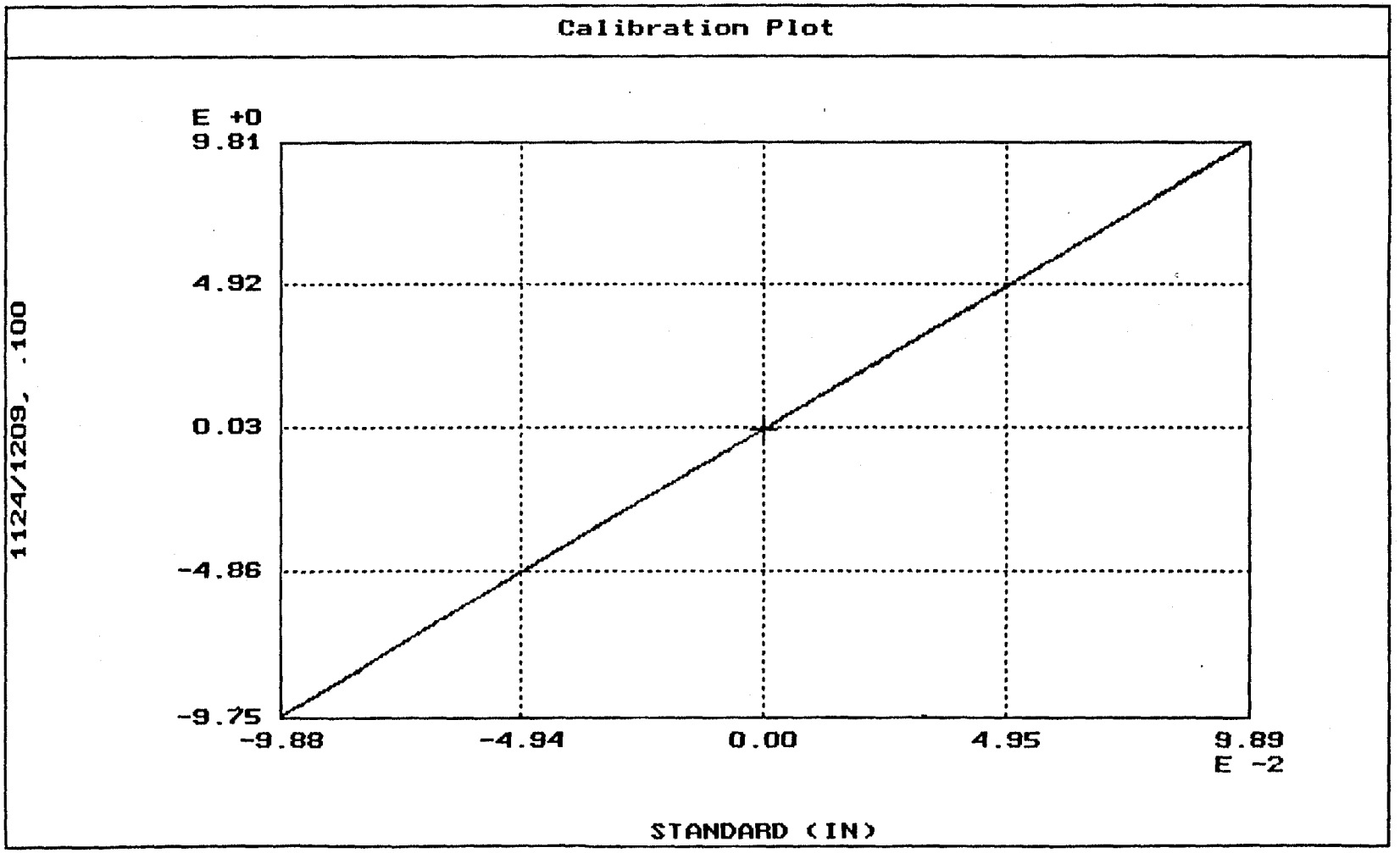

Setup Data

Transducer Calibration by R. D. HARDY, Tue May 10 16:56:07 1994
Standard transducer: SCHAEVITZ, Model PCA-220-100., Serial # 5195
Conditioner: MTS, Model 458.13, Serial No. 134553
Range .050 IN., Gain NA, Zero NA
Transducer Type LVDT, Transducer Serial No. 3518
Excitation Voltage: NA, Shunt Cal. Output: NA
Reciprocal of Slope is 0.005041 IN/V +/- 0.000001 IN/V (95% Confidence)

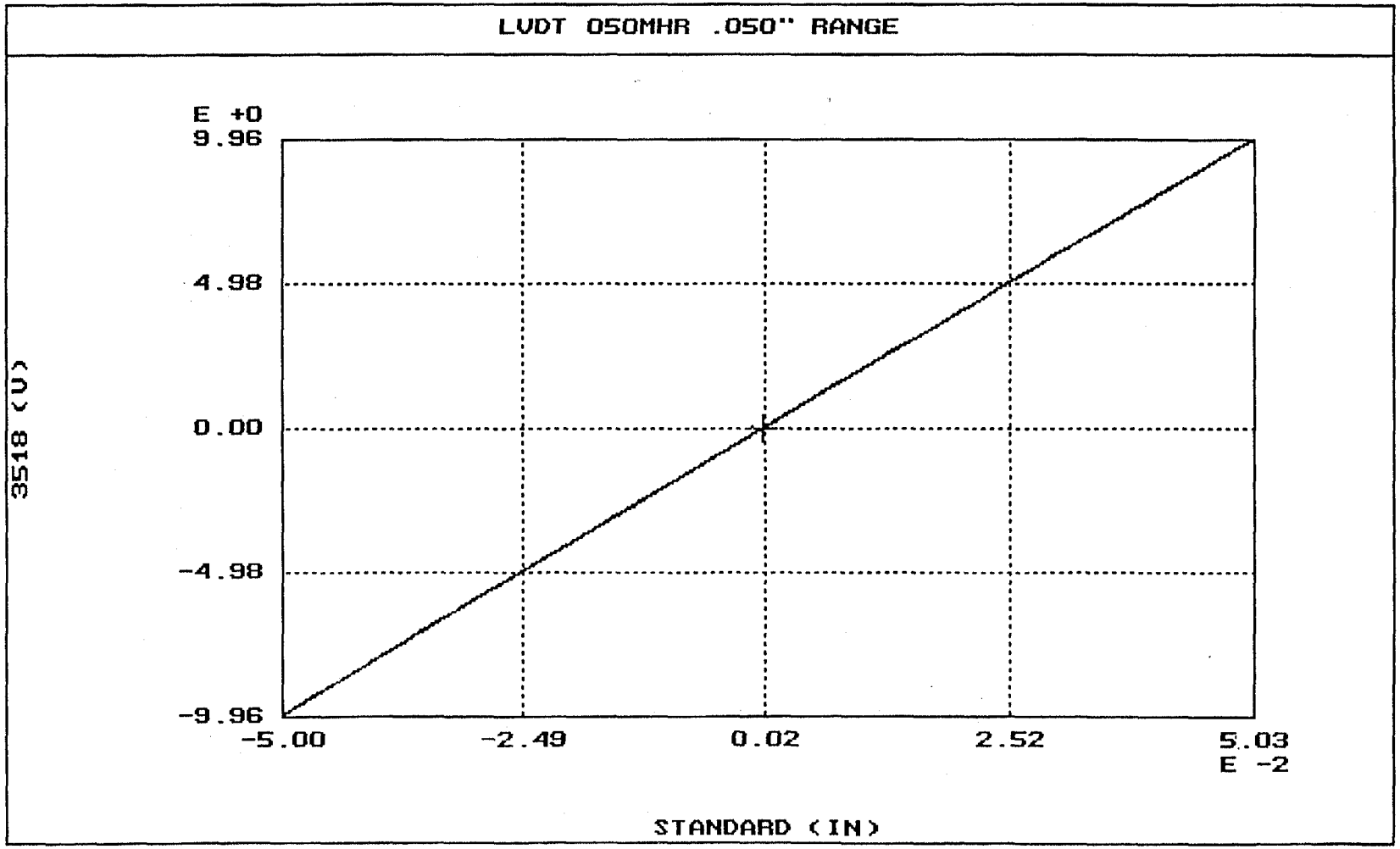

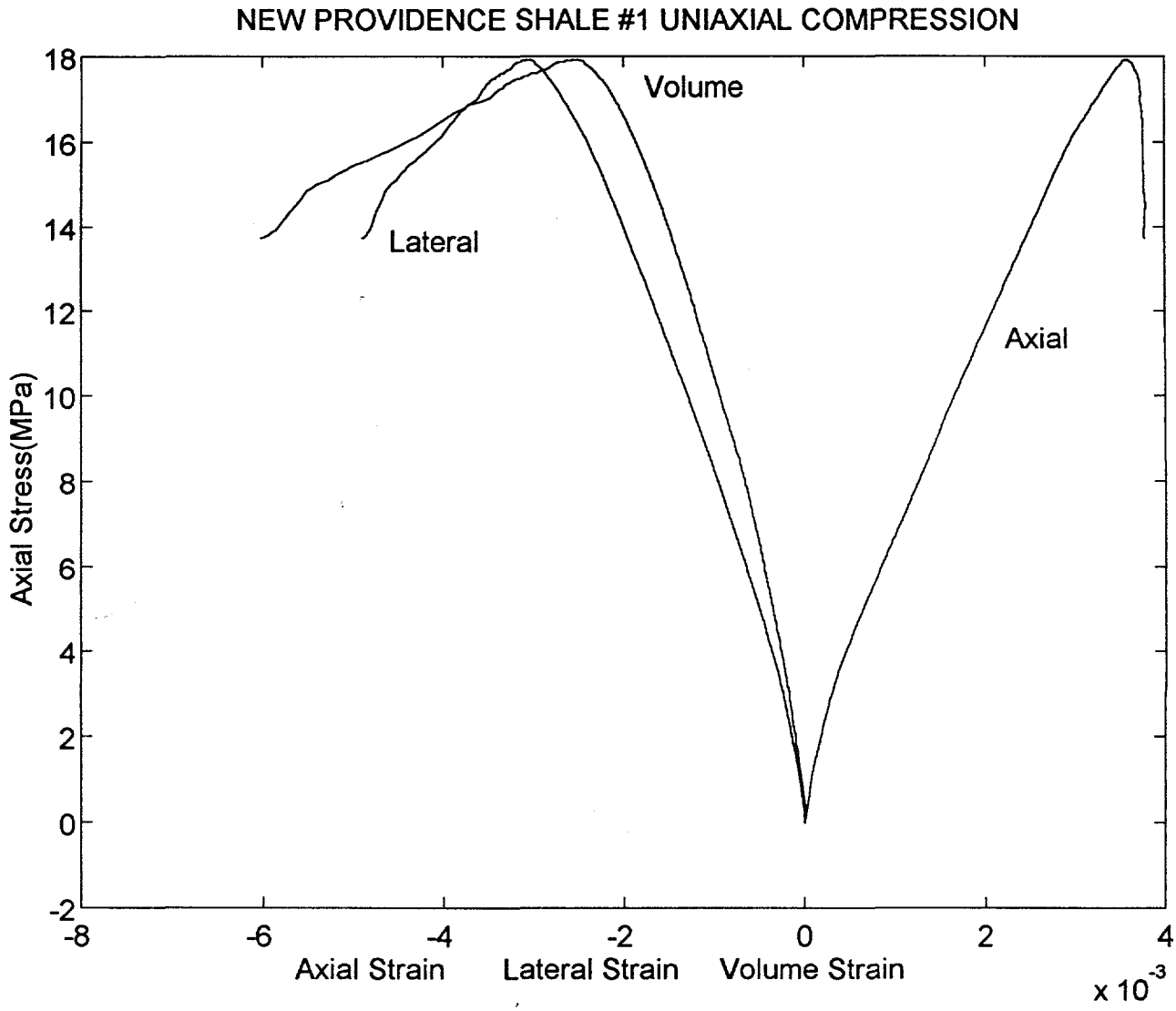
NEW PROVIDENCE SHALE #1 UNIAXIAL COMPRESSION
Volume
Lateral
Axial
Axial Stress(MPa)
18
16
14
12
10
8
6
4
2
0
-2
-8
-6
-4
-2
0
2
4
Axial Strain
Lateral Strain
Volume Strain
x 10^-3

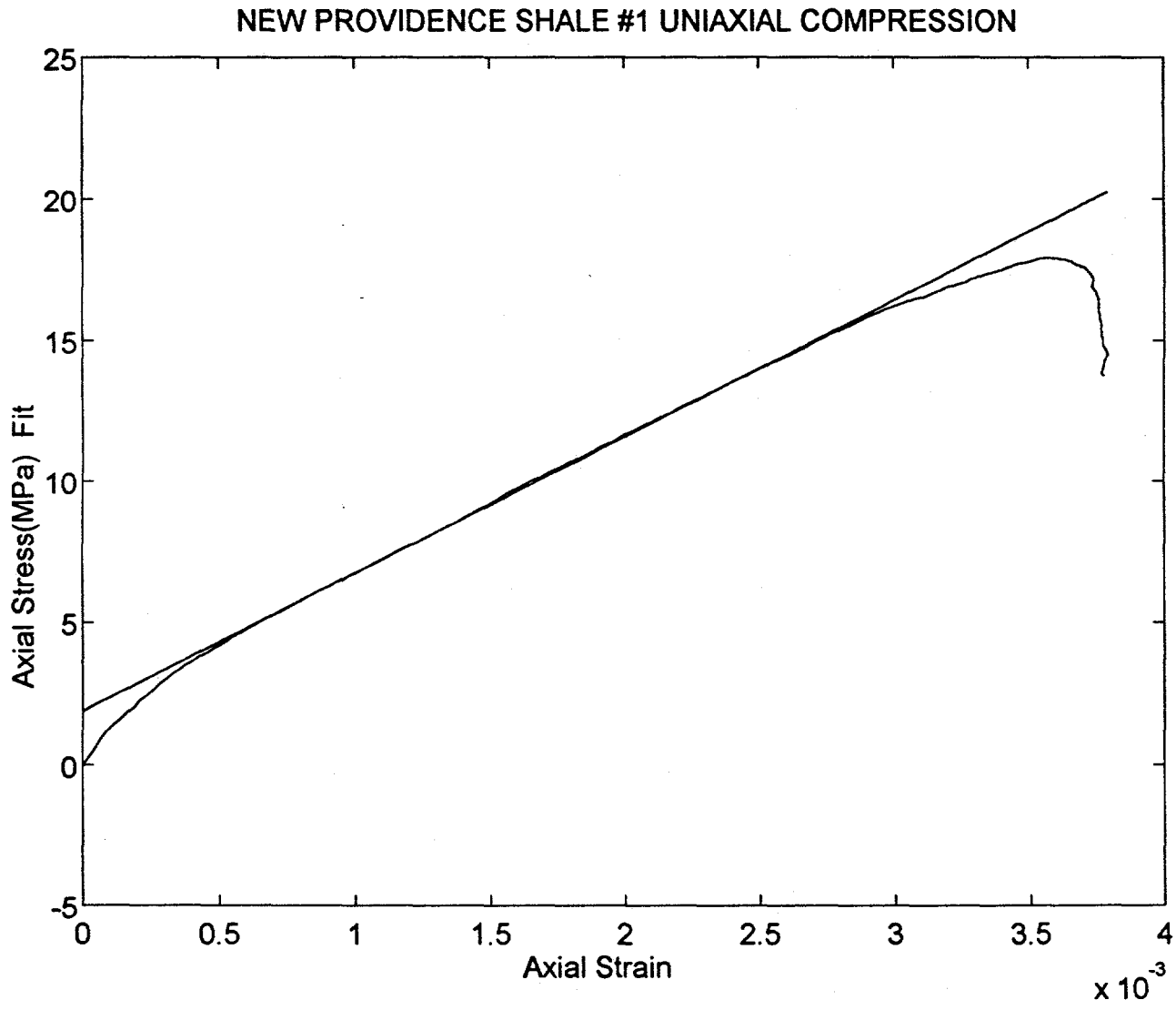
NEW PROVIDENCE SHALE #1 UNIAXIAL COMPRESSION
Axial Stress(MPa) Fit
Axial Strain
x 10^-3
25
20
15
10
5
0
-5
0
0.5
1
1.5
2
2.5
3
3.5
4

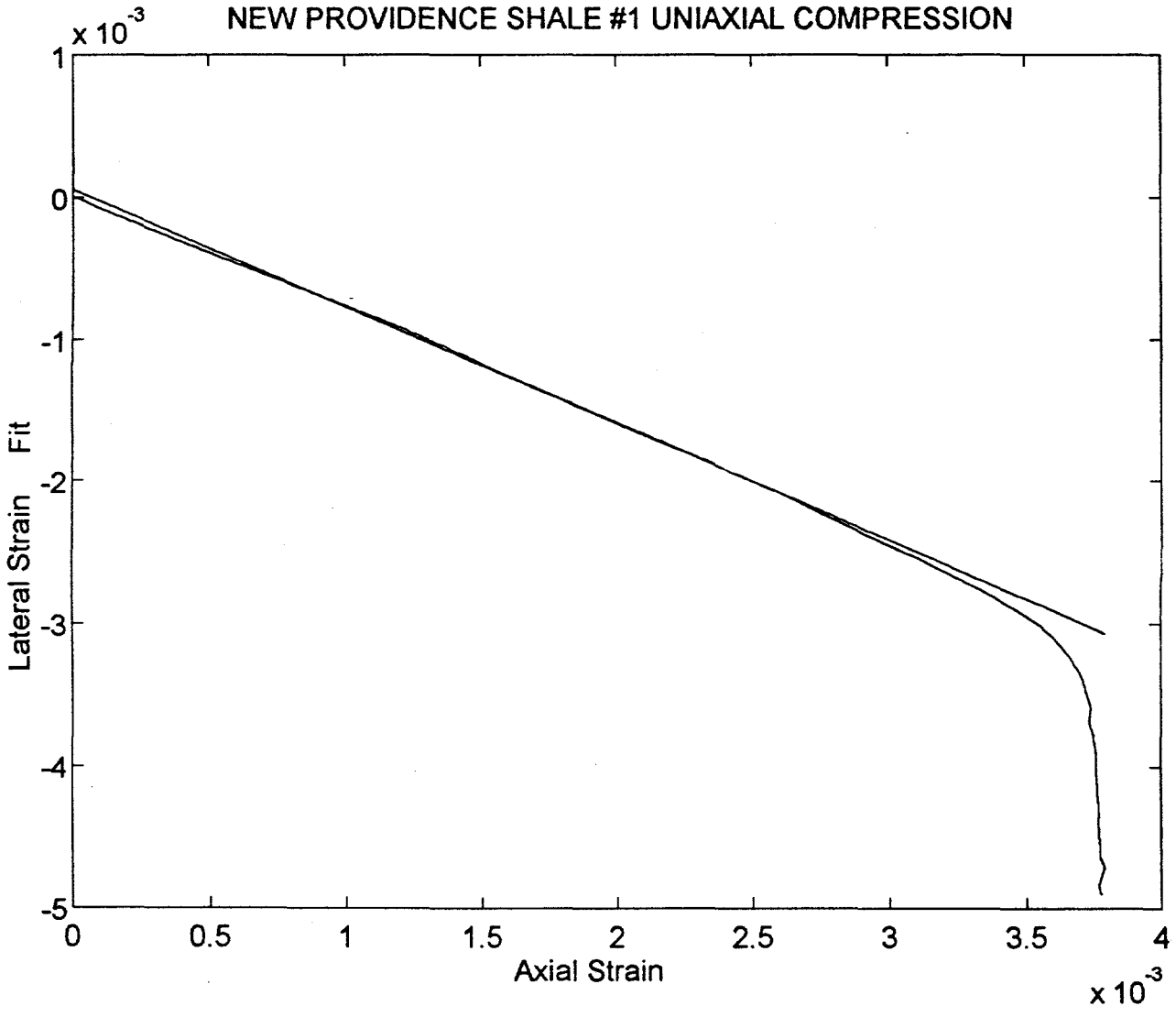
NEW PROVIDENCE SHALE #1 UNIAXIAL COMPRESSION
x 10^-3
1
0
-1
-2
-3
-4
-5
Lateral Strain Fit
0
0.5
1
1.5
2
2.5
3
3.5
4
Axial Strain
x 10^-3

New Providence Shale test NPS1 acoustic wave velocities.

Velocities were measured on the velocity bench. All readings were made using shear transducers which allow us to get both shear and pressure wave velocities simultaneously.

There were a total of six readings made in different orientations as follows:

1) P-wave axial through the sample and the S-wave in the vertical direction.
2) P-wave axial through the sample and the S-wave in the horizontal direction.
3) P-wave in the vertical direction and the S-wave axial to the sample.
4) P-wave in the vertical direction and the S-wave lateral to the sample.
5) P-wave in the horizontal direction and the S-wave axial to the sample.
6) P-wave in the horizontal direction and the S-wave lateral to the sample.

Velocity (mm / μsec)		
Reading #	P-wave	S-wave
1	3.69	2.04/1.16
2	–	1.96
3	2.90	1.24
4	2.88	1.17
5	3.70	1.99
6	3.62	1.17

RML3-1 March 8, 1994

Page: _____ Of: _____

Date: 6/23/94

Initials: ADF

Rock Mechanics Laboratory Test Check List

Test ID: NPS 2

Requester: D. Holcomb

Case Number: 4274.000

Mark those items present and indicate the number of each.

☒ Test Request Form: Pages 1

☒ Test Data Report Form: Pages 3

☒ Data Disk(s): Number 1 combined with NPS 1

☒ Calibration Data: Pages 2

☒ Plots: Pages 3

☒ Additional Notes: Pages 1 - velocities

☐ Analysis Notes: Pages _____

☐ Other: _____ Pages _____

☐ Other: _____ Pages _____

☐ Other: _____ Pages _____

☐ Other: _____ Pages _____

Notes:

Unused spaces intentionally left blank.

RML1-1, February 16, 1994 Page: _____ Of: _____

Date: 6/28/94 Initials: RDT

Rock Mechanics Laboratory Test Request Form

(Use to collect and organize your thoughts when planning a test.)

Test ID: NPS2 Requester: D. Holcomb

Case Number: 4274.000

Type of Test: Uniaxial Compression Confining Pressure: 0

Due Date: _____

Objectives: (Why are we doing this test.) _____

Sample Material: (Specify control number if needed.) #2 New Providence shale

Sample Shape and Dimensions: (Specify units.)

☒ Cylinder: Diameter: 2" Length: 5"

☐ Prism: Width: _____ Height: _____ Thickness: _____

Preparation Details: (Finish, Cautions, etc.)

Core & grind. Keep in water until coating is applied

Instrumentation: (Location and Type. Attach sketch if you feel it will help.)

Axial & lateral LVDTs. Make P & S velocity readings axial, vertical & horizontal.

Special Instructions:

Sample Disposition: Coat & Bag

Data Disposition: _____

Other: _____

Test Control:

Axis:	Control Variable:	Units Desired:	Ramp Rate:
Load			
Stroke			
Pressure			
Axial strain	✓		10^{-5} strain rate
Lateral strain			

Neatness Counts! If your instructions cannot be read, the test may be delayed.
Unused spaces intentionally left blank.
*** Attach continuation pages as needed. ***

RML2-1 March 10, 1994 Page: _____ Of: _____

Date: 6/25/94 Initials: RDT

Rock Mechanics Laboratory Test Data Report

Sample Preparation Details

Test ID: NPS 2 Requester: D. Holcomb

Case Number: 4274.ccp

Technician(s): Hardy

Sample Material: (Specify control number if needed.) #2 New Providence shale

Diameter: 1.997" Length: 5.102" Width: ——— Height: ———

Mass: 675.29 Coating: Bees Wax Other: ———

Sketch: (Include Dimensions & add continuation pages as needed.)

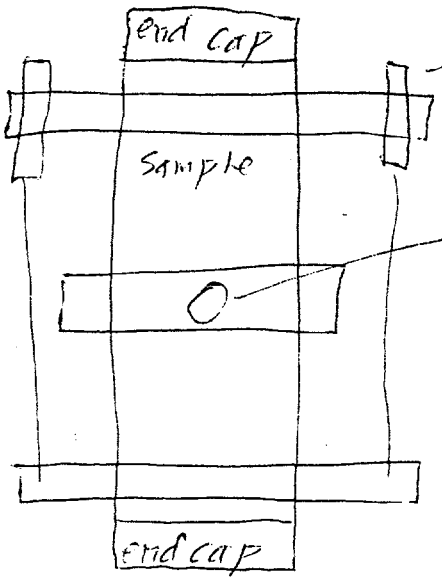

See notes on continuation page

Preparation Details: Sample was cored from original core then ground all surfaces using tap water for coolant sample kept in water between operations. End caps secured with scotch tape and sample coated with bees wax before applying gauge rings.

Instrumentation: Type & Serial No.	(Check Calibration Dates) Gage Length, etc.	Location on Sample
Load Cell		Machine Load
Stroke LVDT		Machine Stroke
Pressure Transducer		Control Pressure
Axial LVDT	75 mm	
Lateral LVDT	50.7 mm	

Unused spaces intentionally left blank.

RML2-4 March 8, 1994 Page: _____ Of: _____

Date: 6/28/94 Initials: LDH

Rock Mechanics Laboratory Test Data Report

Continuation Page

Test ID: NPS2 Requester: D. Holcomb

Notes:

This material is soft. The grinding fixture left groves in the top + bottom surfaces. these groves are about 0.014" deep. There is a flake missing near the center. this flake is about 1/2" long x 1/4" wide and 0.03" deep.

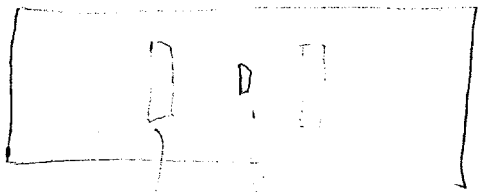

Unused spaces intentionally left blank.

*** Attach continuation pages as needed. ***

RML2-2(April 8, 1994) Page: _____ Of: _____

Date: 6/29/94 Initials: RDH

Rock Mechanics Laboratory Test Data Report

Data Recording Information

Test ID: NPS2 Requester: D. Holcomb

Machine Used: 220 KIP Controller Type: 458

Requested Confining Pressure: 0

Controller Settings:

Variable:	Range Full Scale:	Span %	Function Generator Settings: Rate:	Time:
Load	450 KN			
Stroke	10 MM			
Control Pres.				
Ax. Strain	2.5 mm	100	0.00075 mm/sec	
Lat Strain	1.25 mm			

Attach printout of setup if desired.

Variables Recorded:	Scale Factors:	Shunt Cal. (V)
Load	45.015 KN/V	3.591
Stroke	1 MM/V	NA
Control Pressure		
Ax. Strain	0.2574 mm/V	
Lat. Strain	0.125 mm/V	

Data Storage:

File Names:	Contents:
NPS2.SET	Setup File
NPS2.DAT	Data File
NPS2.HDR	Header File
2TRACK01	Axial, shear Vert.
2TRACK02	Axial, shear Horiz.
2TRACK03	Vertical, shear Axial
2TRACK04	Vertical, shear Lateral
2TRACK05	Horizontal, shear Axial
2TRACK06	Horizontal, shear Lateral

Comments:

Unused spaces intentionally left blank.

*** Attach continuation pages as needed. ***

Setup Data
Transducer Calibration by R. D. HARDY, Tue May 10 16:56:07 1994
Standard transducer: SCHAEVITZ, Model PCA-220-100., Serial # 5195
Conditioner: MTS, Model 458.13, Serial No. 134553
Range .050 IN., Gain NA, Zero NA
Transducer Type LVDT, Transducer Serial No. 3518
Excitation Voltage: NA, Shunt Cal. Output: NA
Reciprocal of Slope is 0.005041 IN/V +/- 0.000001 IN/V (95% Confidence)

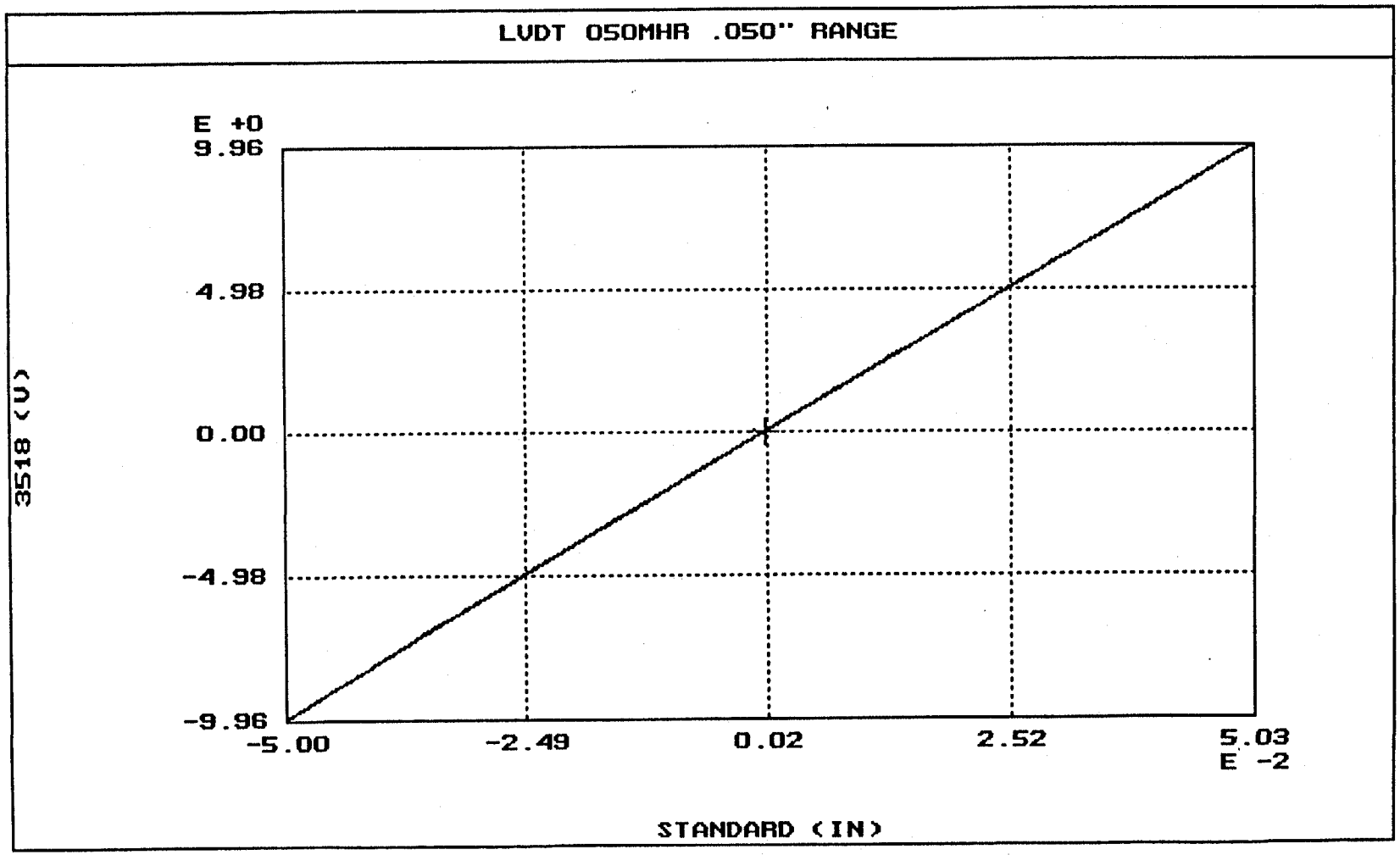

Setup Data
Transducer Calibration on 220 KIP, by R. D. HARDY, Thu Mar 10 11:52:23 1994
Standard transducer: SCHAEVITZ, Model PCA-220-100., Serial # 5195
Conditioner: MTS, Model 458.13, Serial No. 135567
Range .100 IN, Gain NA, Zero NA
Transducer Type LVDT PAIR, Transducer Serial No. 1124/1209
Excitation Voltage: NA, Shunt Cal. Output: NA
Reciprocal of Slope is 0.010135 IN./V +/- 0.000002 IN./V (95% Confidence)

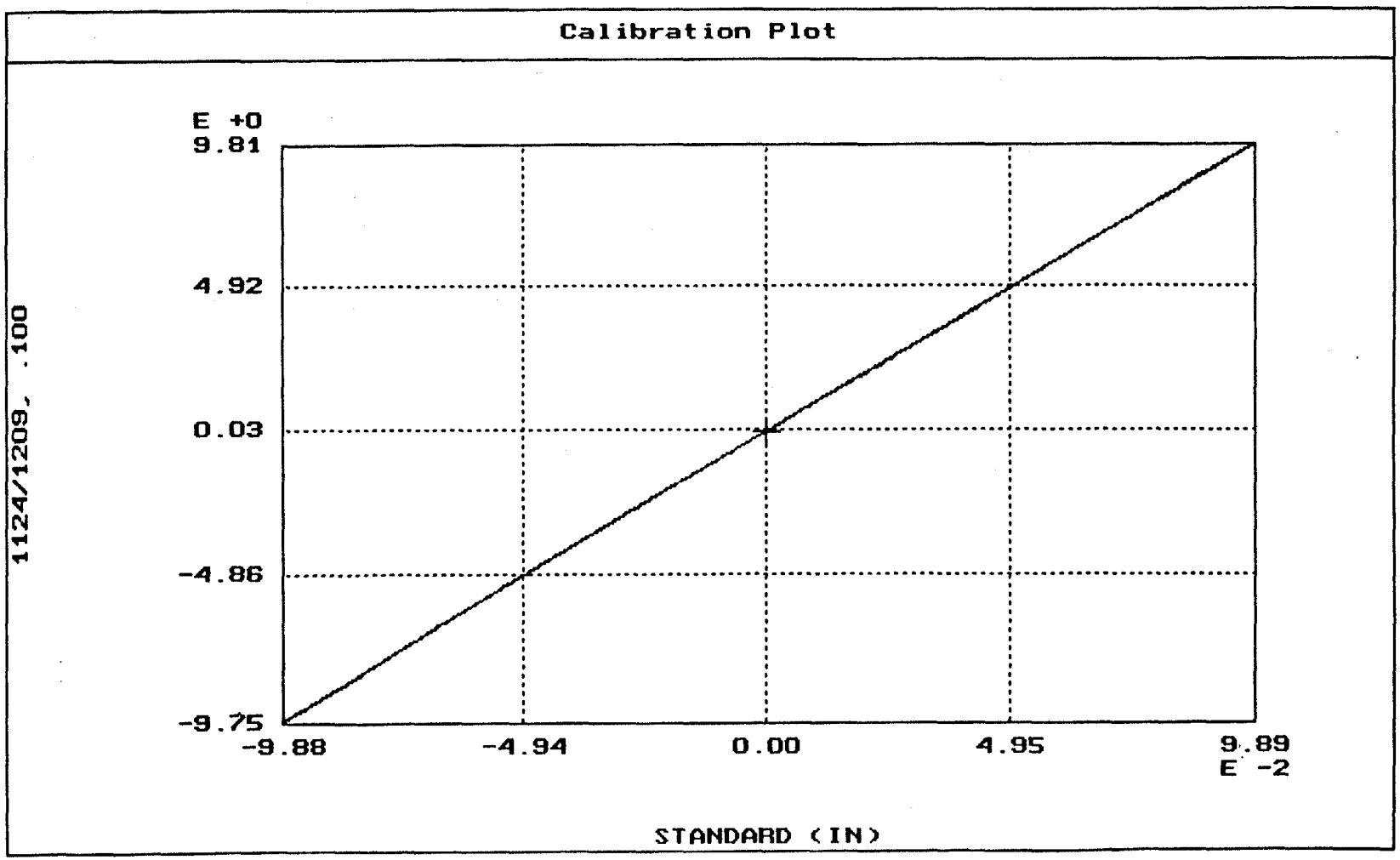

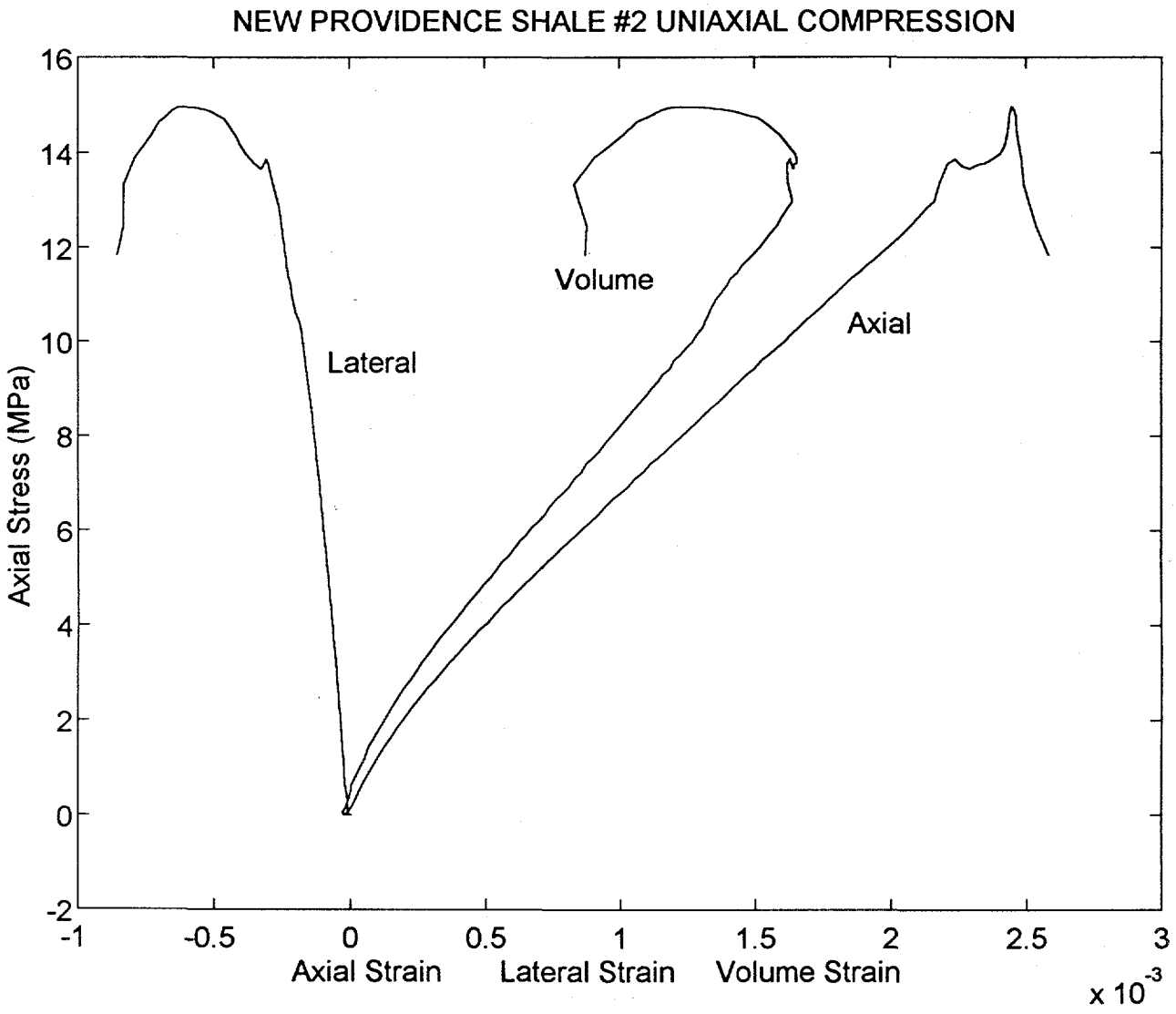
NEW PROVIDENCE SHALE #2 UNIAXIAL COMPRESSION
Axial Stress (MPa)
16
14
12
10
8
6
4
2
0
-2
Volume
Axial
Lateral
-1
-0.5
0
0.5
1
1.5
2
2.5
3
Axial Strain
Lateral Strain
Volume Strain
x 10^-3

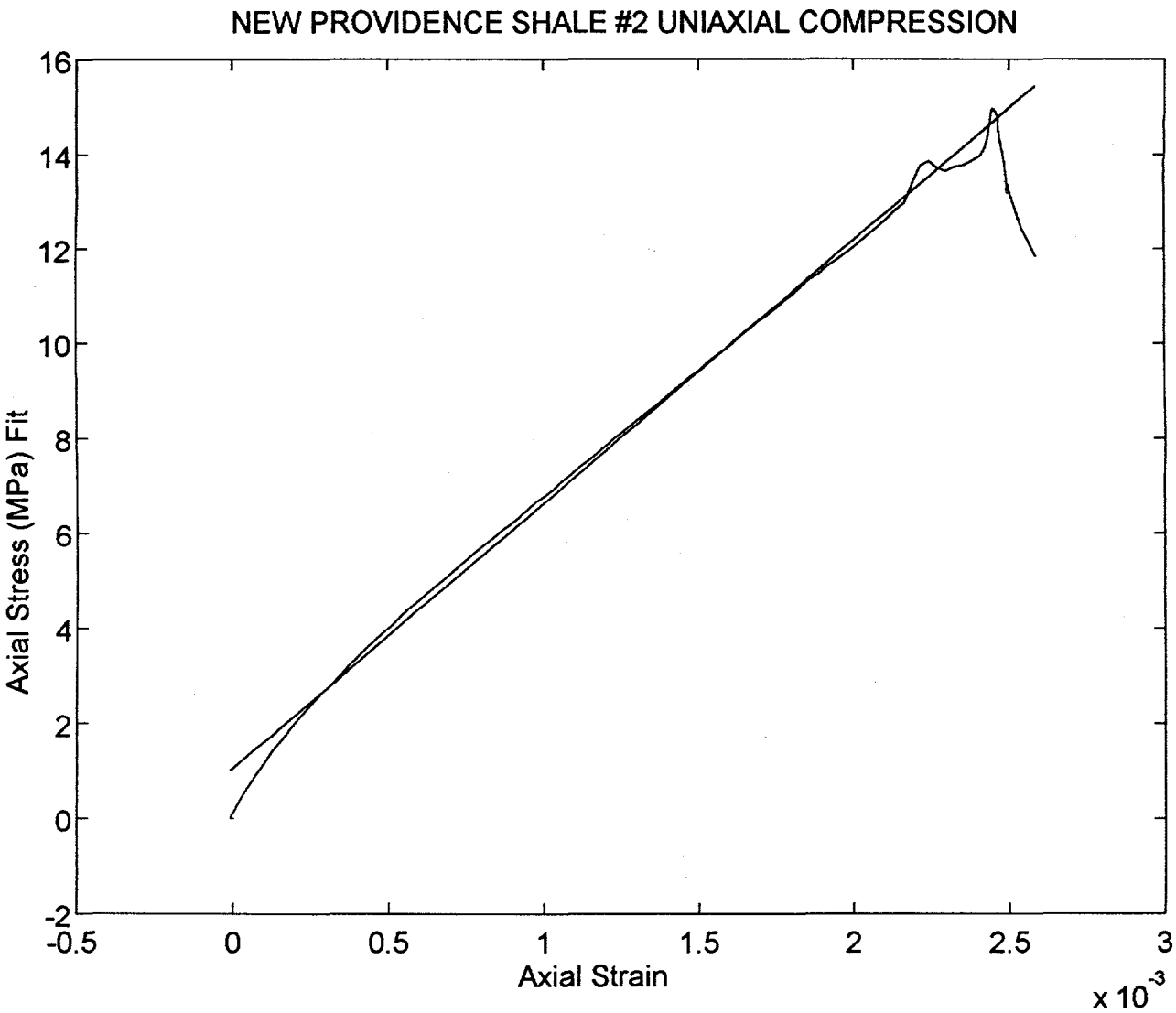
NEW PROVIDENCE SHALE #2 UNIAXIAL COMPRESSION
Axial Stress (MPa) Fit
16
14
12
10
8
6
4
2
0
-2
-0.5
0
0.5
1
1.5
2
2.5
3
Axial Strain
x 10^-3

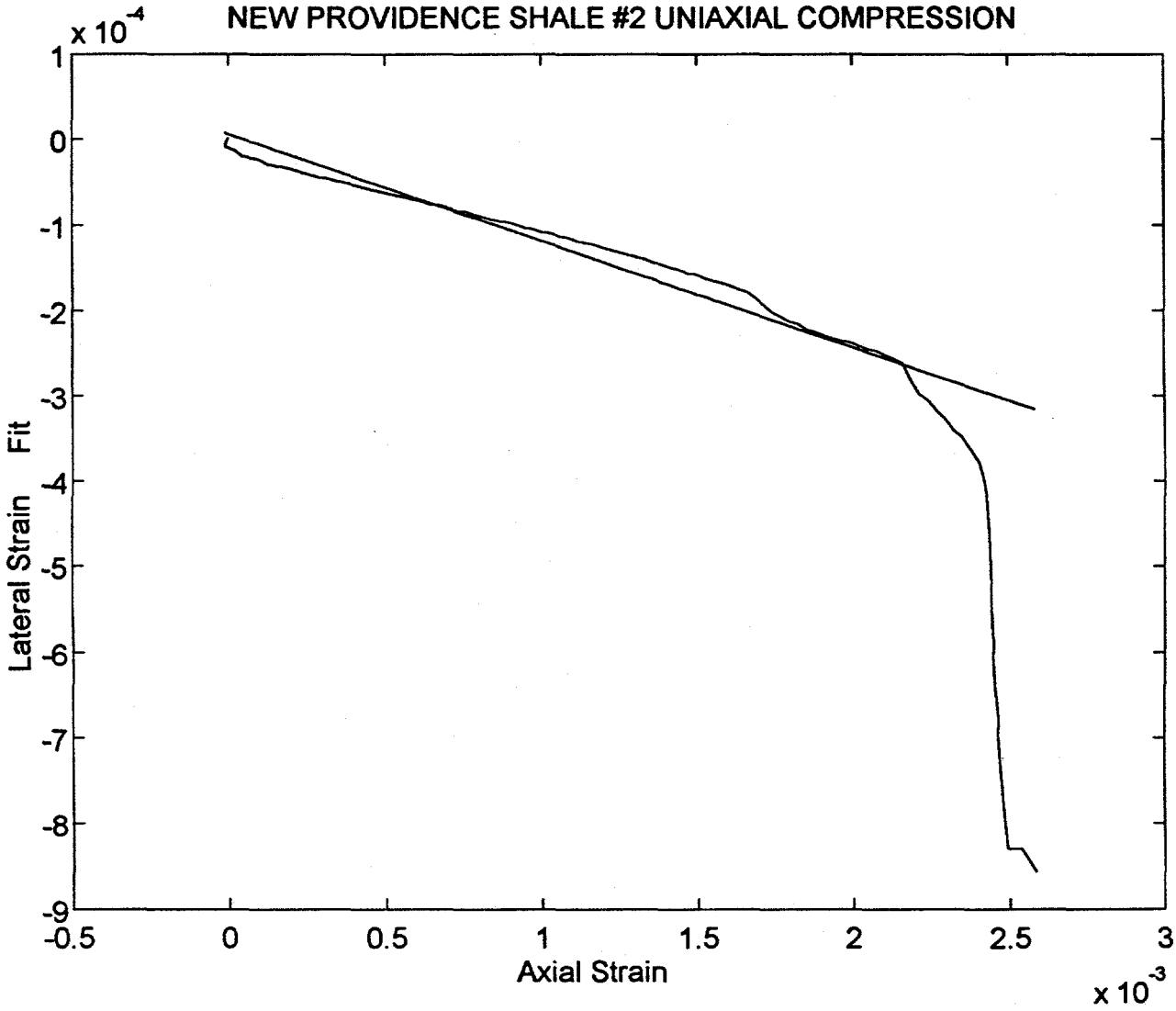
NEW PROVIDENCE SHALE #2 UNIAXIAL COMPRESSION
x 10^-4
1
0
-1
-2
-3
-4
-5
-6
-7
-8
-9
Lateral Strain Fit
-0.5
0
0.5
1
1.5
2
2.5
3
Axial Strain
x 10^-3

New Providence Shale test NPS2 acoustic wave velocities.

Velocities were measured on the velocity bench. All readings were made using shear transducers which allow us to get both shear and pressure wave velocities simultaneously.

There were a total of six readings made in different orientations.

1) P-wave axial through the sample and the S-wave in the vertical direction.
2) P-wave axial through the sample and the S-wave in the horizontal direction.
3) P-wave in the vertical direction and the S-wave axial to the sample.
4) P-wave in the vertical direction and the S-wave lateral to the sample.
5) P-wave in the horizontal direction and the S-wave axial to the sample.
6) P-wave in the horizontal direction and the S-wave lateral to the sample.

Velocity (mm / μsec)		
Reading #	P-wave	S-wave
1	3.77	1.93
2	2.84	2.04
3	–	1.26
4	2.28	1.19
5	3.73	2.04
6	3.81	1.16

The P-wave arrival could not be located in reading three.

APPENDIX B

Pressure Displacement Histories

Vertical and Horizontal Flatjack Tests

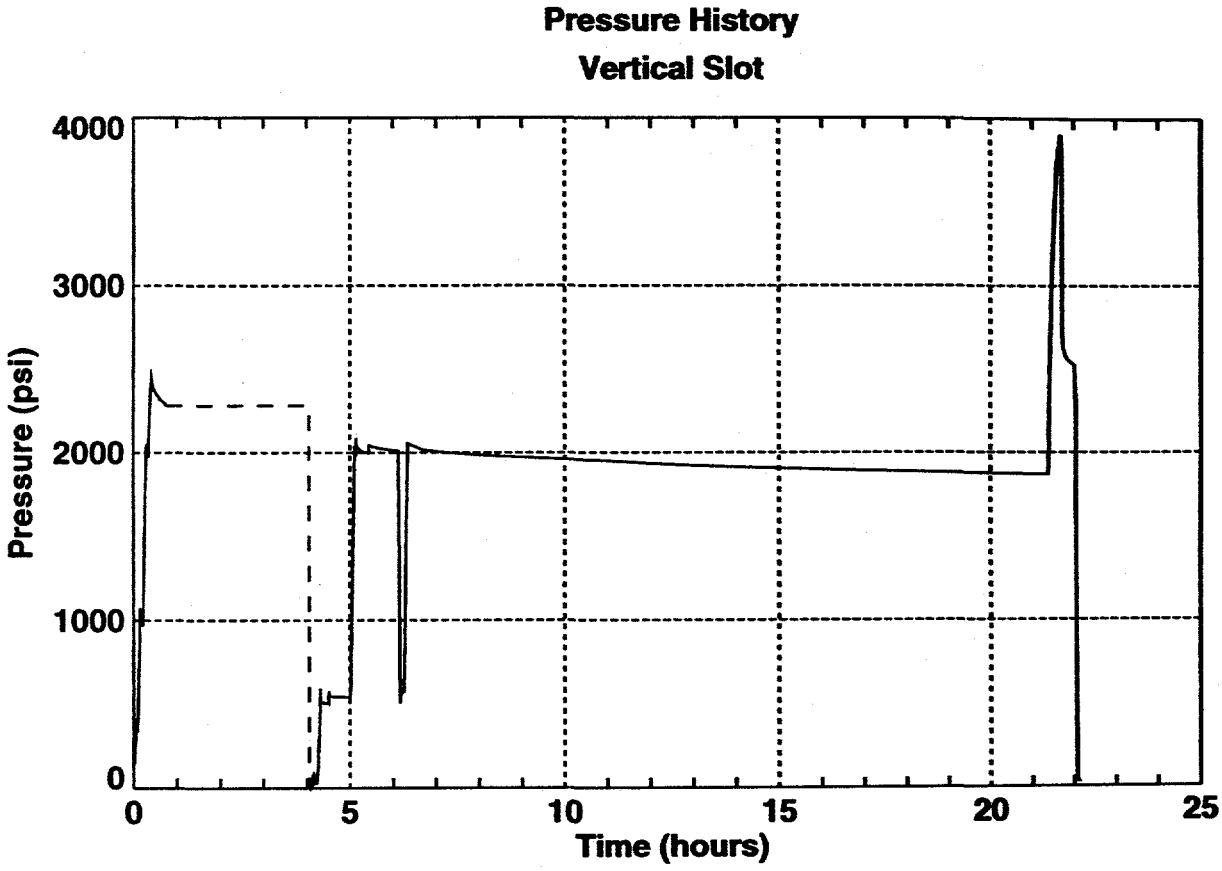
Pressure History
Vertical Slot
4000
3000
2000
1000
0
Pressure (psi)
0
5
10
15
20
25
Time (hours)

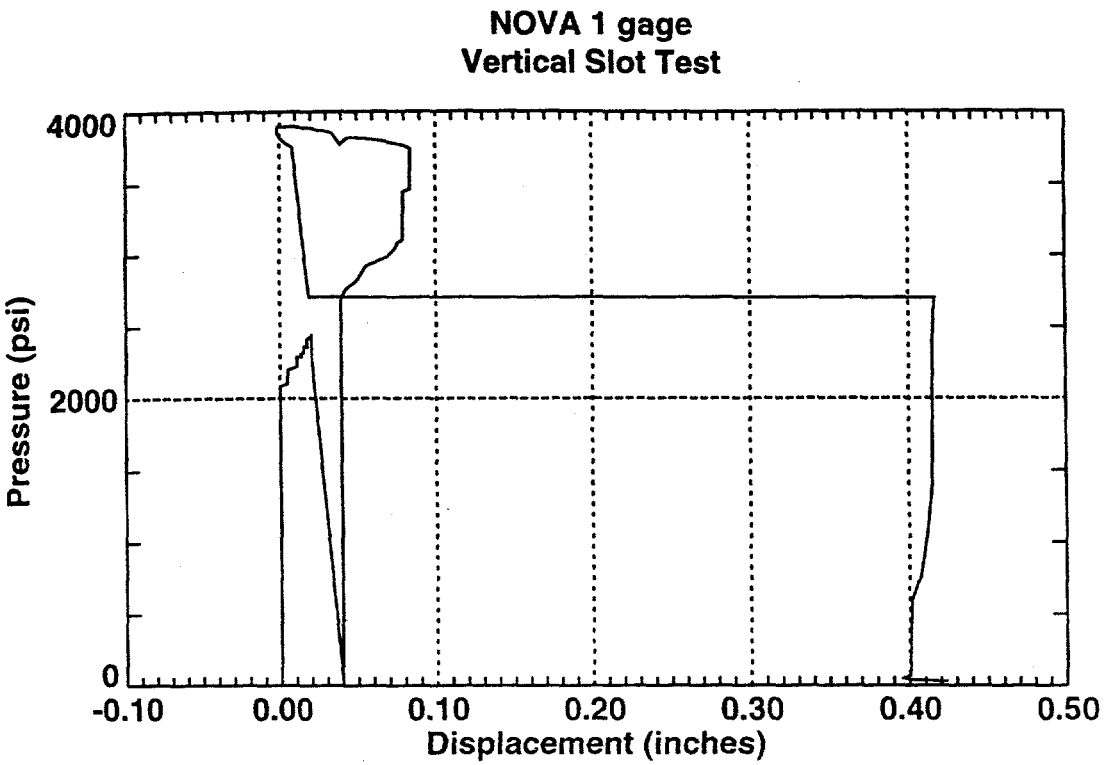
NOVA 1 gage
Vertical Slot Test
4000
2000
0
Pressure (psi)
-0.10
0.00
0.10
0.20
0.30
0.40
0.50
Displacement (inches)

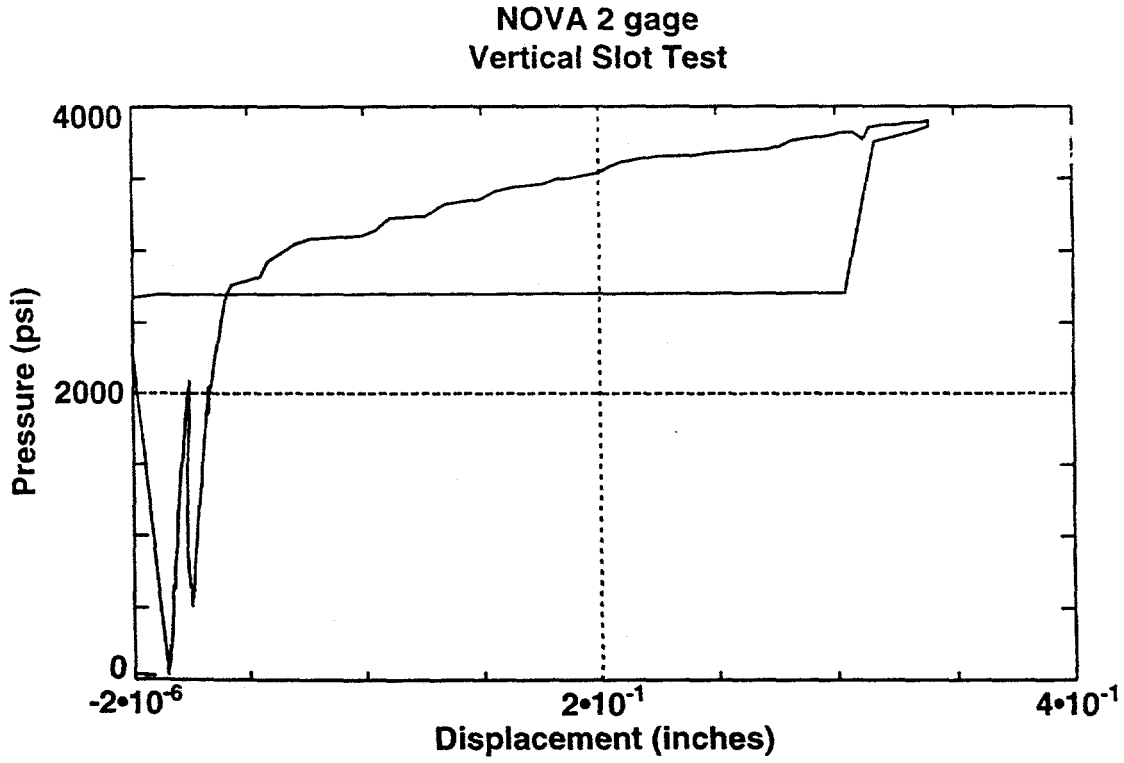
NOVA 2 gage
Vertical Slot Test
4000
2000
0
Pressure (psi)
-2•10-6
2•10-1
4•10-1
Displacement (inches)

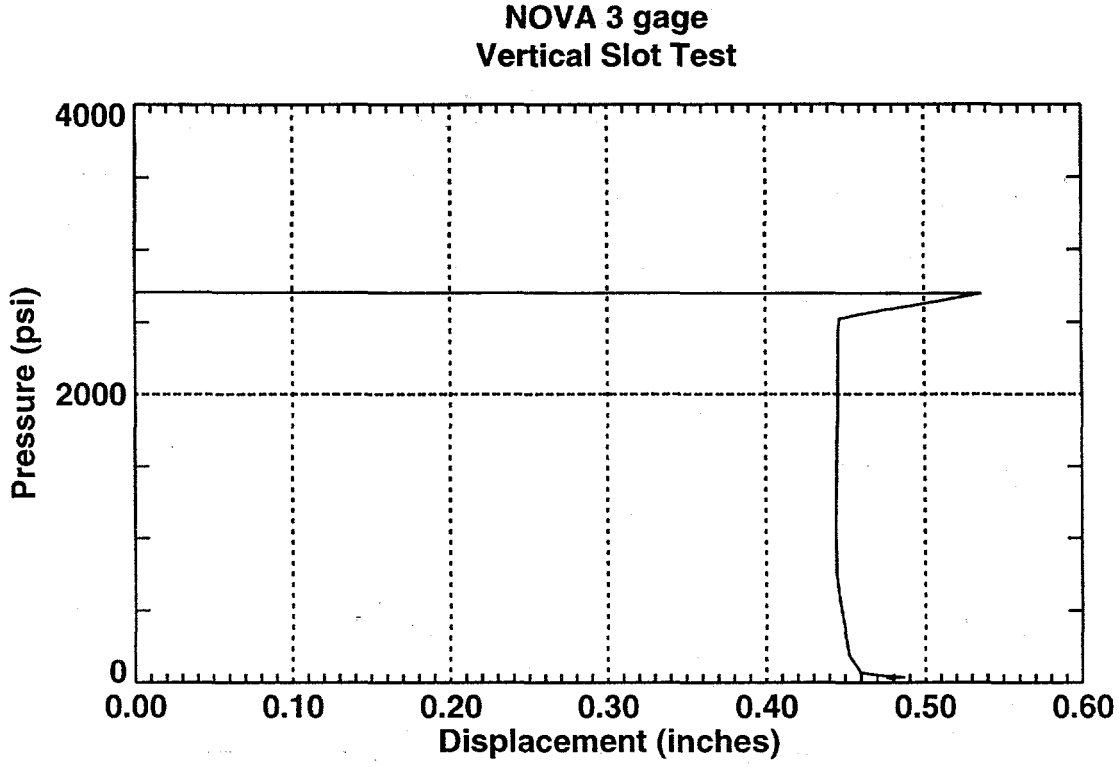
NOVA 3 gage
Vertical Slot Test
4000
2000
0
Pressure (psi)
0.00
0.10
0.20
0.30
0.40
0.50
0.60
Displacement (inches)

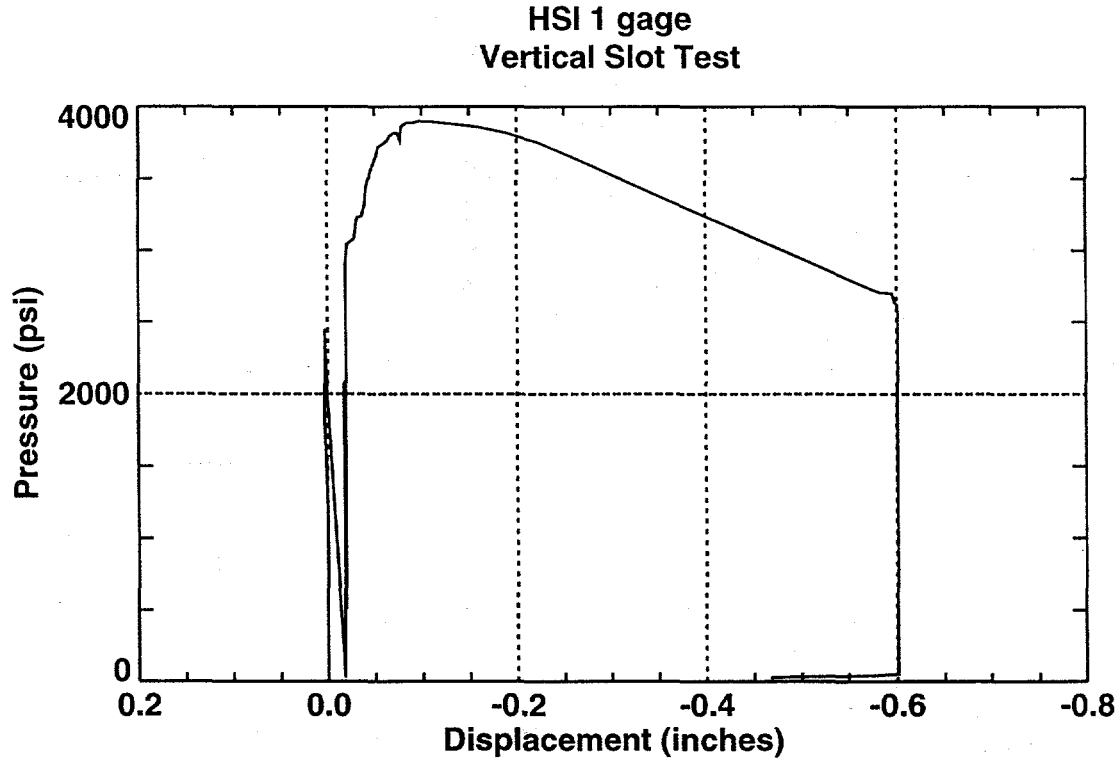
HSI 1 gage
Vertical Slot Test
4000
2000
0
Pressure (psi)
0.2
0.0
-0.2
-0.4
-0.6
-0.8
Displacement (inches)

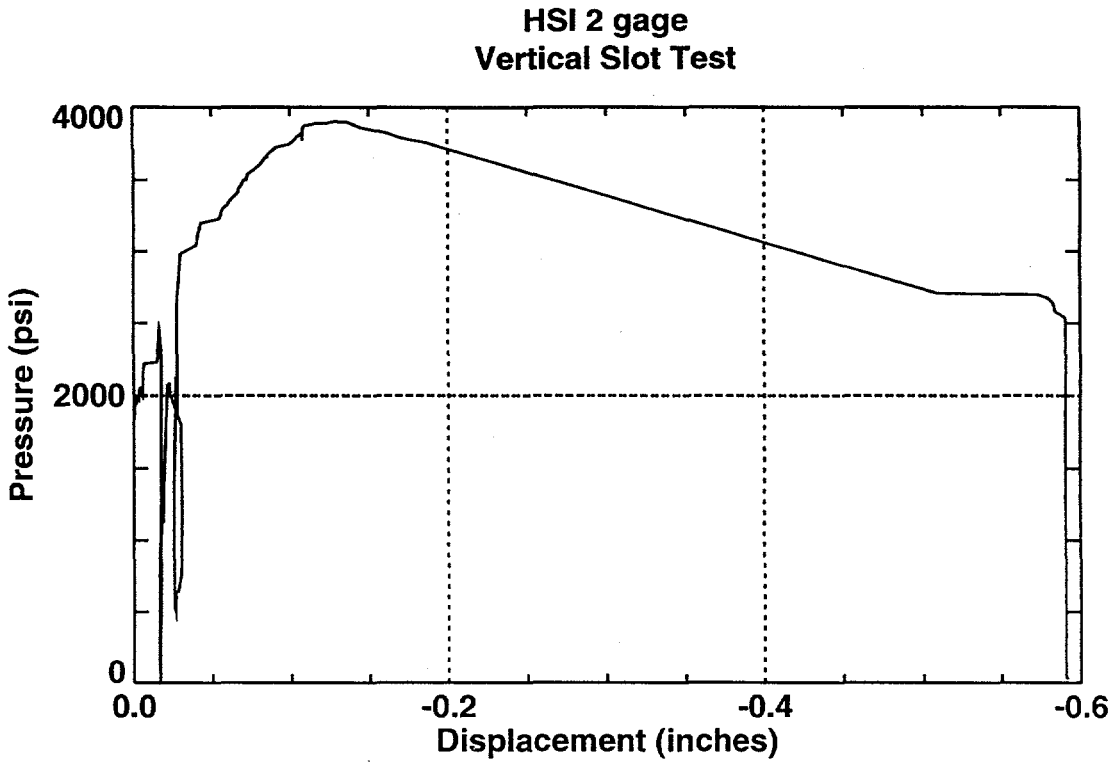
HSI 2 gage
Vertical Slot Test
4000
2000
0
Pressure (psi)
0.0
-0.2
-0.4
-0.6
Displacement (inches)

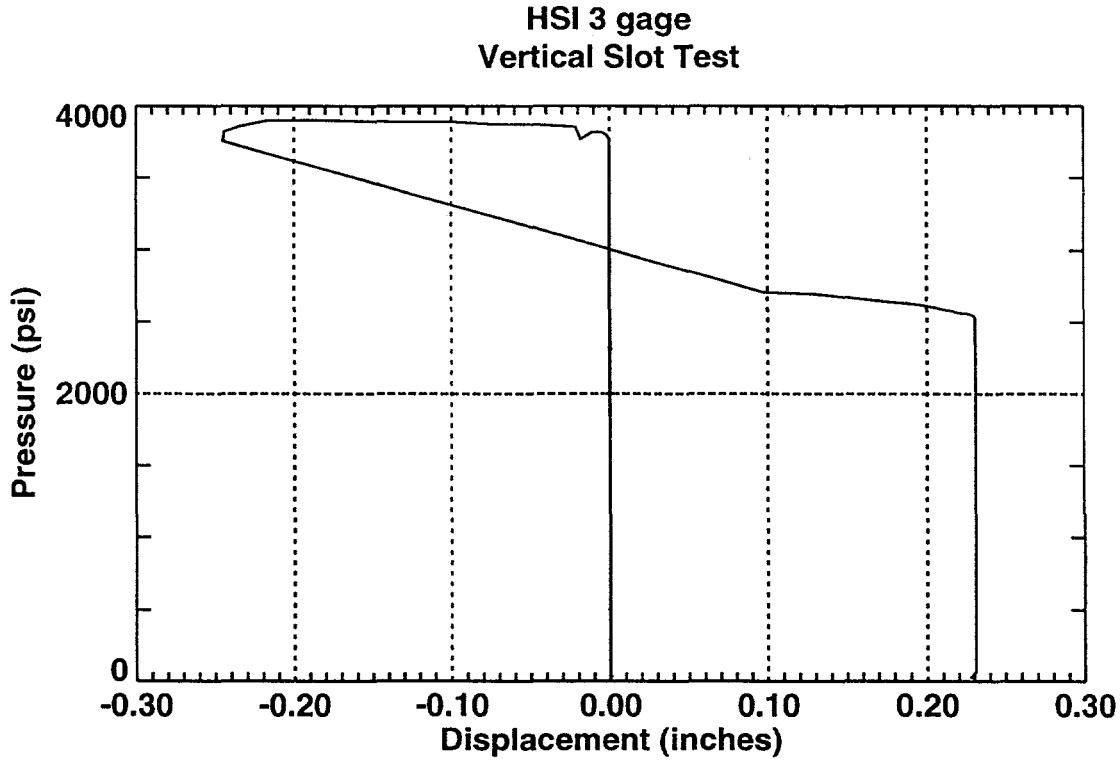
HSI 3 gage
Vertical Slot Test
4000
2000
0
Pressure (psi)
-0.30
-0.20
-0.10
0.00
0.10
0.20
0.30
Displacement (inches)

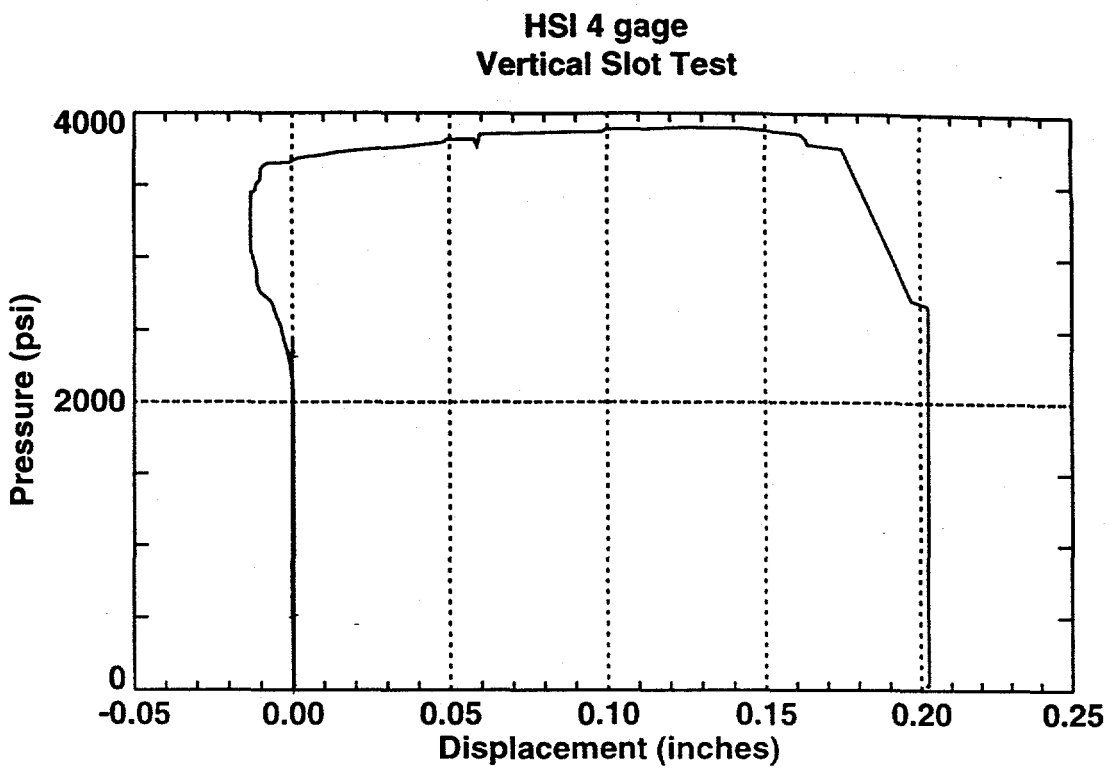
HSI 4 gage
Vertical Slot Test
4000
2000
0
Pressure (psi)
-0.05
0.00
0.05
0.10
0.15
0.20
0.25
Displacement (inches)

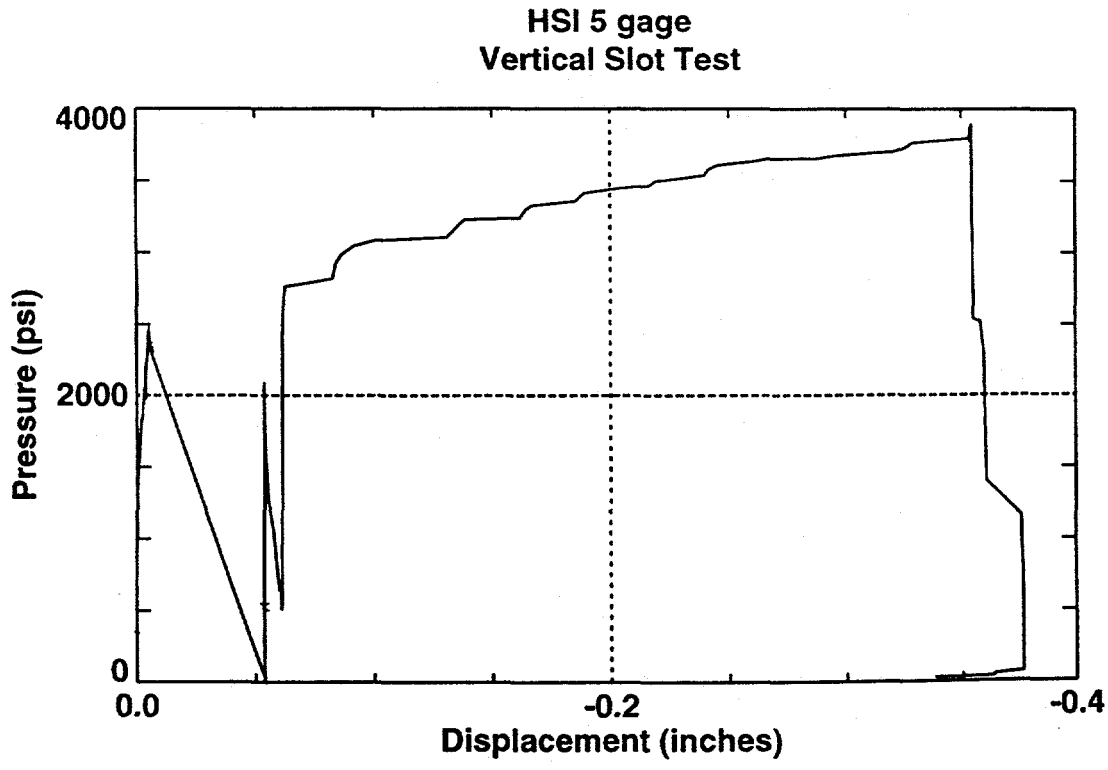
HSI 5 gage
Vertical Slot Test
4000
2000
0
Pressure (psi)
0.0
-0.2
-0.4
Displacement (inches)

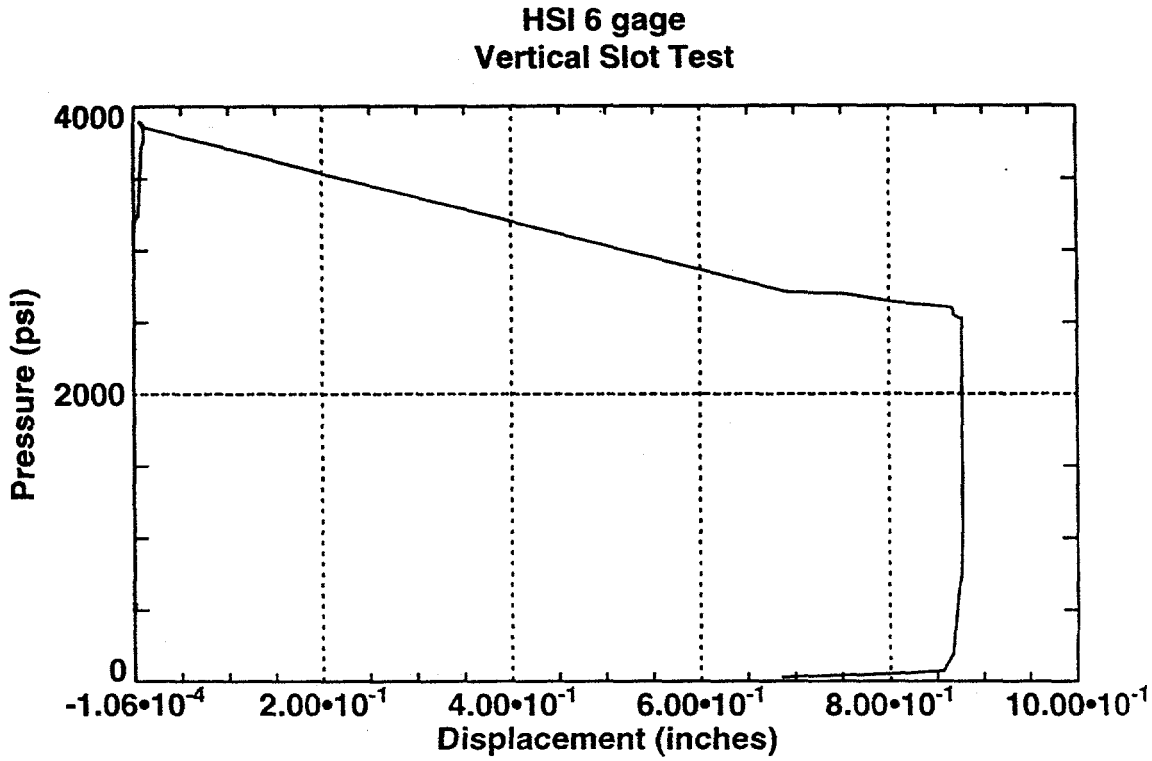
HSI 6 gage
Vertical Slot Test
4000
2000
0
Pressure (psi)
-1.06•10-4
2.00•10-1
4.00•10-1
6.00•10-1
8.00•10-1
10.00•10-1
Displacement (inches)

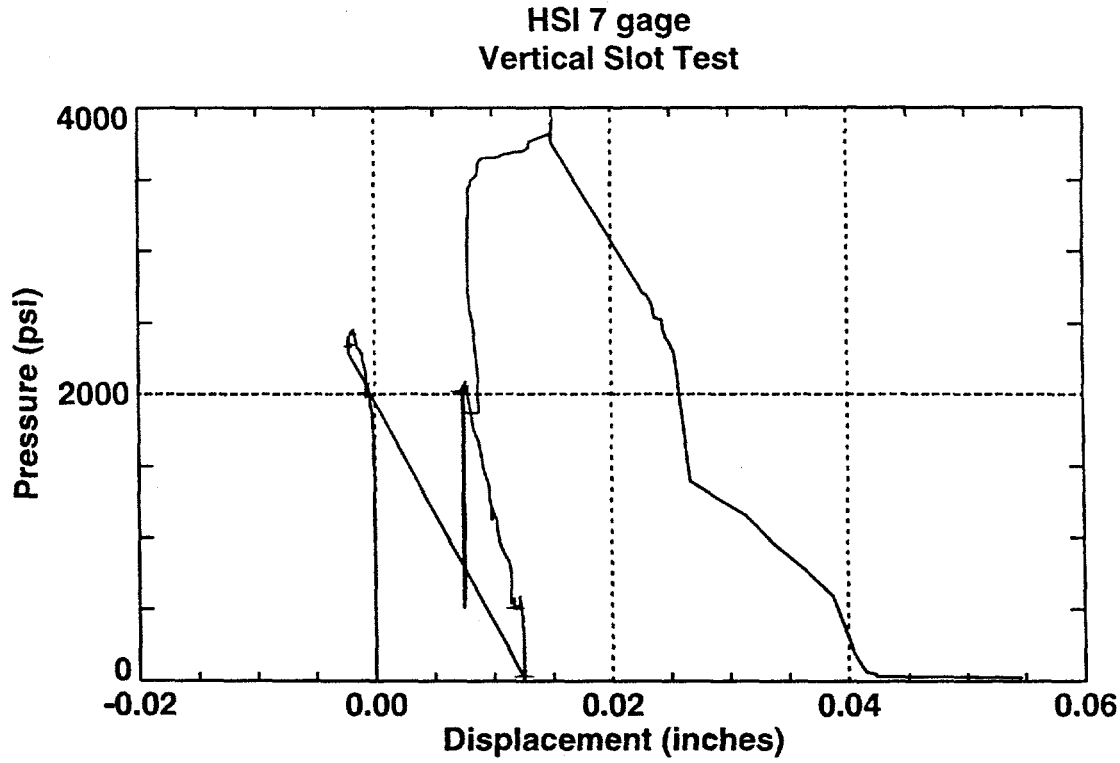
HSI 7 gage
Vertical Slot Test
4000
2000
0
Pressure (psi)
-0.02
0.00
0.02
0.04
0.06
Displacement (inches)

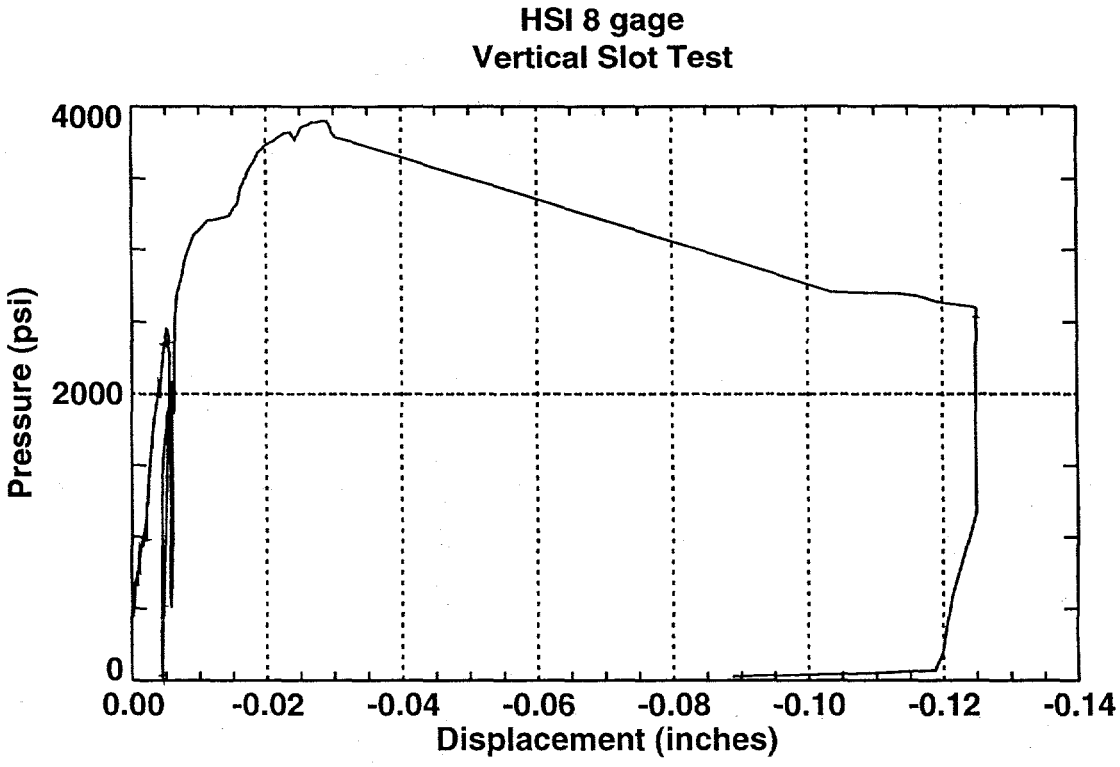
HSI 8 gage
Vertical Slot Test
4000
2000
0
Pressure (psi)
0.00
-0.02
-0.04
-0.06
-0.08
-0.10
-0.12
-0.14
Displacement (inches)

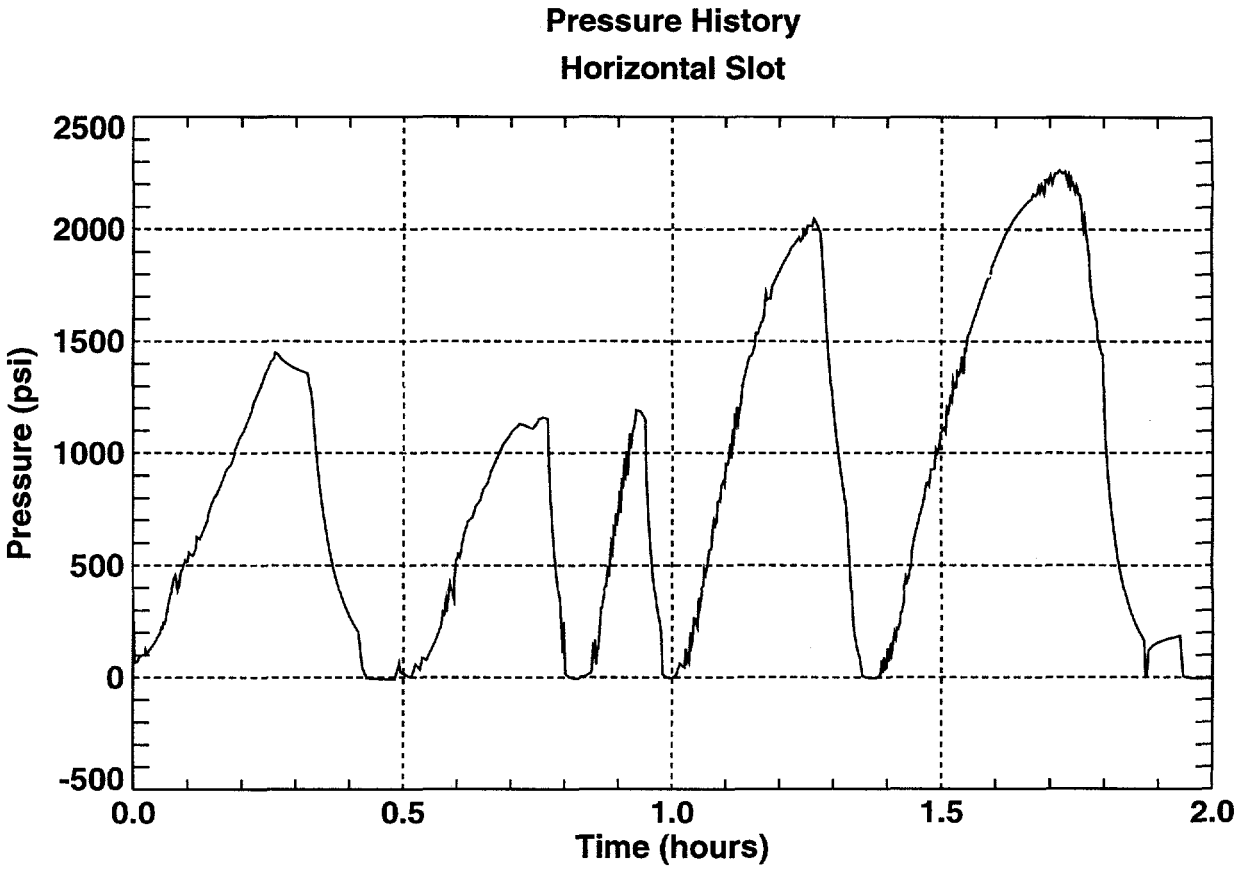
Pressure History
Horizontal Slot
2500
2000
1500
1000
500
0
-500
Pressure (psi)
0.0
0.5
1.0
1.5
2.0
Time (hours)

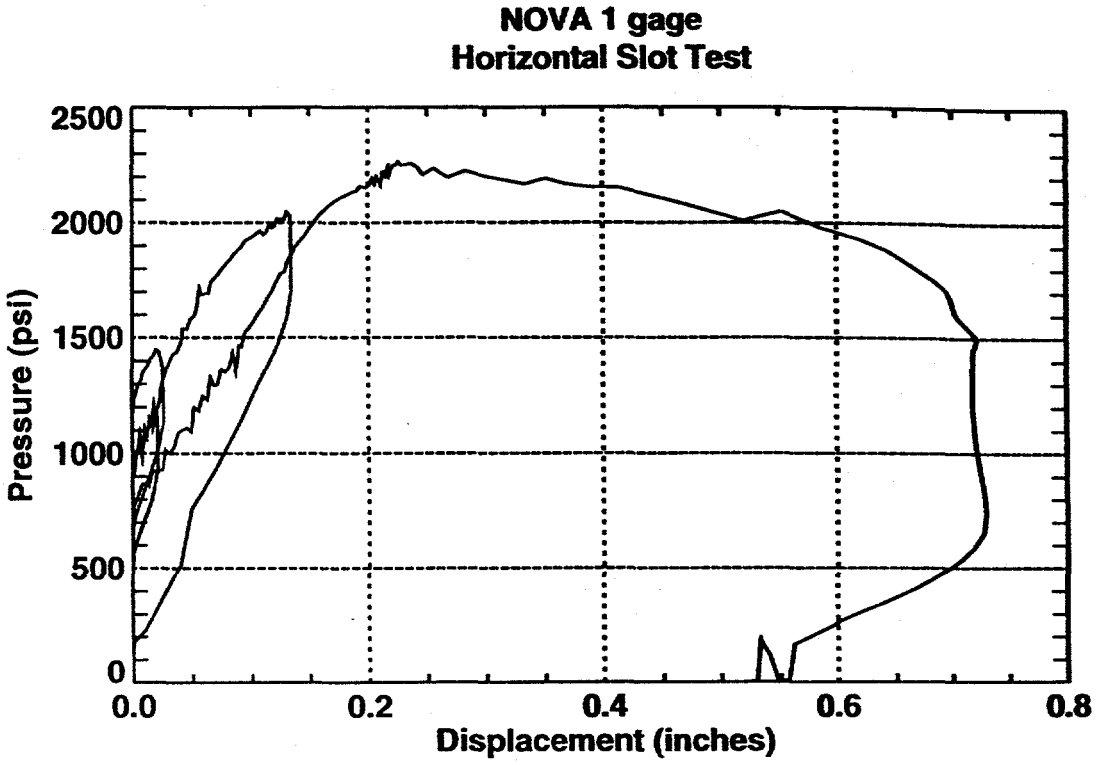
NOVA 1 gage
Horizontal Slot Test
Pressure (psi)
2500
2000
1500
1000
500
0
0.0
0.2
0.4
0.6
0.8
Displacement (inches)

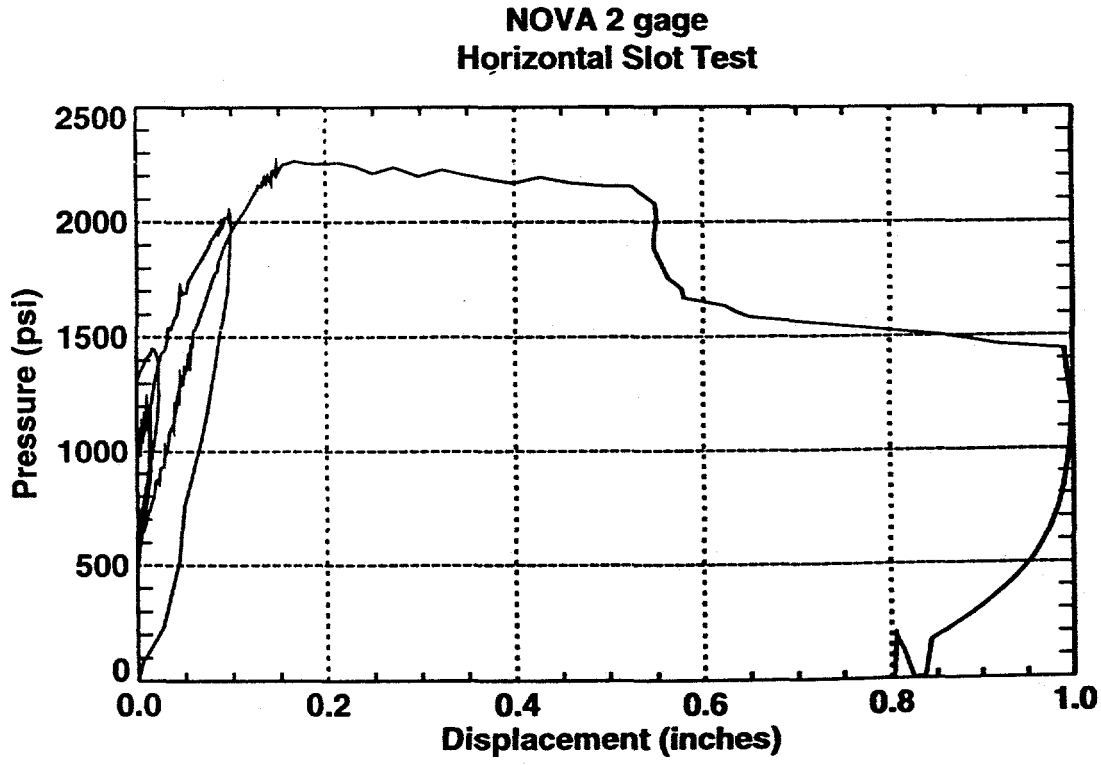
NOVA 2 gage
Horizontal Slot Test
Pressure (psi)
2500
2000
1500
1000
500
0
0.0
0.2
0.4
0.6
0.8
1.0
Displacement (inches)

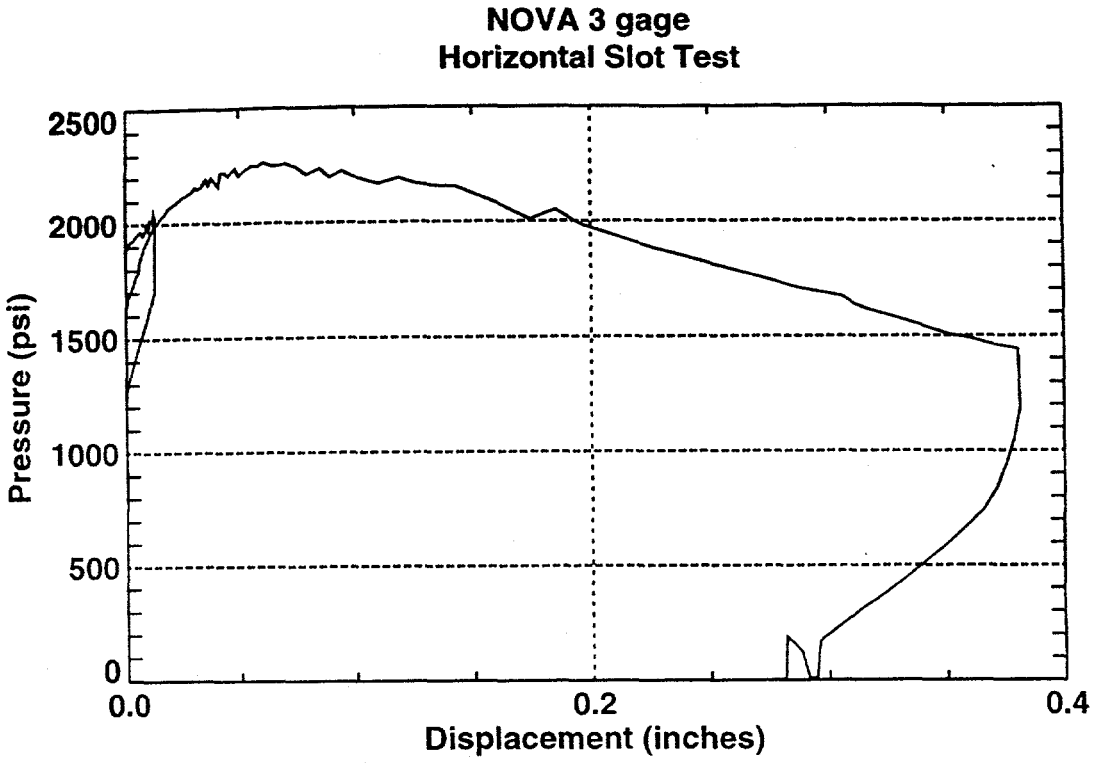
NOVA 3 gage
Horizontal Slot Test
Pressure (psi)
2500
2000
1500
1000
500
0
0.0
0.2
0.4
Displacement (inches)

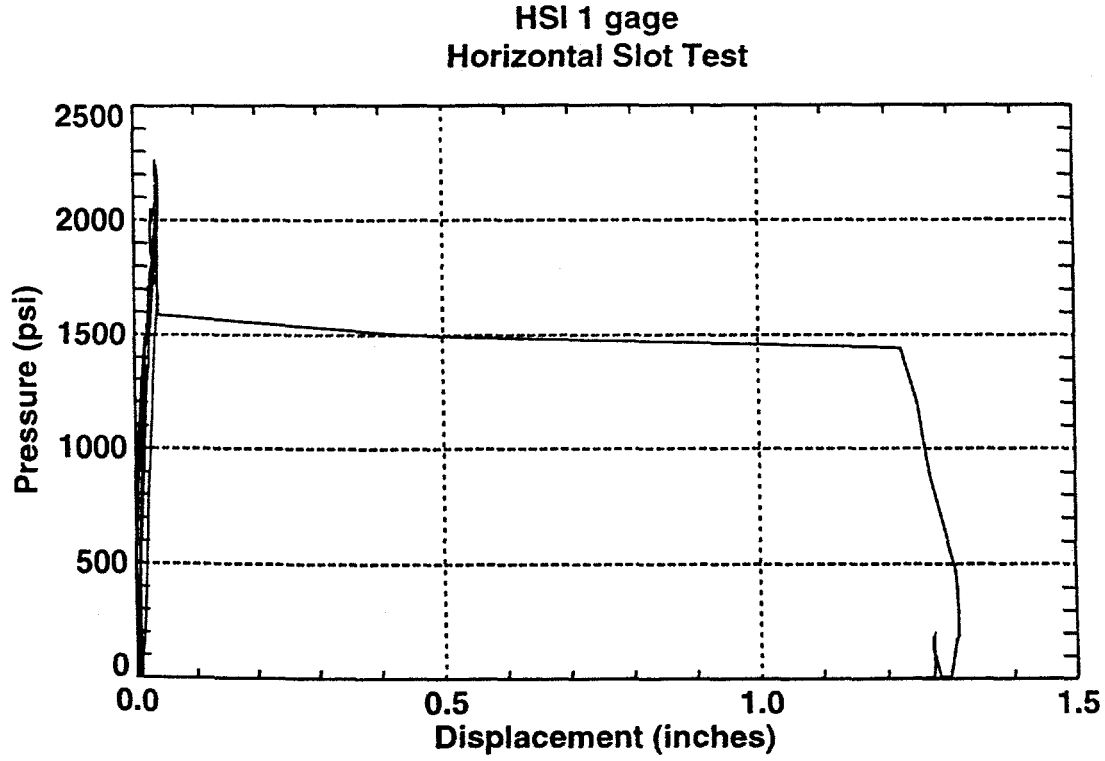
HSI 1 gage
Horizontal Slot Test
Pressure (psi)
2500
2000
1500
1000
500
0
0.0
0.5
1.0
1.5
Displacement (inches)

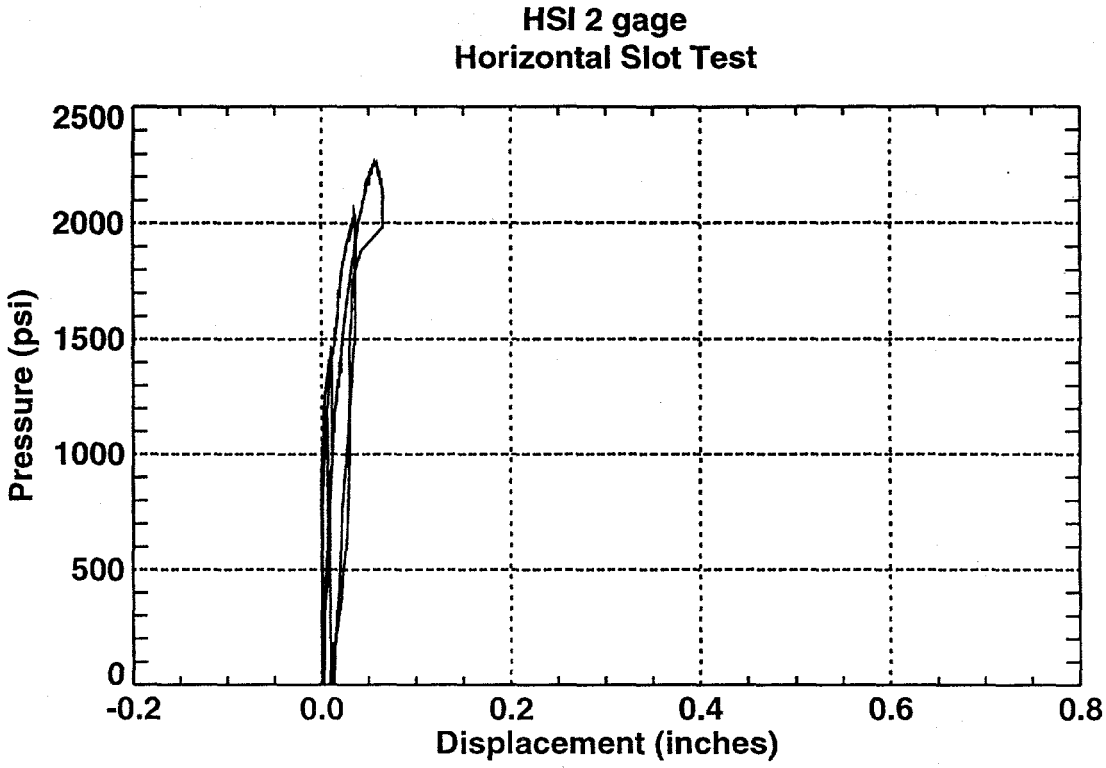
HSI 2 gage
Horizontal Slot Test
Pressure (psi)
2500
2000
1500
1000
500
0
-0.2
0.0
0.2
0.4
0.6
0.8
Displacement (inches)

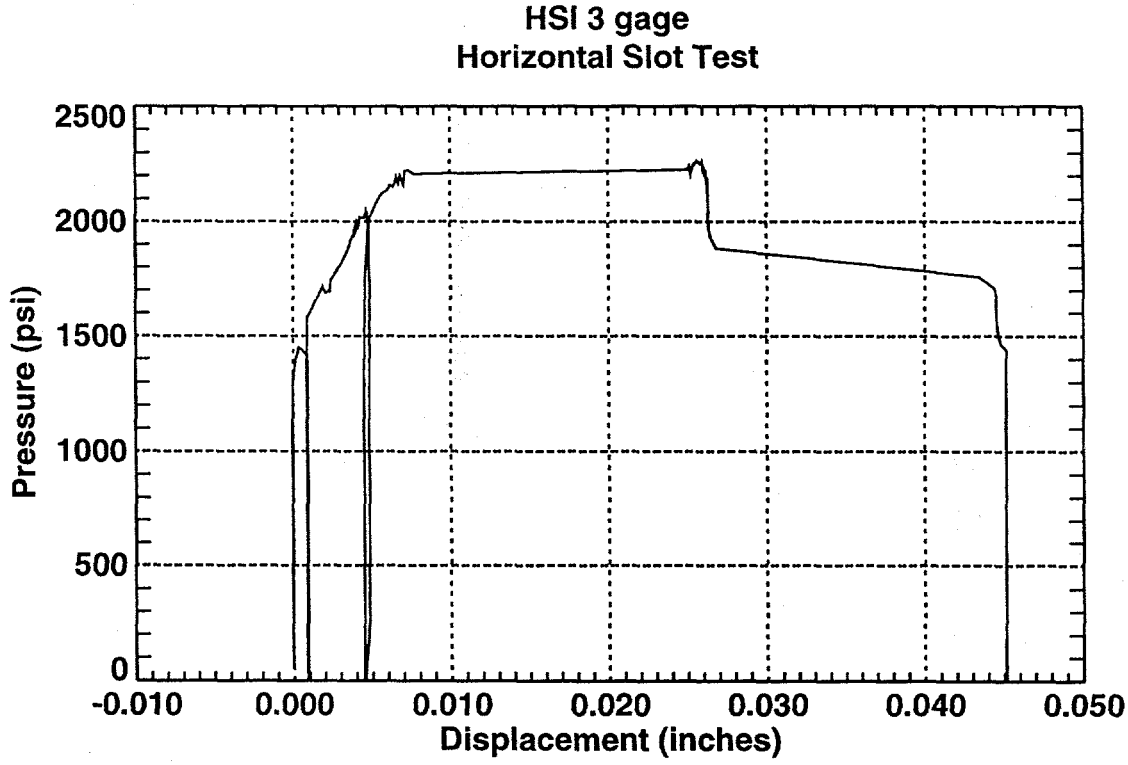
HSI 3 gage
Horizontal Slot Test
Pressure (psi)
2500
2000
1500
1000
500
0
-0.010
0.000
0.010
0.020
0.030
0.040
0.050
Displacement (inches)

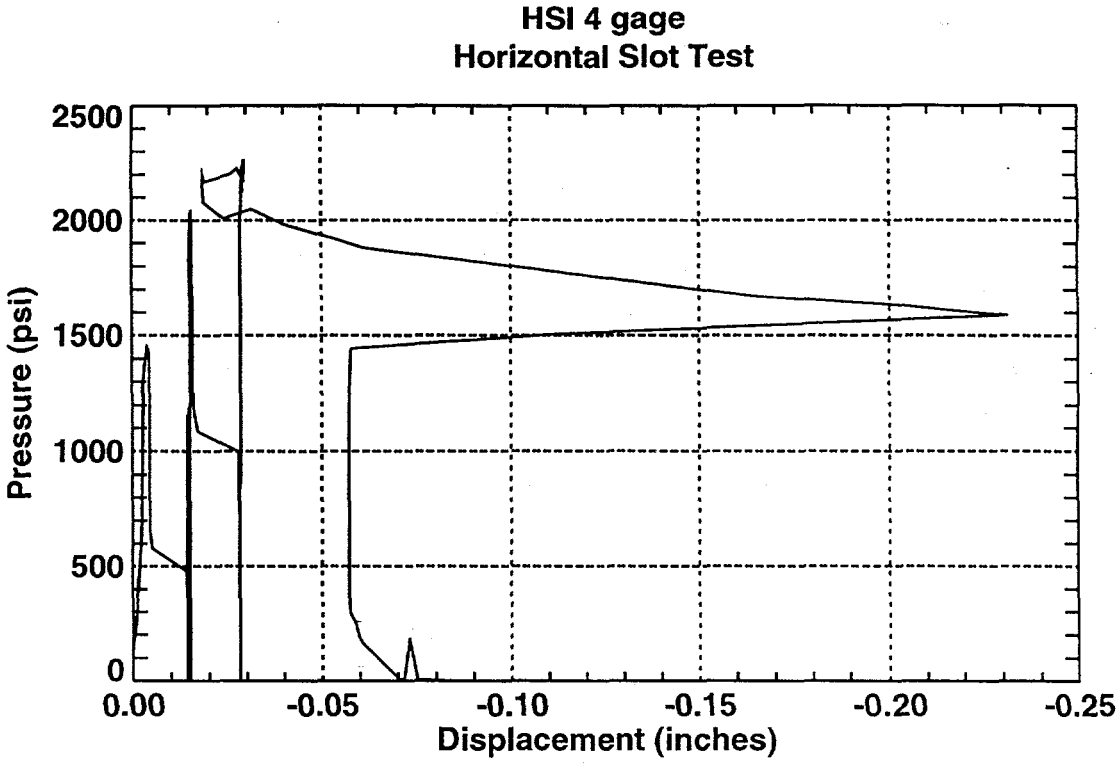
HSI 4 gage
Horizontal Slot Test
Pressure (psi)
2500
2000
1500
1000
500
0
0.00
-0.05
-0.10
-0.15
-0.20
-0.25
Displacement (inches)

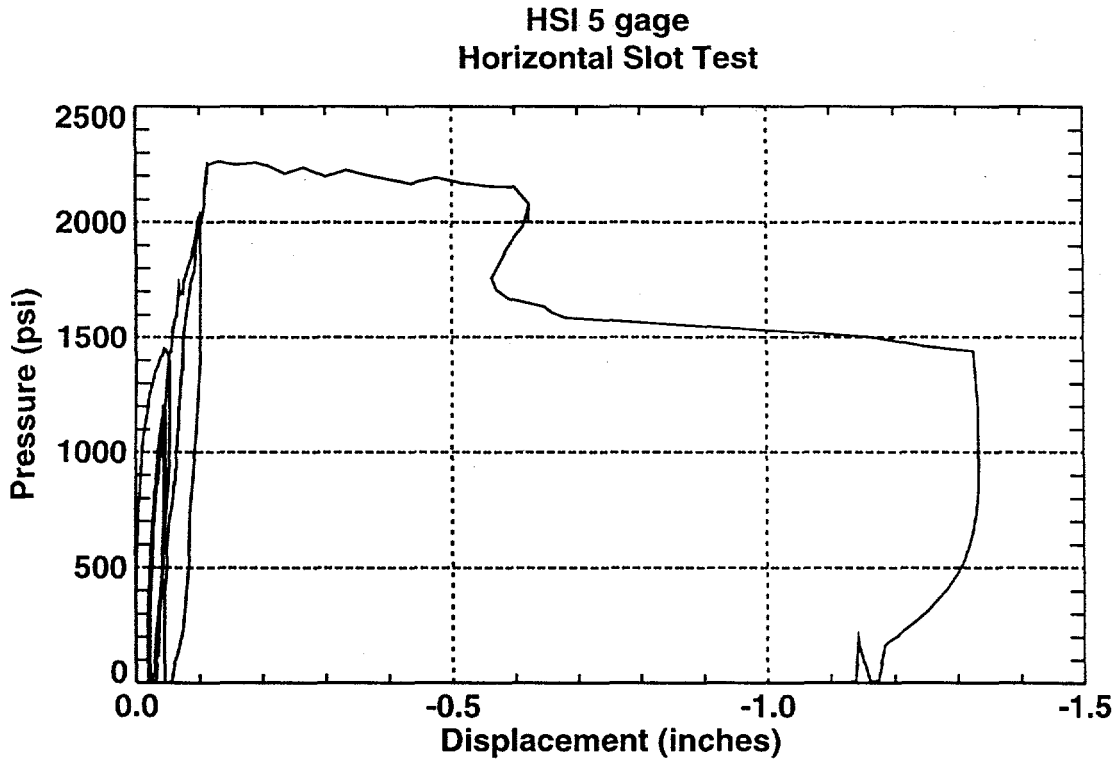
HSI 5 gage
Horizontal Slot Test
Pressure (psi)
2500
2000
1500
1000
500
0
0.0
-0.5
-1.0
-1.5
Displacement (inches)

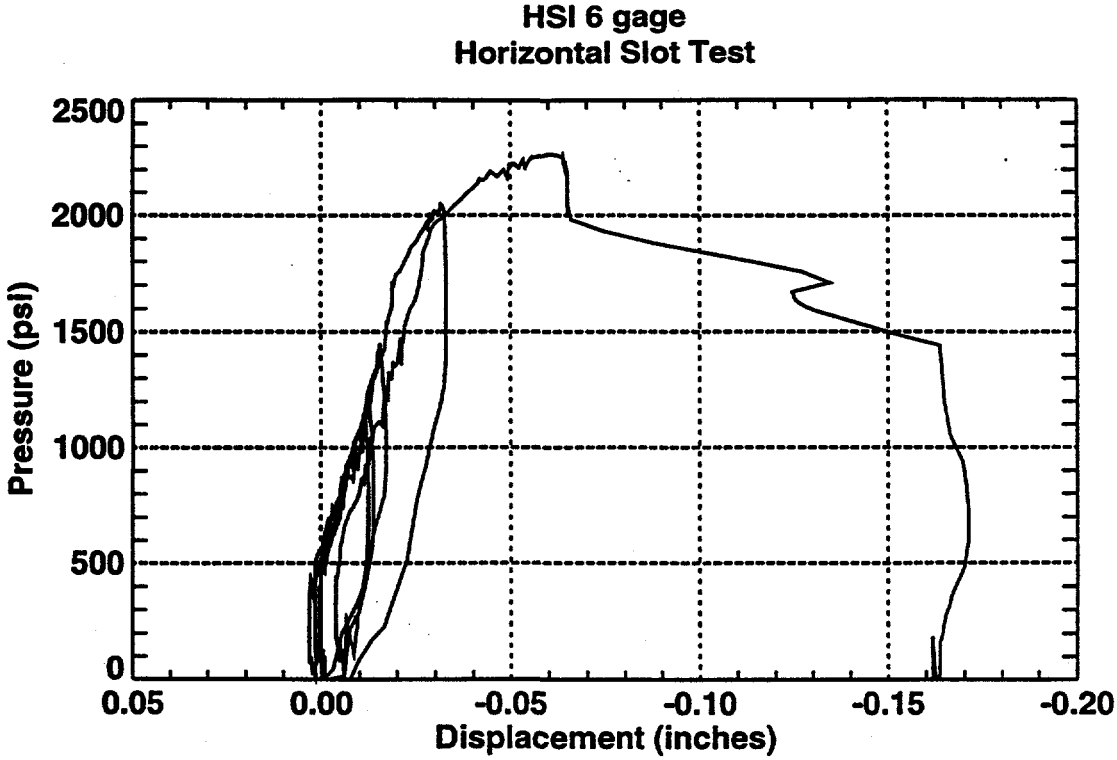
HSI 6 gage
Horizontal Slot Test
Pressure (psi)
2500
2000
1500
1000
500
0
0.05
0.00
-0.05
-0.10
-0.15
-0.20
Displacement (inches)

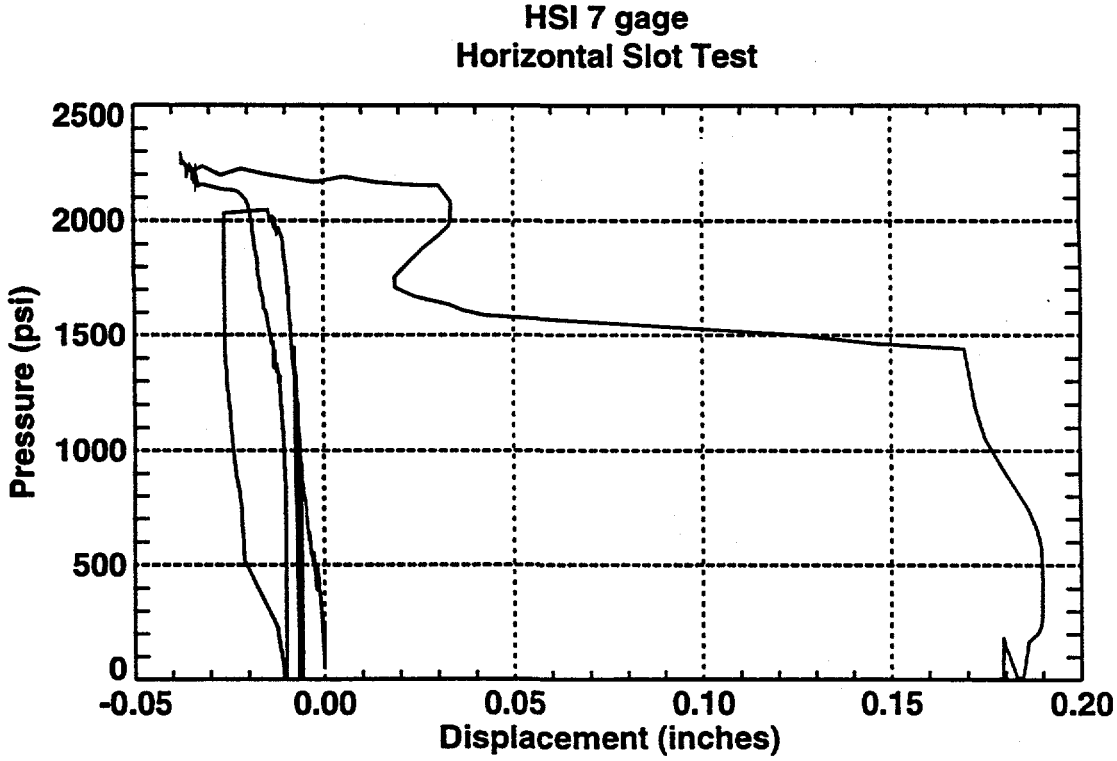
HSI 7 gage
Horizontal Slot Test
Pressure (psi)
2500
2000
1500
1000
500
0
-0.05
0.00
0.05
0.10
0.15
0.20
Displacement (inches)

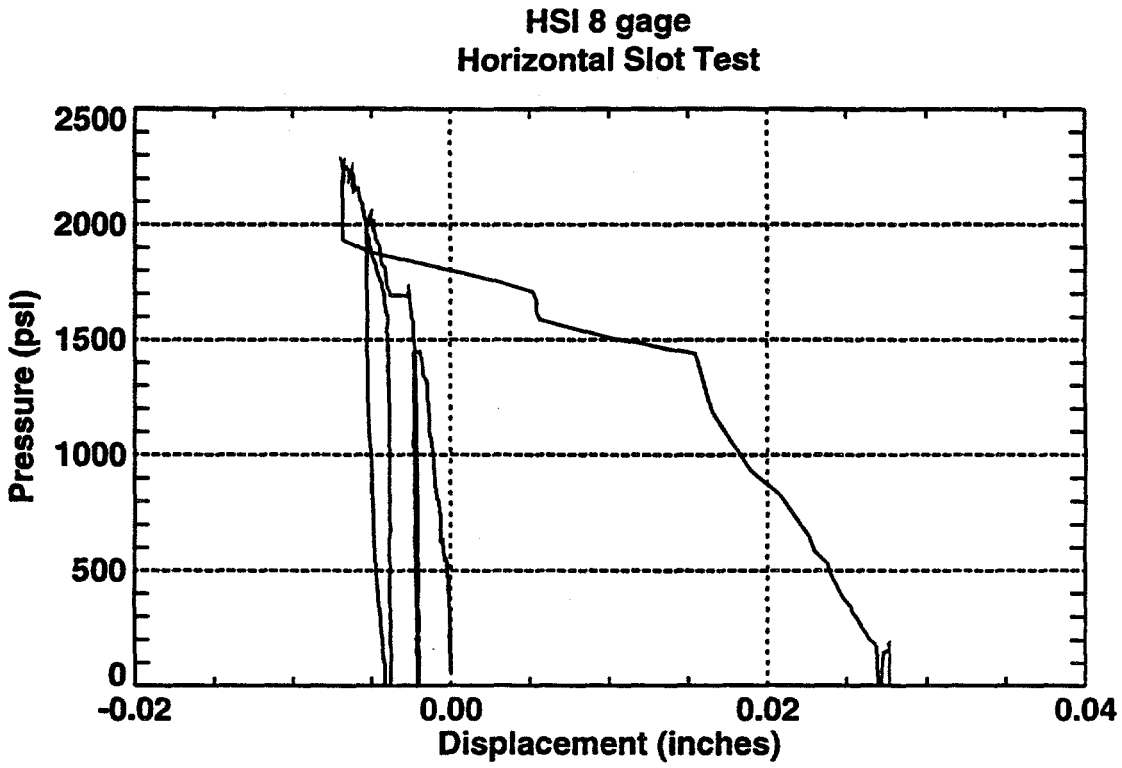
HSI 8 gage
Horizontal Slot Test
Pressure (psi)
2500
2000
1500
1000
500
0
-0.02
0.00
0.02
0.04
Displacement (inches)

DISTRIBUTION

Defense Nuclear Agency
Attn: Dr. Paul Senseny (5)
6807 Telegraph Rd.
Alexandria, VA 22310-3398

BDM Engineering Services, Co.
Attn: Dr. Dan Burgess (1)
Director, Redlands Operations
25837 Business Center Drive
Suite F
Redlands, CA 92374-4514

Petroleum Industry Alliance
Attn: L. Stephen Melzer (1)
Director, Center for Energy and
Economic Diversification
P.O. Box 553
Midland, TX 79702

USAE Waterways Experiment Station
Attn: Gayle Albritton (1)
3909 Halls Ferry Rd.
Vicksburg, MS 39180-6199

Agapito Assoc., Inc.
Attn: Carl Brechtel (1)
3841 W. Charleston
Suite 203
Las Vegas, NV 89102

Agapito Assoc., Inc.
Attn: Dr. Michael Hardy (1)
715 Horizon Drive
Suite 340
Grand Junction, CO 81506

Internal

0751	6117	W.A. Wawersik (1)
0751	6117	D.J. Holcomb (1)
1325	6313	L.S. Costin (1)
1325	6313	R.E. Finley (20)
1325	6313	J.T. George (1)
1325	6313	J. Pott (1)
1325	6313	E.E. Ryder (1)
1322	6121	J.R. Tillerson (1)
1322	6121	F.D. Hansen (1)
0899	13414	Technical Library (5)
0619	13416	Technical Publications (1)
0100	7613-2	Document Processing for DOE/OSTI (2)
9018	8523-2	Central Technical Files (1)